EFFECTS OF SAND ON THE COMPONENTS AND PERFORMANCE OF ELECTRIC SUBMERSIBLE PUMPS

A Thesis

by

NICOLAS I. CARVAJAL DIAZ

Submitted to the Office of Graduate Studies of
Texas A&M University
in partial fulfillment of the requirements for the degree of

MASTER OF SCIENCE

Approved by:

Chair of Committee,	Gerald Morrison
Committee Members,	Sy Bor Wen
	Robert Randall
Head of Department,	Jerald Caton

December 2012

Major Subject: Mechanical Engineering

ABSTRACT

The increasing world demand for oil has pushed oil companies to extract it from the ocean at extreme depths. With the increase in depth comes an increase in operation costs, especially the deep-sea equipment changeover cost. To be able to push the oil to the ocean surface, Electrical Submersible Pumps (ESPs) are commonly used as artificial lift. The changeover cost of these pumps in deep-water has been estimated to sometimes be as much as forty times the cost of a new pump.

One common reason for the failure of ESPs is the erosion and abrasion created by the fine sands that seep through the gravel pack mesh in the well hole. These fine sand particles are most destructive to the bearings and bushings due to their capability to enter the clearances lubricated by the pumped fluid. Over time, the sustained abrasion and erosion in the different components of the ESP will affect the performance of the pump and could lead to its damage.

This work describes the design, construction and evaluation of an erosion test rig built at the facilities of the Turbomachinery Laboratory in Texas A&M University. The test rig is capable of introducing 100 mesh (6 mil) sand into the flow loop, measure its concentration and separate it at the exit with minimal water loss.

The pump under study is a Baker Hughes 10.25” WJE1000. The performance of the pump is described by measuring the head, flow rate, power and efficiency. The pump is

equipped with accelerometers to detect the casing vibration as well as proximity probes in five locations along the pump to detect the internal vibrations of the shaft near the bearings as well as impeller radial movement. The baseline data, to be used for comparison with the worn out pump, has been shown and recommendations for the study method and operation of the rig are given.

DEDICATION

To the people that motivated and supported me the most: Mami, Papi, Nicole and Mami Lina.

ACKNOWLEDGEMENTS

This is about more than a thesis for me; this is about a journey I have undergone, in which I have learned, changed and grown. And it is as much, if not more, about what I learned in life than what I learned in school. I couldn't have accomplished all of the goals I had set for myself in this journey without the help of a lot of incredible and talented people, and for that I am forever thankful.

Dr. Morrison: I always wonder why I was the only one to call him "The Professor", because to me it only made sense; with him you are always learning, whether you are talking about philosophy, history, engineering or life, teaching is just a part of who he is. The ability he has for teaching seems from the naked eye to be innate or subconscious, but a more careful look will easily show that his teaching ability is no accident and is only possible to obtain through many years of hard work and perfecting. I have never met a person that truly enjoys teaching so much and is so good at it. Thanks for always going the extra mile to help all of us, your passion for your work has truly inspired me and has helped me enjoy what I do even more.

Ramy, for teaching me to always look at life lightly, and that in the end, what is important is the friends we make and the journey we go through. Thanks for always reminding me that we are all kids at heart and every once in a while, might as well act like it. The hard work you and I put on this project might sometime be forgotten but the lessons we learned along the way, never will.

Joey, for the welding.

Just kidding, thanks for always listening to me and being a good friend. Your advice was always wise, and I hope you know that I will keep counting on it as you can count on mine. Thanks for reminding us that we're in this world to do some good, and I know you are going to continue doing so, besides being a heck of an engineer.

Hector, for believing in us and in the projects we are working on. For always being interested in our projects and always available and willing to help. For all the life and work advice you always had for us. Without your support, all these projects would not have been possible and for that, all of us will be always grateful.

Sahand, I don't know how you did it but no matter how busy you were, you always managed to find time to help me, and with a big smile to boot. I guess I don't have to linger too much on thanking you since I already named the SahANDometer after you. Working with you and watching you work was a privilege, and a lot of fun.

Ray, thanks for patiently teaching me all the tricks in your bag while in the shop, you have a great talent for teaching and I really enjoyed every time I got to work with or spend time with you.

I would also like to thank Chase and Nick, working with you guys was a lot of fun and I hope you know all the hard work you put into the project didn't go unnoticed. Sujan and Daniel, with whom I did not spend as much time but whom without their hard work I would still be scrambling to finish my degree. Thanks for your patience with me,

especially every time you asked me a question and I (accidentally) ignored you because I was too absorbed writing the thesis.

Finally, to all my friends not mentioned above (Abhay, Daniel, Emmanuel, Scott and Shankar) and didn't contribute directly to the project but were always willing to help in and made it a point to put a smile in my face when I was having a bad day. I hope to see you guys soon and I wish you all the best.

Thanks to my family and friends in Puerto Rico, especially my mom, dad, my sister and my grandma. I love you all and look forward to catching up to the time we couldn't spend together these past couple of years.

I was blessed to work in such an interesting project and with so many talented and wonderful people. There are a lot more people that in some way or another helped me in this project and/or in my life. I might not have mentioned you here, but you know that I am always extremely grateful.

NOMENCLATURE

η	Pump efficiency
$\dot{m}_m$	Mass flow rate of slurry in CFM
$\dot{m}_s$	Mass flow rate of sand in the CFM
ΔP_{OFM}	Differential pressure in OFM
BHP	Brake horsepower
BPD	Barrels per day
CFM	Coriolis flow meter
DHF	Down hole failure
ESP	Electrical submersible pumps
FHP	Fluid horsepower
H-Q	Head to flow rate curve
NPSHR	Net positive suction head required
OFM	Orifice flow meter
P	Pressure
P&ID	Piping and instrumentation diagram
PID	Proportial,-Integral-Derivative controller
Q	Flow rate
Q_{FP}	Volume flow rate of feed pump
RPM	Rotational speed in revolutions per minute
T	Torque

VFD	Variable frequency drive

TABLE OF CONTENTS

Page

LIST OF FIGURES

Page

LIST OF TABLES

Page

1. INTRODUCTION

Over the past few decades, as technology has improved, oil companies have expanded their offshore drilling areas to depths previously thought impossible. But, as the distance from the oil rig at the ocean's surface to the bottom of the ocean increases, so does the cost of production, including installation and maintenance of down-hole equipment.

A very significant part of these costs is not in the unique but commonly used pumps, known as Electric Submersible Pumps (ESPs) used as artificial lift where the installation and removal of these pumps is sometimes more than a mile deep, but in the changeover itself. For this reason, more emphasis has been placed on extending the useful lives of these pumps.

Electric Submersible Pumps are centrifugal pumps with a hermetically protected motor that is close coupled to the pump's body. To avoid cavitation and multiple other problems that arise when trying to lift the working fluid to the surface, the ESP and all its components (including the motor) are submerged in and cooled by the working fluid being pumped; pushing the fluid instead of pulling it from the surface.

In order to generate the pressure required to elevate the fluid the amount necessary while overcoming losses, the ESP is comprised of multiple stages; each stage consists of an impeller stacked under a diffuser. The impeller (rotor) is keyed to the shaft and therefore rotates with it, imparting the torque energy from the shaft into the liquid as

kinetic energy, which is then transformed into pressure energy by the diffusers. The diffusers are fixed in place (stators) and slow down the velocity of the fluid, turning the kinetic energy into pressure rise. The process is then repeated on each subsequent stage.

Theoretically, ESPs can generate any needed pressure if enough stages are put together, coupled to a big enough motor. Common ESPs can have anywhere from tens to hundreds of stages. Due to limited lateral space inside the well hole, motors have to be small in diameter but very long. To achieve the required length and horsepower, sometimes up to three motors, of up to 30 feet each, are stacked one on top of the other, linked together with special mechanical couplings [1].

The top motor is attached to the protector (also known as mechanical seals). The protector is what prevents the well fluids from entering the motor coils and contaminating the oil and/or damaging the motor.

Coupled in a similar way as the other accessories, is the pump on top of the protector. As with the motor, individual pumps are limited in length and multiple pumps may be coupled together for proper assembly and ease of handling. Individual pumps can range from 20-25 feet. A diagram of a conventional ESP installation can be found in Figure 1.1.

Two types of submersible pumps are commonly used: fixed impeller (also called compression) and floating impeller pumps. The impellers in fixed impeller pumps are fixed axially to the shaft, which supports the entire axial load; this load is transferred to

the thrust bearings in the protector. In floating impeller pumps, the impellers are free to move up and down the shaft. In these pumps, the axial loads from the impellers are supported by the up and down thrust bearings, allowing for smaller thrust bearings to be used in the protector.

There are also two types of impellers used in ESPs: radial flow and mixed flow impellers. Radial flow impellers are typically used for lighter applications where the flow is less than 3,000 bpd and mixed flow impellers are used on larger capacity pumps (up to 40,000 bpd).

The inherent problem created by the placement of ESPs in subsea wells, besides the impracticality and difficulty of periodic maintenance, is the high cost of installation and removal of the pump. The cost of removing and installing a faulty pump could be, depending on the depth, up to forty times the cost of a new pump. For this reason, more emphasis is now being placed on research to extend the useful life of the pump to at least five years, and to locate, predict and mitigate any and all causes of pump failure.

One possible cause of submersible pump failure, depending on the nature of the oil bearing strata, is the damage incurred to the bearings, shaft and other components due to the presence of fine sand in the fluid. The sand present in the fluid originates either from the well itself or from the hydraulic fracturing of the well and thus its type, size and concentration will vary from well to well. Most wells have some type of sand control, usually gravel pack covered with a mesh. This will filter out the coarser gravel, but finer sands will seep through the mesh. The fine sand can pass through the product-lubricated

bearings and small clearances inside the pump, creating erosion problems, which in turn could lead to wear, vibration and possible pump failure.

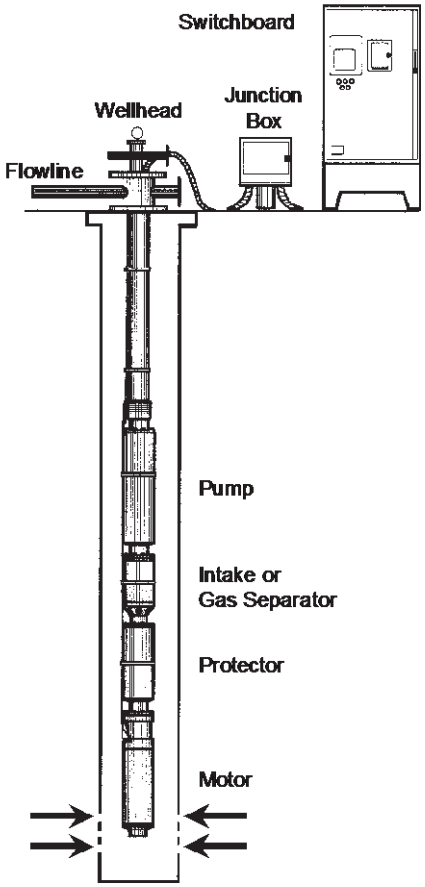

Figure 1.1 Conventional ESP installation. (Takacs 2009)

This thesis will describe the experimental facility designed and constructed to study the effects of these fine sands on ESPs. The initial investigation will consist of running 100 mesh (6 mil) sand through the pump in a controlled laboratory environment in order to determine the root cause failure modes of the pump and propose design improvements and/or recommend operation modes to minimize or avoid these failures. This work will

describe in detail the experimental design and construction of the test loop, procedures to be used in the experiments, baseline tests, and provide important information and recommendations to be used during testing.

A custom-made for laboratory environment, fixed impeller and mixed flow electrical submersible pump will be used for this study (referred from now on as ESP). For space constraint issues and unavailability of a well in the laboratory, only three stages of the pump will be tested and, since standard ESP motors are designed to be inserted inside the well, a regular 250 HP induction motor will be used instead. The three stages of the pump are installed inside a special casing built for the sole purpose of laboratory experiment; the ESP is shown in Figure 1.2. A thorough description of the experimental setup can be found in Section 3. The ESP is a 10.25" WJE1000 fixed impeller, mixed flow pump, manufactured and provided by Shell and Baker-Hughes.

The ESP will be disassembled and studied periodically and whenever a performance loss, change in vibration patterns or abnormal operation in the pump is detected. The pump will be disassembled on site, using the facilities at the Turbomachinery Laboratory of Texas A&M University. During disassembly, all components of the pumps will be measured and/or weighed and logged. This data will be used to quantify material loss and erosion on the pump's components such as bearings, sleeves, shaft, etc.

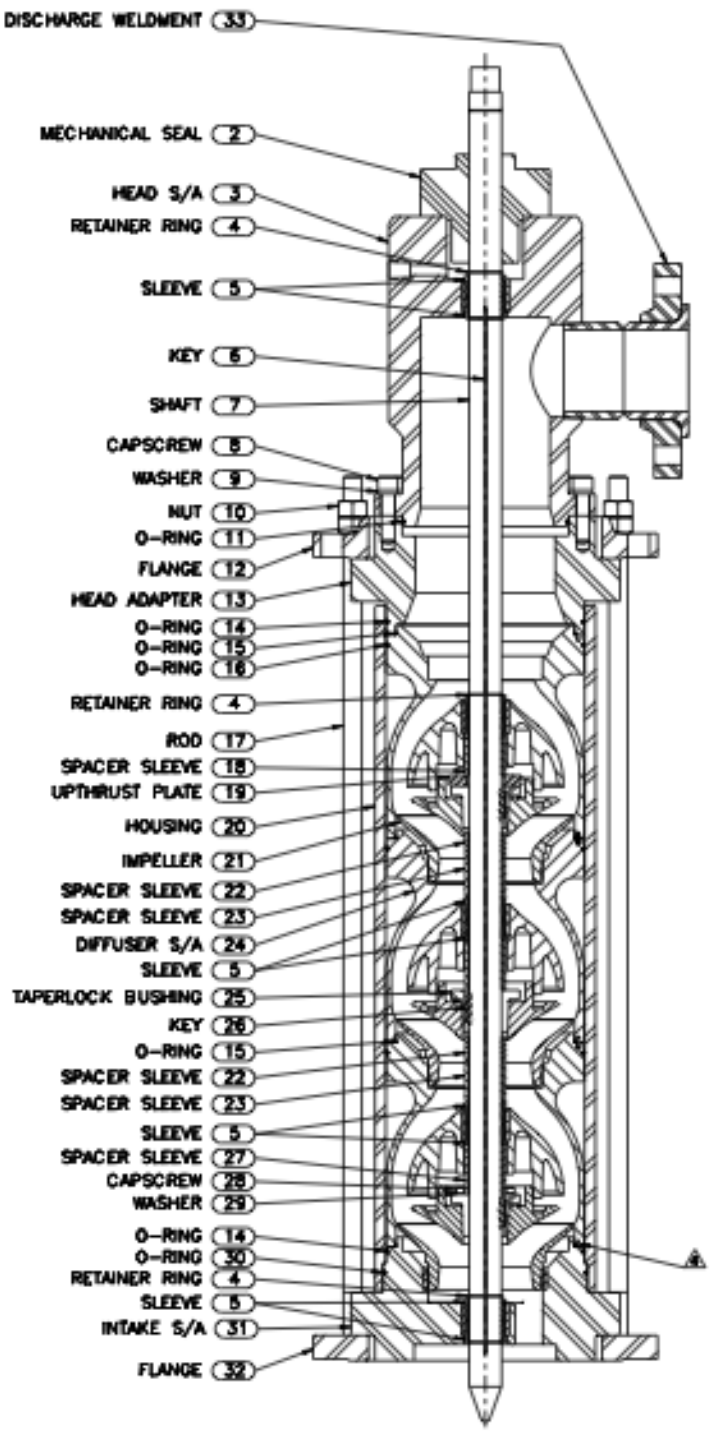

Figure 1.2 Cross-section and Bill of Materials of ESP under study.

The sand to be used in the experiment is rated as 100 mesh “frac” sand used to mimic the fine sand that seeps through the sand control screens and gravel installed in wells.

Sand that is used for hydraulic fracturing is commonly referred in the industry as frac sand. The frac sand is usually screened to a desired mesh, and is used in the oilfields to keep fractures in the rock open. The sand will be analyzed, before and after use, in the laboratory using sieves to determine its size distribution and microscope images to determine its shape.

Some of the questions hoped to be cleared in the future by the experiment described:

- How much do clearances grow for a given amount of sand (or run time)?
- Is there a point where clearances stop growing?
- What are the effects of the increased clearances on the rotor-dynamics of the pump?
- What are the effects of the increased clearances on the performance of the pump?
- What operating conditions accelerate the wear on the pump?
- What type of sand is most damaging to the pump?

Due to the length of the experiment, the scope of this work only includes the design, construction and guidelines of operation of the experiment. Besides serving as a handbook for running the experiment, the paper will post questions that need to be answered and provide the data necessary for comparison upon completion of the experiment.

2. LITERATURE REVIEW

2.1 Electrical Submersible Pumps

Typically, in their early stages, oil wells flow naturally to the surface propelled by pressure at the well bore; these wells are called "flowing wells". When the pressure in the well is not enough to lift the liquid to the surface, the well is considered to be "dying". Artificial lift is used to produce oil on dying wells or increase the production rate of flowing wells. Artificial lift methods include: ESPs, beam pumps, jet pumps and gas lifting (injecting compressed gas down hole). Electrical Submersible Pumps are one of the most commonly used artificial lift methods, a thorough review of ESPs, their history, design, operation and maintenance can be found on Gabor Takacs' book *The Electrical Submersible Pump Manual* [1].

Some advantages of the ESP include [1]:

- Capable of achieving high volume flow rates (over 30,000 barrels per day (bpd) from 1,000 feet).
- Energy efficiency (over 50% on high flow rate pumps).
- Well suited for offshore environments due to their small footprint and capability of being submerged.
- Well suited for urban areas due to their small footprint.

An ESP in its simplest form consists of two components: the rotor (impeller) and the stator (diffuser). Each pair of these components is known as a stage, shown in Figure 2.1. The ESP is comprised of multiple stages stacked on top of each other.

The impeller (Figure 2.2) consists of a set of vanes driven by a prime mover (motor) that impart kinetic energy to the fluid. The torque imparted by the motor is converted to kinetic energy by the vanes in the impeller, accelerating the fluid. The high velocity liquid is then slowed down and converted into pressure energy in the diffuser (Figure 2.3), where the liquid enters the next stage and repeats the process [1].

Since kinetic energy is proportional to the term $\rho\, v^2$ (density times velocity squared), a centrifugal pump at a constant speed transfers different amounts of energy to liquids of different density. The pressure rise on the liquid is directly proportional to the density of the fluid and, all else equal, the pressure increase imparted by a centrifugal pump divided by the liquid density is constant for all fluids. For this reason, when dealing with centrifugal pumps the pressure rise in the pump is given in terms of length (i.e. meters or feet) [1].

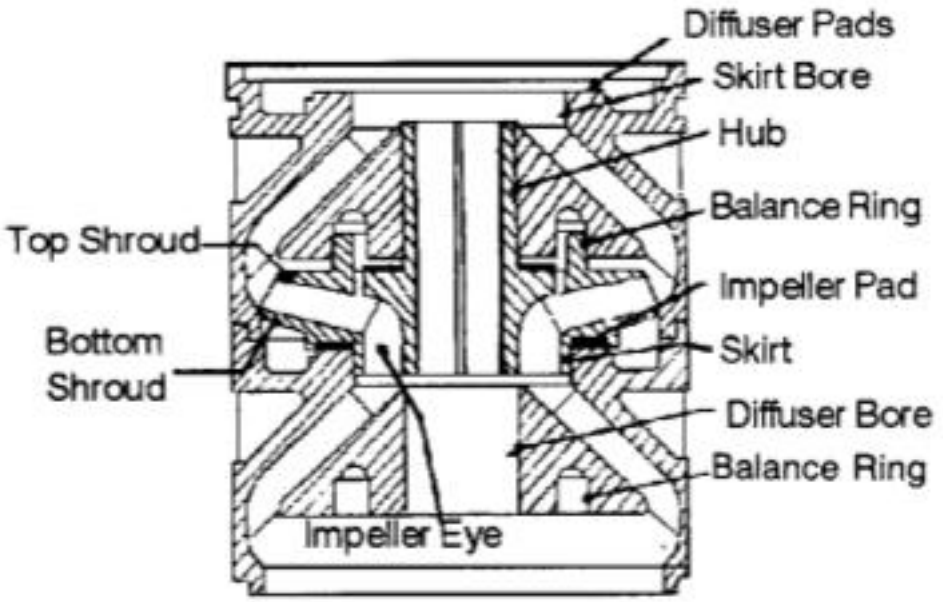

Figure 2.1 Common ESP mixed flow pump stage, consisting of an impeller and a diffuser, direction of flow is upward. (Divine et al. 1993)

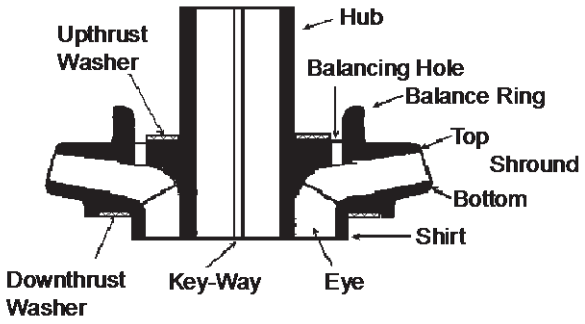

Figure 2.2 Nomenclature of impeller parts, direction of flow is upward. (Takacs 2009)

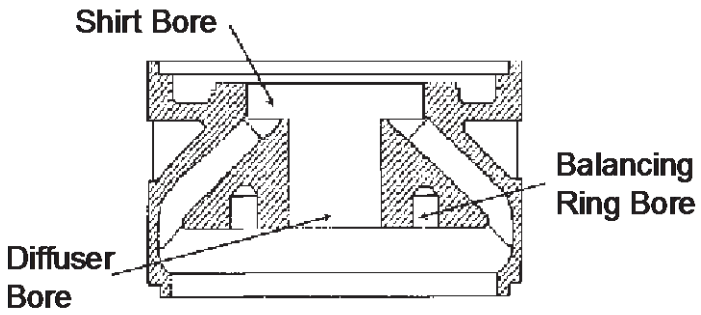

Figure 2.3 Nomenclature of diffuser parts, direction of flow is upward. (Takacs 2009).

In order to properly compare different designs of centrifugal pumps, the specific speed term has to be introduced. Specific speed, N_s, is defined as the rotational speed required to produce a liquid rate of one gallon per minute against one foot of head [1]. The formula for specific speed is:

$$\mathrm{N}_s = \frac{N\sqrt{Q}}{H^{.75}} \qquad 2.1$$

N is the pump speed in RPM, Q is the pumping rate in gpm and H is the head (pressure rise) per stage in feet. All parameters have to be taken at best efficiency point (BEP).

Common centrifugal pumps can be classified according to their flow direction: radial, axial and mixed flow pumps. In ESPs however only radial (Figure 2.4) or mixed flow (Figure 2.5) pumps are used. Radial flow pumps are used for low flow rates (under 3,000 bpd) and they work by transferring all their kinetic energy into centrifugal force

before converting into head. Mixed flow pumps will develop their head by converting the centrifugal force and by the lifting action of the impeller [1].

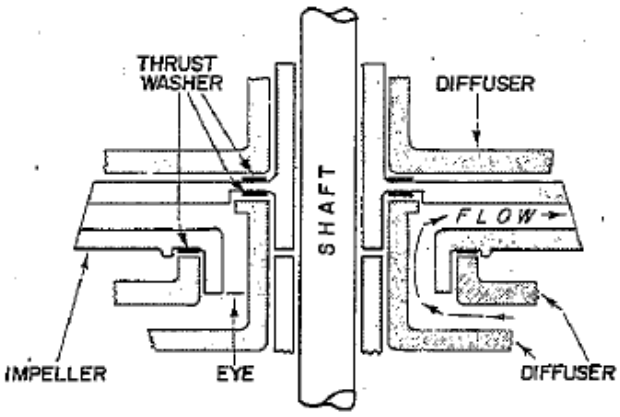

Figure 2.4 Cross section of a radial flow ESP. (Powers 1987)

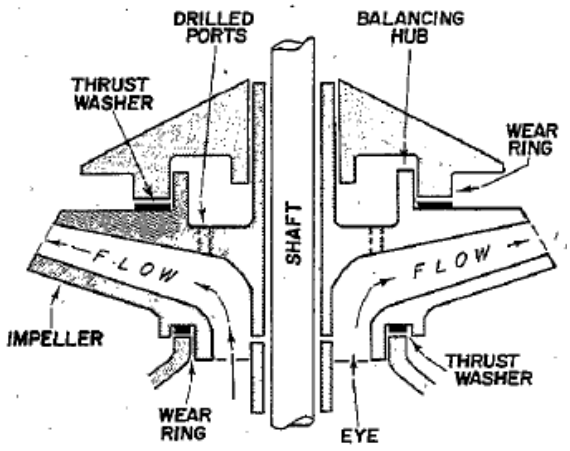

Figure 2.5 Cross section of a mixed flow ESP. (Powers 1987)

Developed in the 1910's by Armais Arutunoff, the ESPs have undergone few changes since then. Of these changes, one of the most significant was the development, in the

early 1950's, of a mechanical protector that kept well fluids out of the motor, substantially increasing pump life.

Another breakthrough in ESP technology was the introduction of Variable Frequency Drives (VFDs), also known as Variable Speed Drives, in 1977 [1]. The VFD is a device capable of changing the electric frequency of an alternate current in order to control the speed of a motor. In the case of the ESPs, the ability to control the pump's speed meant that a single pump would be capable of operating under a wider range of well conditions, saving the work-over cost previously required to change the pump once the condition of the well changed. Apart from the benefits of using a VFD to control ESPs, they do present certain challenges. The running of the pump outside its design operating ranges leads to extra wear on the pump due to abnormal thrust and/or vibrations.

Powers [2] studied the effects of the speed variation on the ESPs, focusing mainly on the relationship between pump thrust and its useful life. A pump that has been running normally for years can wear out in a few days when operated under hostile thrust conditions [2] . Thrust is the sum of the axial forces on the pump. These can be classified into two categories: dynamic and static. Static forces include the buoyancy weight of the impeller and shaft. Figure 2.6 demonstrates the dynamic forces, which include: forces due to the pressure gradient between the inlet and exit of the impeller (always downward), the net inertial force from the change of direction of the fluid in the pump stage (upward) and the axial pressure due to the discharge pressure of the pump acting downwards on the shaft.

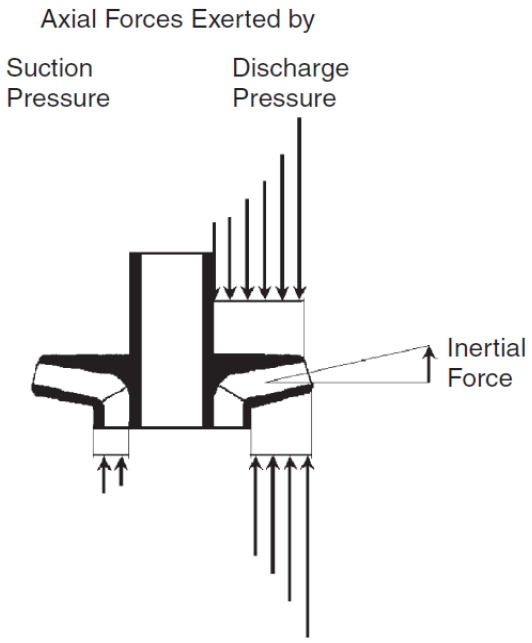

Figure 2.6 Distribution of axial forces (thrust) in mixed flow impeller. (Takacs 2009).

Due to the high costs of installation and removal of an ESP pump working in deep-sea wells, some petroleum companies, as Upchurch [3] mentions, have applied very strict standards for their pumps. These standards include manufacturer's testing of every pump delivered and requiring the installation of only new pumps and equipment in subsea wells.

In his paper, Upchurch [3] attempts to find a correlation between the type of ESP failure and the inherent condition of each reservoir encountered in the East Wilmington field of California. This reservoir is divided into three major producing zones, the descriptions

of which provide an example of the variety between different types of wells within an oil field:

- The Ranger Zone depth ranges from 2100’ to 3200’ and is considered the most prolific of the three zones. It’s low temperature and gas-oil ratio also makes it the easiest zone to produce but the presence of fine sands results in erosion of the pump.
- The Terminal Zone depth ranges from 2800’ to 4200’, as this depth increases, so does the temperature and gas-oil ratio, making the extraction of oil more challenging.
- The Union-Pacific-Ford zone is the deepest (4100’ to 7100’) and thus contains the highest fluid temperature as well as gas-oil ratio. This combination is the harshest for the ESP, mainly because of the limited cooling provided by the working fluid.

Upchurch [3] also identifies five common down-hole failures (DHF) encountered in these zones: cable, pothead, pump, motor and protector. He also notes that after any other type of failure, the cable also failed (i.e. a motor failure would also create a cable failure); therefore, a cable failure is only considered a failure in which the cable failed when everything else was in operable condition. A pothead or protector failure would cause the well fluids to enter the motor, causing motor failures; repeated startup attempts will also cause cable failure. A pump failure could consist of the stages seizing or

plugging with foreign materials, including sands, this seizing would in turn also damage the motor and cable.

2.2 Performance of ESPs, Wear and Losses

To describe the performance of a centrifugal pump, a pump curve is used. A typical pump curve includes pressure rise, brake horsepower and efficiency plotted vs. flow rate. A pump curve can also include these same parameters at different pump speeds. The head vs. flow rate curve of a typical pump will be maximum at zero flow rate and zero at maximum flow rate. Centrifugal pump curves are produced by testing the pump at constant speed while throttling the flow at the pump discharge to vary its exit pressure, while measuring necessary parameters.

In their paper, Divine et al. [4] used ESP test curves (head and brake horsepower to flow rate curves) to try to determine pump wear and remaining useful life of the pump. The purpose of the paper was to develop a qualitative and quantitative technique to determine whether a pump should be returned to service without repair. Due to the stricter quality control measures in the industry, as mentioned by Upchurch [3] , a used pump is not commonly returned to service in subsea environments; however, the ability to track pump performance using the sophisticated sensors available in ESPs would allow the ESP operators or engineers to use this and other information to track the performance of the pump, allowing them to make inferences on its condition and control operation to maximize remaining life.

Losses in ESPs and all pumps are the reason that more energy is required to be imparted to the pump than the energy gained by the fluid. The energy imparted to the pump is the energy on the motor shaft known as brake horsepower (BHP) and can be found using the following formula:

$$\mathrm{BHP} = \frac{\mathrm{T} * \mathrm{RPM}}{5{,}252} \qquad 2.2$$

Where BHP is the power imparted to the pump (does not include losses in the motor) by the shaft, in horsepower. T is the torque on the shaft in lbf-ft and RPM is the rotational velocity of the shaft in revolutions per minute.

The fluid (or hydraulic) horsepower (FHP) of the pump is calculated using the following formula:

$$\mathrm{FHP} = \frac{\mathrm{Q} * \Delta\mathrm{P}}{1{,}714} \qquad 2.3$$

Where Q is the flow rate in gallons per minute (gpm) and ΔP is the pressure increase across the pump in pounds per square inch (psi).

The efficiency of the pump is:

$$\eta = \frac{FHP}{BHP} \qquad 2.4$$

Due to the losses inside the pump, the FHP is always going to be lower than the BHP, and thus the efficiency, η will always be less than 1. Common losses on ESPs are bearing losses, disk friction, leakage, friction, and turbulence [4] .

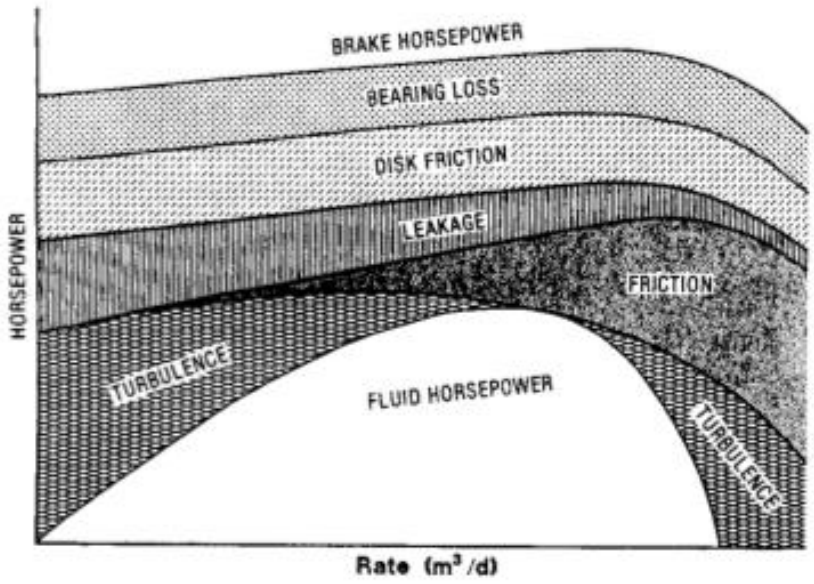

Figure 2.7 BHP losses in ESPs. (Divine et al. 1993)

All the existing losses in the pump are further increased by wear, leading to loss in pump performance and eventually can lead to pump failure. Divine et al. [4] describe different types of wear that commonly occur inside the ESPs: radial wear, loss of compresion, upthrust wear, downthrust wear, and sand wear. These problems may or may not lead to ESP failure, but will most certainly lead to increased losses and/or reduced efficiency.

Radial wear causes the clearances between the impeller hub (Figure 2.2) and the diffuser bore (Figure 2.3) to increase. These increased clearances allow higher leakage

losses from the impeller discharge to the impeller suction (also known as slip), thus reducing the head to flow rate curve (H-Q).

Upthrust wear usually occurs when the pump is operated at flow rates larger than the Best Efficiency Point (BEP) flow rate, where the upward hydraulic force from the impact on the impeller eye (Figure 2.2) is larger than the hydrostatic force from the pressure downstream of the pump. As seen on Figure 2.2, the bearing surface in this situation would be the upthrust washer on the impeller.

Downthrust wear occurs when the pump is operated at flow rates to the left of the BEP (lower flow rates than the flow rate at BEP). The downthrust washer in Figure 2.2 is the bearing surface for this running conditions. Divine et al. [4] showed that this type of wear would increase the bearing losses on the pump.

2.3 Sand Wear

The type of wear of most interest for this study is wear caused by sand around 100 mesh or smaller. Divine et al. [4] state that in general, this type of wear is similar to radial wear in that it increases the clearances in the same way, resulting in an increase in BHP also. Due to the small size of the particles of sand to be used in the study and their ability to fit inside the small clearances between bearings, hub and bore (Figure 2.2 and Figure 2.3), etc.; this is where most of the sand wear is expected.

Due to the geological composition of the reservoir rock, sand is usually present in normal quantities in the extracted petroleum. Normal quantities can range from 10-50

ppm by weight and particle size of 100- 350 μm (4 to 14 mil) [5]. In the mid-to-late 1900's extensive studies of sand erosion were performed in the petroleum industry.

True and Weiner [6] performed general research on the effects of sand erosion on equipment used to produce oil and gas. This research was limited to equipment such as valves, chokes and fittings (tees, elbows, etc.) and did not include pumps. Experiments were conducted using sand injected into compressed air streams at several velocities. They concluded that sand erosion increased linearly with fluid velocity and sand concentration.

On an ESP, metal loss caused by erosion and abrasion on critical points in the pump may lead to catastrophic failure. The removal of metal particles from different parts of the pump can be classified as [1]:

- Erosion on a metal surface hit by abrasive particle in the fluid.
- Abrasion caused by the presence of the foreign material between two moving metal surfaces.

Sand erosion is a form of wear caused by particles hitting against a target face and removing material. Several properties such as size, density, sharpness and hardness of sand influence the severity of the erosion incurred on the chafed material. Natural dusts in oil wells carry a variety of materials of which quartz, SiO_2 (sand) is usually the most abundant, hardest and most erosive. Studies have shown that the erosive potential of natural sands is directly proportional to its quartz content [7]. Figure 2.8 illustrates the

relative hardness of several materials typically present in ESPs and in sands normally found in an oil well.

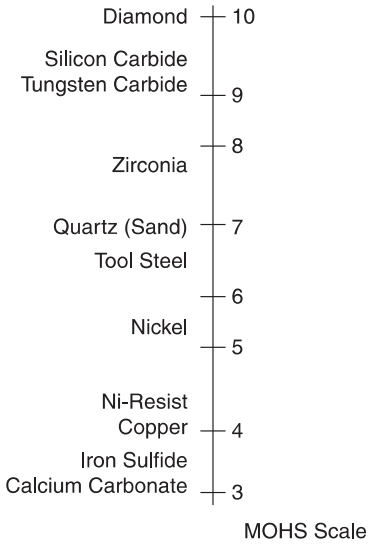

Figure 2.8 Approximate hardness of several materials found in ESPs and common minerals found in wells (Takacs 2009).

Another important factor in the erosion rate is the impact angle on the surface. The influence of impact angles depends on the material being eroded: ductile materials exhibit maximum damage for low angle impacts, whereas brittle materials are most affected by normal impacts [7].

Abrasion is highest when the majority of solid particles' size is comparable to the clearances inside the pump, sizes between two and ten mils are considered to be the most damaging on ESPs. Solid concentration in the produced fluid also has a crucial effect on erosion and abrasion in ESP equipment. Typical concentrations found in oil wells range from 10 mg/lit (light) to more than 200 mg/lit (severe) [1]. Since the purpose of these

studies is to find the failure modes and not the mean time to failure, concentrations of 2,000 mg/lit (more than ten times of those considered severe) will be used in order to achieve the desired results (abrasion and erosion) in a timely manner.

Different parts of the pump undergo different types of damage, which can be classified as [1]:

- Erosion in the pump stage.
- Abrasion in the radial bearings (radial wear).
- Abrasion in thrust washers and thrust bearings (axial wear).

Erosion in the pump stages, while not entirely negligible, seldom leads to failure since the pump will usually fail for other reasons before then. Radial abrasion is caused when the sand particles enter the clearance spaces between the bearing and the journals. These clearances depend on pump design and machining tolerances. Larger particles, upon entering the clearances will be crushed and remove metal from the bearing surfaces while smaller particles may go through without touching the metal. This type of wear will increase the clearances in bearings and sleeves, which will in turn make the shaft rotate eccentrically causing side loads that further accelerate the wear. The increase in radial clearances combined with the high axial loads and slender shaft will cause buckling which will create severe vibration and destruction of the pump, protector and/or motor [1].

Axial wear is caused by abrasion in thrust bearings on the thrust washers and the mating surfaces of the pump stage. Fixed impeller pumps, like the one currently used for this study, have no contact between the impellers and diffusers and thus are protected against axial wear. Floating impeller pumps, when operated in upthrust conditions, will have clearances large enough for the sand enter the thrust bearing, leading to worn-out washers and bearings.

From the available literature, it is clear that the erosion and abrasion on ESPs from small particles necessitates further study in order to understand the mechanism behind the erosion and abrasion in ESPs. In the current era of oil and gas production, where more emphasis is being placed on longer equipment run life, it is imperative that the erosion mechanisms that affect the ESPs be understood in order to be mitigated.

3. EXPERIMENTAL SETUP

A flow loop must be designed and constructed for this study. It must provide sufficient NPSHR to the ESP and deliver correct sand concentrations. The loop must also have the capability to separate the sand at the exit of the ESP in order to avoid recirculating the crushed particles, which would lead to decreased wear. A numbered illustration of the test rig assembled can be found on Figure 3.1, Table 3.1 describes the items numbered in the figure. For a more detailed description of the test loop, refer to the Piping and Instrumentation Diagram (P&ID) in Appendix A. The test rig consists of a 5,000 gallon tank supplying the necessary water for the pump; on top of the tank, connected to the exit of the pump, are 20 hydro-cyclone separators on top of a screen shaker. Feeding the ESP are two pumps and a sand auger, which will be controlled automatically using a Proportional Integral Derivative (PID) Controller to regulate the flow rates and sand concentration. The feed pump flow rate is measured using an orifice flow meter (OFM), while the flow rate and density of the slurry pump is measured using a Coriolis flow meter (CFM); the sum of both is the ESP's flow rate. A 250 HP induction motor controlled by a VFD (VFD1) powers the ESP. The exit pressure at the pump can be controlled using a pinch valve (V3) in conjunction with a choke (C1).

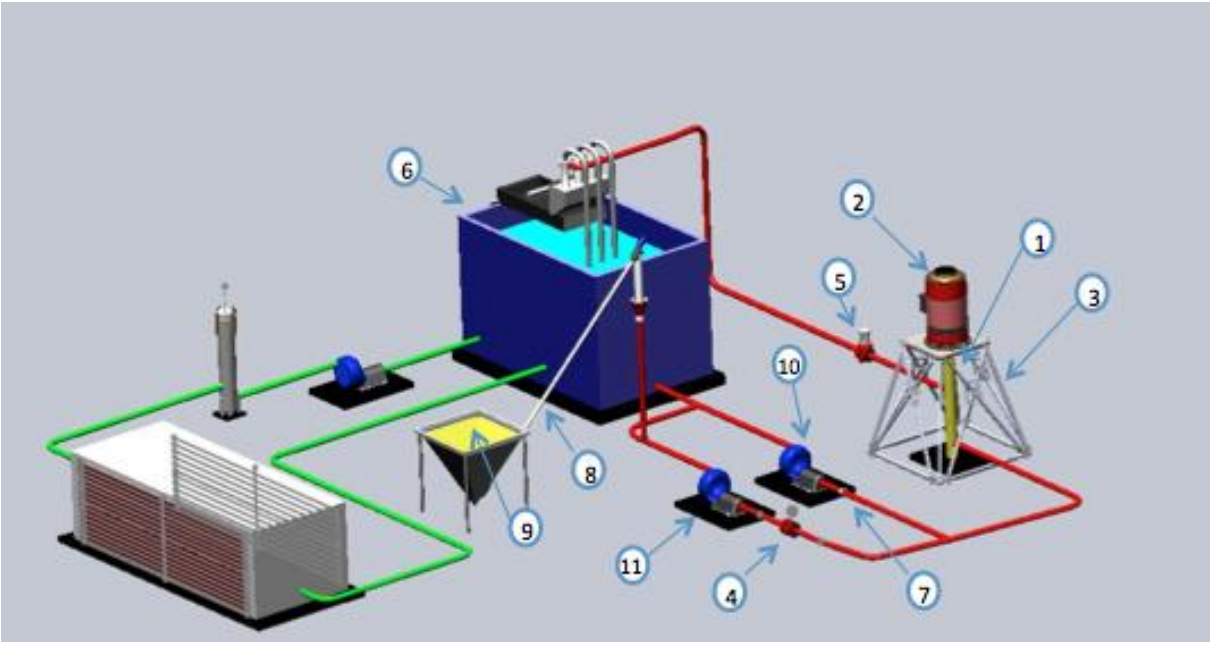

Figure 3.1 Experimental Setup Diagram. The red piping represents the test loop, green piping represents the cooling loop.

Table 3.1 Identification for items in Figure 3.1

No.	Item
1	ESP Pump
2	ESP Motor
3	Derrick
4	Coriolis Flow Meter
5	Pinch Valve
6	Tanks and Separators
7	Orifice Flow Meter
8	Sand Auger
9	Sand hopper
10	Feed Pump
11	Slurry Pump

Data to be measured and logged during testing includes:

- Pump input shaft thrust
- Pump input shaft torque
- Pump input shaft rotational speed
- Horsepower
- Radial position of components inside the housing
- Acceleration of the housing
- Flow rate and Head
- Inlet and Exit pressure
- Sand Concentration

Thrust and torque will be measured using strain gages placed in a special coupling between the pump and motor. With a calibration curve found experimentally in the laboratory, axial strain can be used to determine the thrust and torsional strain can be used to determine the torque. Rotational velocity will be measured using one of the proximity probes measuring the position of a rotating component with a small notch (phasor) cut on it, the phasor will act as a once per revolution trigger used to calculate the velocity. The rotational velocity and torque will be used to calculate the brake horsepower on the pump according to equation 2.2 .

Selected components inside the housing (both rotors and stators) will have at least two proximity probes (10 total) measuring their position in the radial direction. These probes

will monitor the movement of the components with respect to each other. Besides demonstrating the vibration patterns inside the pump, these probes can also provide rotational velocity as well as torsional strain on the shaft. Lastly, three probes (2 in the radial and one in the axial direction) will be used on the coupling to ensure alignment between the pump and motor and monitor coupling's movement. Vibration on the casing will be measured using tri-axial accelerometers placed near the inlet and outlet of the ESP.

Flow rate will be measured using the OFM and CFM. The OFM will be used to measure the volume flow rate of the feed pump and the CFM for the mass flow rate and density in the slurry pump. The mass flow rate and density can be converted to volume flow rate for the slurry pump, and the sum of the two volume flow rates is the volume flow rate of the ESP. Sand concentration can also be calculated by measuring the change in density with the CFM. The head generated by the pump will be estimated using pressure transducers in the inlet and outlet of the pump.

3.1 ESP

The ESP under study consists of three stages of the pump mounted inside a casing adapted for laboratory environment (Figure 1.2). The pump will be cantilevered on a derrick inside the laboratory in a vertical position to maintain as much resemblance as possible with down-hole ESPs. A 250 HP induction motor mounted on top of the derrick, controlled by a VFD will power the ESP.

The pump curves from the manufacturer for three stages of the pump are shown in Figure 3.2. According to the manufacturer's curve, each stage of the pump is capable of generating 51 psi of head at approximately 1100 gpm at the BEP with 75% efficiency. The head-flow rate curves at different speeds, given by the manufacturer are shown in Figure 3.3.

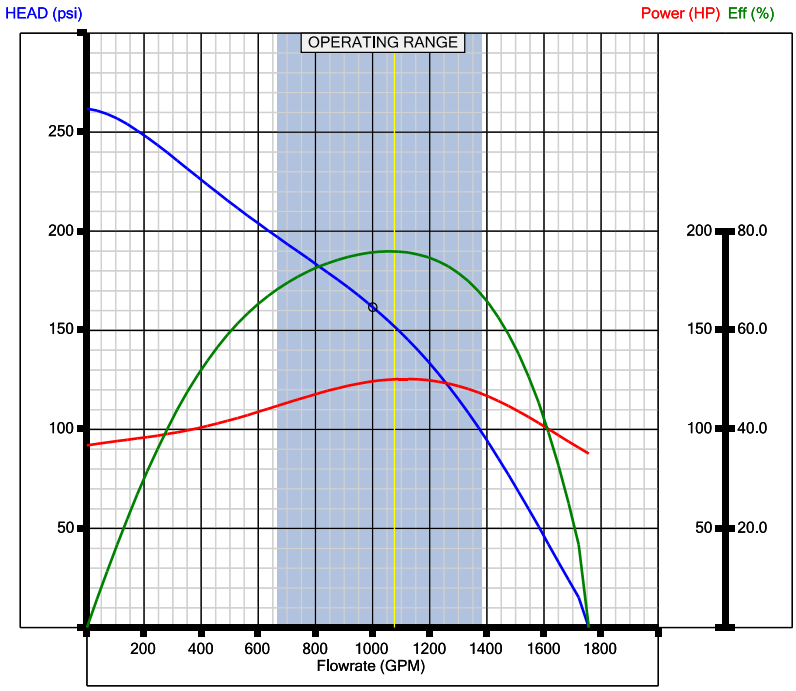

Figure 3.2 Catalog performance curve for three stages of ESP under study at 3600 RPM, S.G.=1.0.

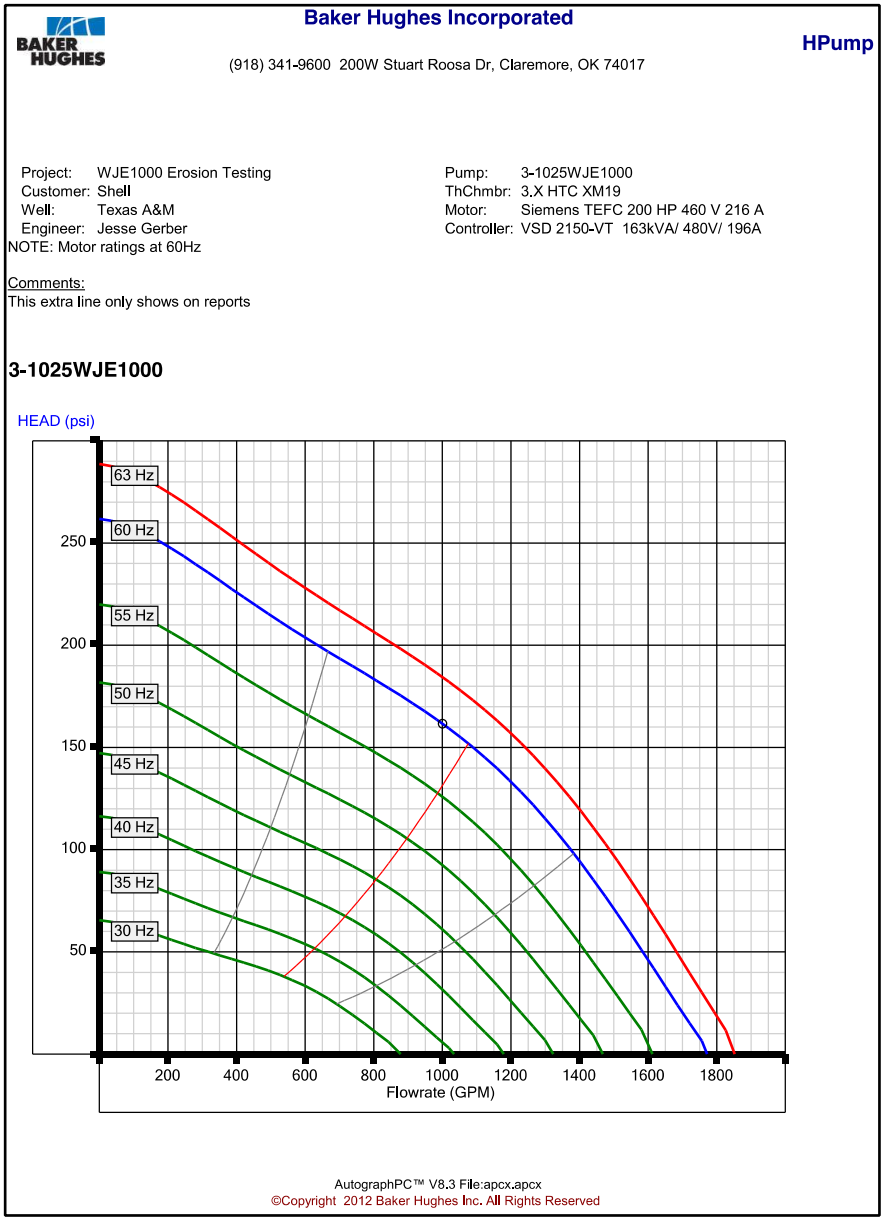

Figure 3.3 Catalog head flow rate curves for different pump speeds.

The pump in use will be a Centrilift WJE1000, this mixed flow, fixed impeller pump has a 10.25" stage diameter, and is considered large for an ESP, therefore the 250 HP needed for only three stages. The impeller in this pump has five vanes, while the diffuser has seven. The impeller and diffuser pictures, taken prior to assembly of the pump can be seen on Figure 3.4 and Figure 3.5. The figures show the five vanes on the impeller and the seven vanes on the diffuser.

Figure 3.4 Impeller picture taken prior to assembly of the pump.

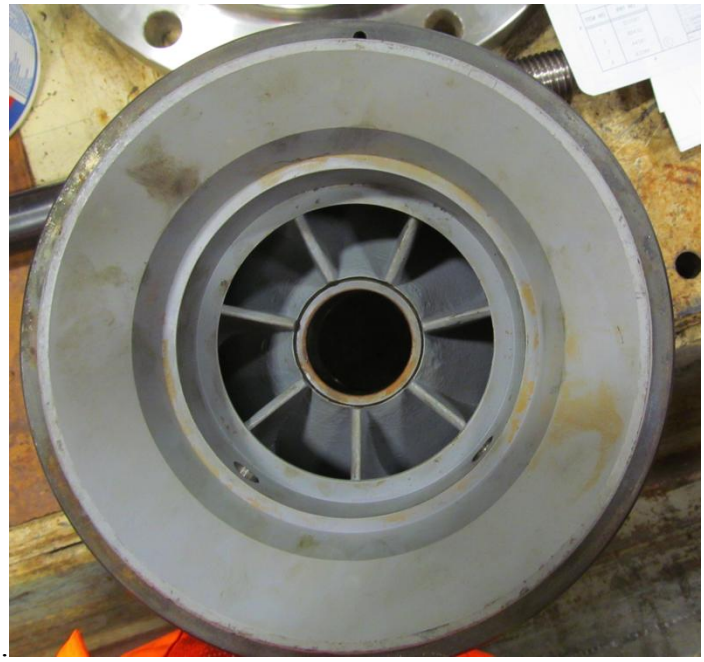

Figure 3.5 Diffuser picture taken prior to assembly of the pump.

The pump and all its components were measured and weighed before assembly with the intention of keeping an accurate log of the wear and material loss on the pump. It is critical that these components be accurately measured and weighed on each disassembly of the pump. Figure 3.6 shows the drawing of the impeller in use and its dimensions according to the manufacturer, the dimensions and weight as measured in the laboratory can be found in Table 3.2. The same data for the diffuser can be found in Figure 3.7 and Table 3.3, the numbering refers to the stage, where the first stage is the nearest to the inlet and the third is the nearest to the exit. Data for the rest of the components and larger size figures can be found in Appendix A.

(21) IMPELLERS			
Location	Impeller 1	Impeller 2	Impeller 3
1			
2			
3			
4			
5			
6			
7			
Weight (lbs)			

Test Cell no.:	**Project:** Shell ESP Erosion Study	
Author: Ramy Saleh	Page 01 of 01 **Measurement / Job Aid** **Title: Impeller Measurement**	
Approved by: Dr. Gerald Morrison		
Objective: To provide the best method to measure ESP impeller erosion		
Run Hr:	Filled by:	Date:

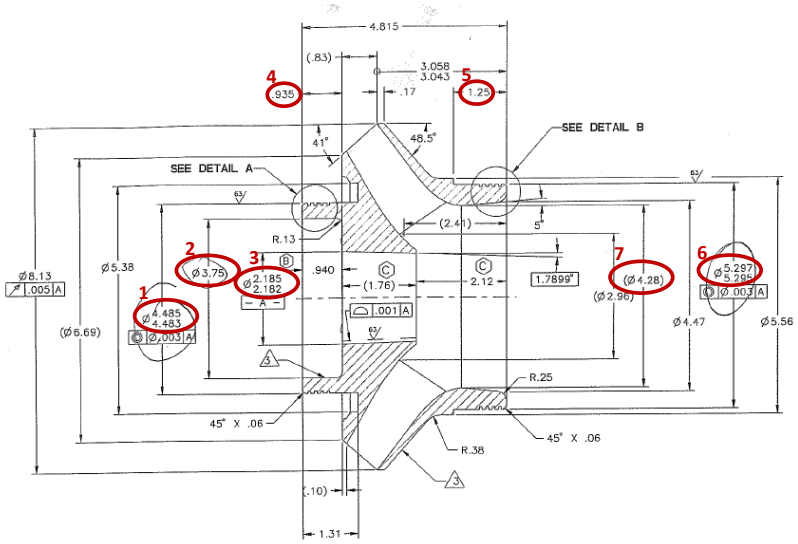

Figure 3.6 Impeller, dimensions as measured are presented in Table 3.2.

Table 3.2 Impeller dimensions, locations are found in Figure 3.6.

(21) IMPELLERS			
Location	Impeller 1	Impeller 2	Impeller 3
1	4.485	4.485	4.486
2	3.752	3.735	3.745
3	4.354	4.34	4.347
4	5.305	5.3	5.3
5	1.248	1.245	1.247
Weight (lbs)	13.55	13.35	13.55

(24) DIFFUSERS			
Location	Diffuser 1	Diffuser 2	Diffuser 3
1			
2			
3			
4			
5			
6			
7			
8			
9			
10			
Weight (lbs)			

Test Cell no.:	Project: Shell ESP Erosion Study	
Author: Ramy Saleh	Page 01 of 01 **Measurement / Job Aid** **Title: Diffuser Measurement**	
Approved by: Dr. Gerald Morrison		
Objective: To provide the best method to measure ESP diffuser erosion		
Run Hr:	Filled by:	Date:

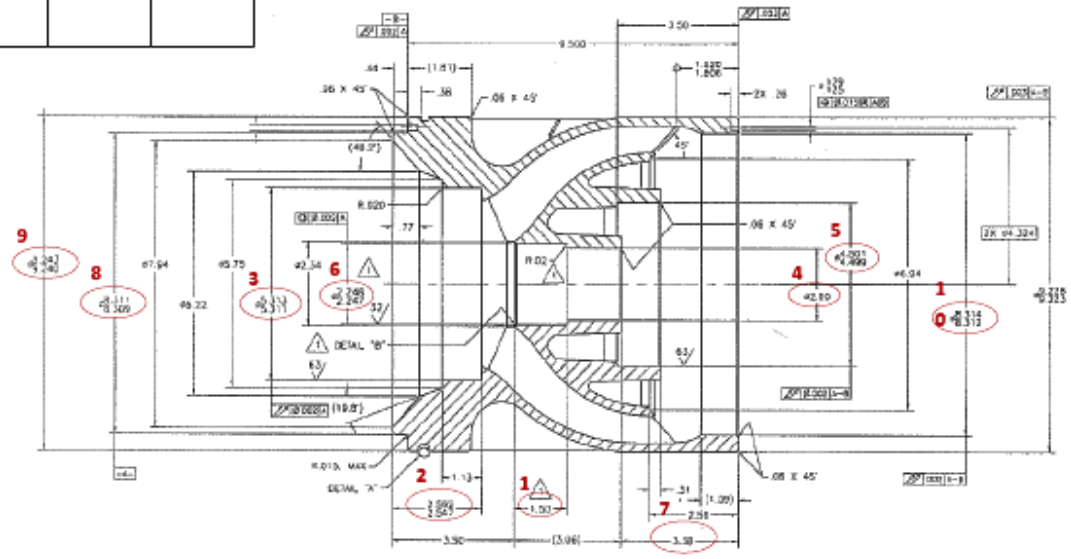

Figure 3.7 Diffuser, dimensions as measured are presented in Table 3.3.

Table 3.3 Diffuser dimensions, locations can be found in Figure 3.7.

(24) DIFFUSERS			
Location	Diffuser 1	Diffuser 2	Diffuser 3
1	1.43	1.43	1.43
2	2.562	2.547	2.555
3	5.313	5.311	5.312
4	2	2	2.000
5	4.501	4.499	4.500
6	2.25	2.25	2.250
7	3.38	3.38	3.380
8	8.314	8.312	8.313
9	9.242	9.240	9.241
10	8.31	8.312	8.313
Weight (lbs)	13.55	13.35	13.55

3.2 Motor

Due to the nature of ESP motors, their geometry and their requirement to be product cooled, it is impossible to install one inside the test cell; instead, the ESP under study will be powered by a regular (non-submersible) 250 HP induction motor. A VFD (VFD1) will control the motor's speed. The brake horsepower to the pump will be estimated using the power output from the VFD (electrical power) and multiplying it by its efficiency on the curve given by the motor manufacturer. The position of the motor on the curve can be found using the slip, the slip on an asynchronous motor is defined by:

$$s = \frac{n_s - n_r}{n_s} * 100\% \qquad 3.1$$

Where n_s is the synchronous speed (the speed of the magnetic field), which is usually 60 Hz in the United States, and n_r is the rotor speed which can measured very accurately using the proximity probes and the phasor in the impeller (Section 4.5). With the value of slip, the position on the curve can be used to determine the % Full Load Output of the motor, and consequently, the efficiency of the motor.

% OF RATED OUTPUT	125%	115%	100%	75%	50%	25%	0%
OUTPUT (HOIRSEPOWER)	312.5	287.5	250	187.5	125	62.5	0
CURRENT (AMPS)	351.2	317.8	271.0	199.5	136.7	81.6	48.1
POWER FACTOR (%)	85.4%	86.8%	88.4%	89.6%	87.9%	77.0%	13.3%
EFFICIENCY (%)	93.4%	93.6%	93.7%	93.4%	91.8%	86.1%	0.0
SPEED (RPM)	3568	3571	3576	3584	3589	3595	3600
SLIP (PER UNIT)	0.0090	0.0079	0.0065	0.0046	0.0029	0.0015	0.0001

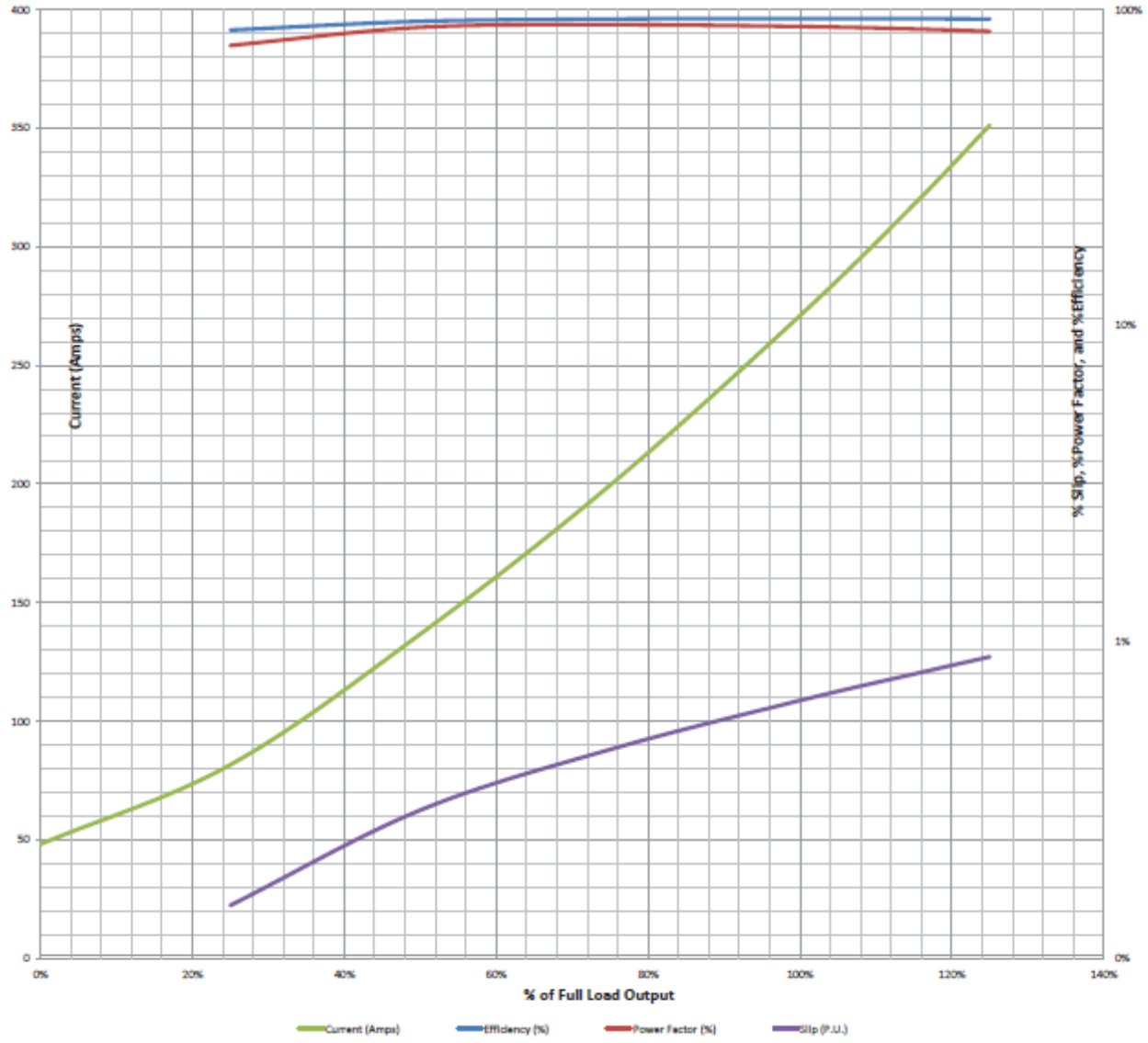

Figure 3.8 Motor efficiency curves, efficiency and slip are shown in a logarithmic scale on the left y axis.

3.3 Pinch Valve

An automatically controlled pinch valve (Figure 3.9) and a choke will be used to control the exit pressure of the ESP. The Larox pinch valve consists of a 4 inch flexible rubber hose pinched between two bars that can control the cross sectional area of the valve. Closing the valve will create a restriction that will raise the pressure at the exit of the ESP, simulating the pressure on the exit of down-hole ESPs due to the weight of the fluid and losses. A pinch valve was chosen because of the simplicity and low-cost of changing the rubber hose if and when the sand erodes it.

To guard against cavitation inside the valve, a choke will be placed after the pinch valve; the choke consists of a simple plate with a smaller diameter orifice, placed in between two flanges located a moderate distance after the pinch valve (to avoid turbulence from either equipment affecting the other). This choke will undertake the majority of the pressure drop, while the pinch valve will be used to fine-tune the exit pressure to the desired amount. The reduced pressure drop undergone inside the pinch valve, due to the presence of the choke plate will help avoid cavitation inside the valve.

The pinch valve is controlled by a 4-20 mA signal from the computer, and powered by compressed air. If the signal for the computer is lost (0 mA) the valve will shut itself (fail close) as a safety mechanism.

Figure 3.9 Larox Pinch Valve

3.4 Auxiliary Pumps

The auxiliary pumps are two centrifugal pumps installed in parallel connected to the inlet of the ESP. The auxiliary pumps are used for two purposes:

- Ensure there is enough pressure at the inlet of the ESP to avoid cavitation.
- Concentrate the mixture of sand and water in a slipstream in order to be able to measure the amount of sand accurately.

The feed pump is controlled by a VFD (VFD2) to regulate the flow-rate or inlet pressure of the ESP. This pump is a 75 HP centrifugal pump whose primary purpose is to provide the necessary pressure (NPSHR) at the inlet of the ESP to avoid cavitation. The feed pump's outlet has an orifice flow meter (OFM) connected in series before joining the slurry pump (P2) in a tee at the inlet of the ESP. The feed pump will provide the ESP with approximately 97% of the flow rate, while the slurry pump will provide the remaining 3%.

The slurry pump carries the mixture of sand and water with a concentration of sand between 20-30% by weight. This pump, a pump identical to the feed pump except smaller (20 HP), will be fed by clean water from the same tank as the feed pump; the inlet between the pump and tank has a stand pipe where the sand auger drops the sand into the stream at controlled rates. The flow rate in the slurry pump will be about 25 times smaller than the flow rate of the feed pump but it will receive all of the sand being run through the ESP; this means that the concentration of sand at the slurry pump line is

about 25 times the concentration of sand in the mixture flowing through the ESP, this allows for higher accuracy when measuring the amount of sand. The mixture discharged by the slurry pump passes through the Coriolis flow meter (CFM) to detect density and flow rate, before joining the larger stream of water discharged by the feed pump, where the mixture is diluted to approximately .2% (2,000 ppm).

3.5 Screw Conveyor

The screw conveyor (SSC) or sand auger consists of a spiral auger inside a tube connected to the bottom of a hopper full of sand on one side and a gear motor controlled by a VFD on the other end (Figure 3.10). The hopper has a static blade on top to pierce the bag of sand and allow the sand to fall into the hopper. The VFD speed will be controlled by a PID controller, which uses the measured concentration value and adjusts the speed accordingly, maintaining the concentration at the required value. The amount or concentration of sand will be measured and recorded using a Coriolis flow meter as detailed in section 4.2. Running the screw conveyor without material in it would eliminate all damping on the system and will lead to its damage.

Figure 3.10 Screw Conveyor

The sand exiting the screw conveyor is dropped into a standpipe at the suction side of the slurry pump. The first design used, shown in Figure 3.11, consisted of a 3" PVC pipe connected through a tee to the hose going from the tank to the inlet of the slurry. This design however was unsuccessful as it plugged with sand after running for a short amount of time. The design was replaced by a 6" PVC pipe connected to the suction hose of the pump through a vertical wye as shown in Figure 3.12.

Figure 3.11 First design of auger standpipe, sand is dropped from the top, the tee is connected to the suction of the slurry pump.

Figure 3.12 Improved design on the auger standpipe, the wye and bigger pipe prevent plugging.

3.6 Separators

The separating system consists of 20 hydro-cyclones of 4" diameter and a capacity of 65 gpm each, mounted on top of a screen shaker. The whole system is mounted on top of the tank, and connected to the discharge of the ESP. The hydro-cyclones (Figure 3.13) are cones that use centrifugal force to separate the sand from the water. Sand, being heavier than water, is pushed towards the walls of the cones by the centrifugal force, this makes it slow down and fall, while the clean water flushes out of the top of the cone. The wet sand coming out of the bottom of the cones falls onto a screen shaker (Figure 3.14) where the water in the sand is drained and returned to the tank. The sand is then collected on a permeable bag to be analyzed, and reused or discarded properly.

Figure 3.13 Hydrocyclone Separators

Figure 3.14 Screen shaker.

Each cone is designed for a flow rate of 65 gpm, and each individual cone is equipped with a valve, this valve can be used to control the amount of separators in use according to the flow rate. To calculate the number of separators that should be open the simple formula $N = Q/65$, can be used, where N is the number of separators open and should be rounded to the next integer and Q is the flow rate. The pressure on the inlet of the separators is also a good clue of proficient operation. A pressure of 25 psi is an indication that the correct number of valves are open, if the pressure is lower than 25 psi, then the valves should be closed starting from the upstream valves first until a pressure of 25 psi is reached.

3.7 Seal

The mechanical seal, is an apparatus designed to keep the water from leaking through the shaft. The seal in use is a John Crane and its drawing can be found in the Appendix B; it requires a flow of clean water of about 3 GPM for cooling and lubrication, known as the seal flush. The seal uses two different seal flush setups, known in the industry as flush plans. A plan 32 uses water injected from an external source, in this case a piston pump shown in Figure 3.15 fed by tap water (to make up the water lost in the sand separation). A plan 13 is also used to inject the exit of the seal flush out of the seal back into the inlet of the ESP. To ensure the pressure in the seal housing is higher than in the exit of the pump and therefore prevent the contamination of the seal with sand particles, the plan 13 is only opened to vent the gases out of the seal and will be closed during normal operation of the pump.

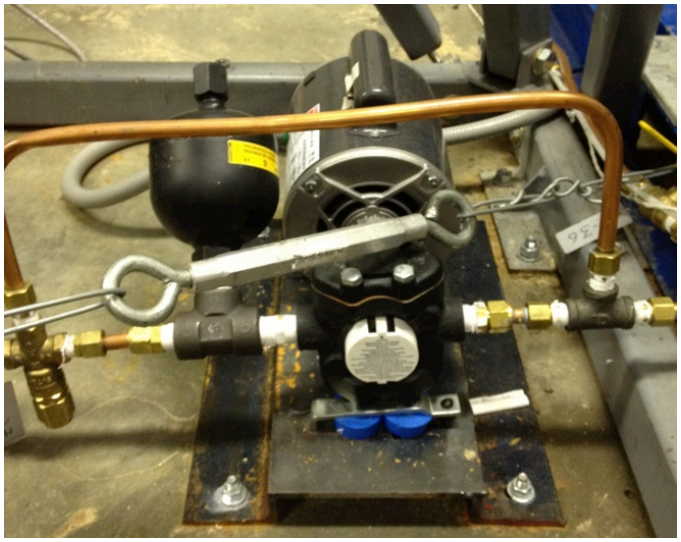

Figure 3.15 Seal flush pump.

3.8 Cooling Loop

The cooling loop, shown in the P&ID in Appendix A consists of a simple 100 GPM centrifugal pump connected to a heat exchanger. The loop has several drain valves that should be opened if freezing temperatures are expected, to prevent damage to the heat exchanger coils.

3.9 Sand

The sand to be used as the abrasive agent for the initial testing will be 100 mesh frac sand. The sand is delivered in 1.5 ton bags Figure 3.16, each bag will be tagged with an identification number for analysis and tracking purposes. The bags will be picked up by a forklift and placed on top of the screw conveyor's hopper (Figure 3.10) where a static blade will pierce through it, allowing the sand to drop in the hopper.

Figure 3.16 Sand bag with its identification number (red tag).

Two types of analysis are to be performed periodically on the sand: a sieve analysis to determine the mass distribution of sand according to size, and a microscope analysis to determine the angularity of the sand. Both tests should be performed periodically before and after running it through the pump.

The sieve analysis consists of placing a weighed sample of sand on the top of a series of sieves with different sized mesh placed on top of each other, where each subsequent screen is smaller than the next, with the top sieve having the largest mesh and the bottom sieve being a pan to collect the smallest particles (Figure 3.17). The sieves are then put on a shaker to ensure the particles fall on the correct sieve. After the shaking is complete, the material in each sieve is weighed and expressed as a percentage retained of

each mesh size. Table 3.4 shows the standard mesh sizes and its diameter equivalents in mils and micrometers.

Figure 3.17 Sieves and shaker.

Table 3.4 Sand mesh size conversion chart.

U.S. MESH	Thousands of an inch	Microns	U.S. MESH	Thousands of an inch	Microns
3	265	6730	40	16.5	400
4	187	4760	45	13.8	354
5	157	4000	50	11.7	297
6	132	3360	60	9.8	250
7	111	2830	70	8.3	210
8	93.7	2380	80	7	177
10	78.7	2000	100	5.9	149
12	66.1	1680	120	4.9	125
14	55.5	1410	140	4.1	105
16	46.9	1190	170	3.5	88
18	39.4	1000	200	2.9	74
20	33.1	841	230	2.4	63
25	28	707	270	2.1	53
30	23.2	595	325	1.7	44
35	19.7	500	400	1.5	37

The microscope analysis consists of measuring the sand particles using software that counts the pixels where the number of pixels has been calibrated to a known length. The measurement with the microscope will be used to corroborate the sieve results (and vice-versa) and to find the eccentricity of the sand. The eccentricity of the sand will be a ratio of the shortest distance to the longest distance given by the equation $\epsilon = \sqrt{1 - \frac{b^2}{a^2}}$, where ϵ is the eccentricity, always less than 1, a is half the longest distance between two opposite points and b is half the shortest distance between two opposite points in the particle and perpendicular to a, as shown Figure 3.18. An eccentricity of 0 would describe a circle, and an eccentricity of 1 would describe a line.

The microscope analysis will be performed on each sample collected from the sieves where the average eccentricity and standard deviation for each mesh size will be

tabulated. A decreasing eccentricity value for a given mesh size will indicate that the sand is being crushed and thus is probably abrading the pump. A strong statistical correlation between decreased eccentricity and pump degradation or clearance growth could isolate the most destructive mesh sizes for the pump.

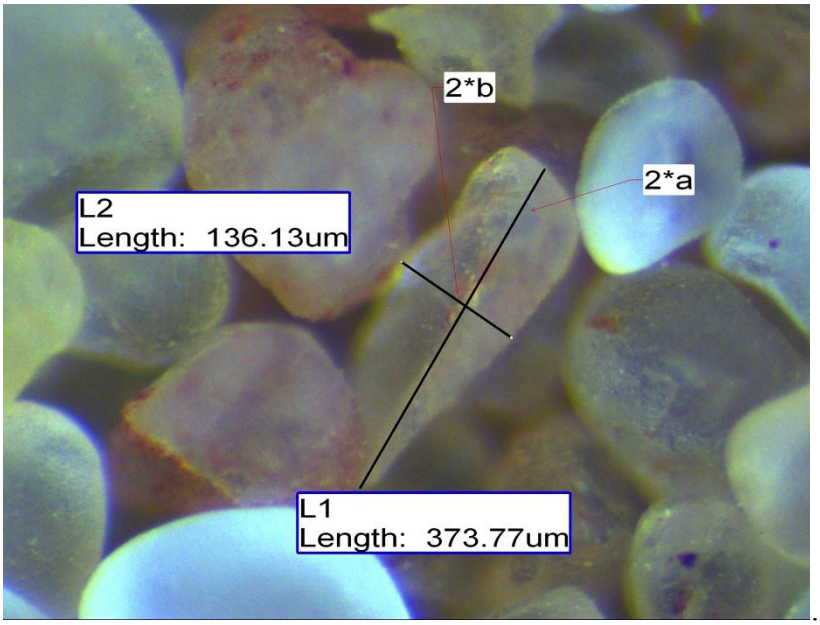

Figure 3.18 Sample of sand and its respective a and b measurements taken to calculate eccentricity.

4. INSTRUMENTATION

The P&ID is found in Appendix A, Table 4.1 shows the instrument nomenclature along with their description and manufacturer. Unless specified, specific instruments will be referred by their item number throughout this work.

Table 4.1 Instrument list.

Instrument List		
Item No.	**Description**	**Manufacturer**
A1	Accelerometer Inlet X	PCB
A2	Accelerometer Inlet Y	PCB
A3	Accelerometer Inlet Z	PCB
A4	Accelerometer Outlet X	PCB
A5	Accelerometer Outlet Y	PCB
A6	Accelerometer Outlet Z	PCB
PP1	Proximity Probe Shaft 1 X	Bently Nevada
PP2	Proximity Probe Shaft 1 Y	Bently Nevada
PP3	Proximity Probe Impeller 1 X	Bently Nevada
PP4	Proximity Probe Impeller 1 Y	Bently Nevada
PP5	Proximity Probe Shaft 2 X	Bently Nevada
PP6	Proximity Probe Shaft 2 Y	Bently Nevada
PP7	Proximity Probe Impeller 2 X	Bently Nevada
PP8	Proximity Probe Impeller 2 Y	Bently Nevada
PP9	Proximity Probe Shaft 3 X	Bently Nevada
PP10	Proximity Probe Shaft 3 Y	Bently Nevada
PP11	Proximity Probe Coupling X	Bently Nevada
PP12	Proximity Probe Coupling Y	Bently Nevada
PP13	Proximity Probe Coupling Z	Bently Nevada
OFM	Orifice Flow Meter	Lambda Square
CFM	Coriolis Density Meter	Emerson
LS1	Tank Level Sensor L	

Table 4.1 Continued.

Item No.	Description	Manufacturer
LS2	Tank Level Sensor M	
LS3	Tank Level Sensor H	
LS4	Sand Level Sensor M	IFM
LS5	Sand Level Sensor L	IFM
PT1	Pressure Transducer Inlet ESP	Omega
PT2	Pressure Transducer Outlet ESP	Omega
PT3	Pressure Transducer Outlet Choke	Omega
PT4	Pressure Transducer	Omega
PT5	Pressure Transducer	Omega
PT6	Pressure Transducer	Omega
PT10	Differential Pressure OFM (FM1)	Rosemount
SG1	Axial Strain Gauge	Binsfield
SG2	Radial Strain Gauge	Binsfield
TT1	ESP Inlet Temperature	Omega
VFD1	ESP VFD	Yaskawa
VFD2	Main Pump VFD	Toshiba
VFD3	Slurry Pump VFD	Toshiba
VFD4	Sand Handling VFD	Altivar

4.1 Orifice Flow Meter

The orifice flow meter (OFM), shown in Figure 4.1, is placed at the exit of the feed pump before the mixing tee (where both auxiliary pumps flows join before the inlet of the ESP), as shown in Figure 4.2. The OFM consists of a plate with a hole that creates a pressure drop that is proportional to the velocity, and therefore, volumetric flow rate of the fluid. The pressure drop is measured by using a differential pressure transmitter

calibrated experimentally (Section 4.3). Equation 4.4 shows the relationship used to calculate the volume flow rate using the obtained values of differential pressure.

$$Q_{FP} = 44.748 * d^2 * K * \sqrt{\Delta P_{OFM} / \rho_w} \quad 4.1$$

Where d is the bore in inches, K is the flow coefficient calculated using equation 4.2, ΔP_{OFM} is the differential pressure (in inches of water) as measured by the differential pressure transmitter and converted using the calibration on Appendix C and ρ_w is the density of water at the given temperature.

$$K = C * \frac{1}{\sqrt{1 - \beta^4}} \quad 4.2$$

C is the discharge coefficient found using equation 4.24.3 and β is the beta ratio, the ratio of the orifice diameter to the inside diameter of the pipe.

$$C = .5959 + .0312\beta^{2.1} - .1840\beta^8 + 91.71\beta^{2.5} \quad 4.3$$

The values in use with the current OFM setup are listed in Table 4.2.

Table 4.2 Parameters for the orifice flow meter in use.

Parameter	Value	Units
d	4.245	inches
K	.7813	dimensionless
ρ_w	f(T)	lb/ft^3
C	.6510	dimensionless
β	.7435	dimensionless

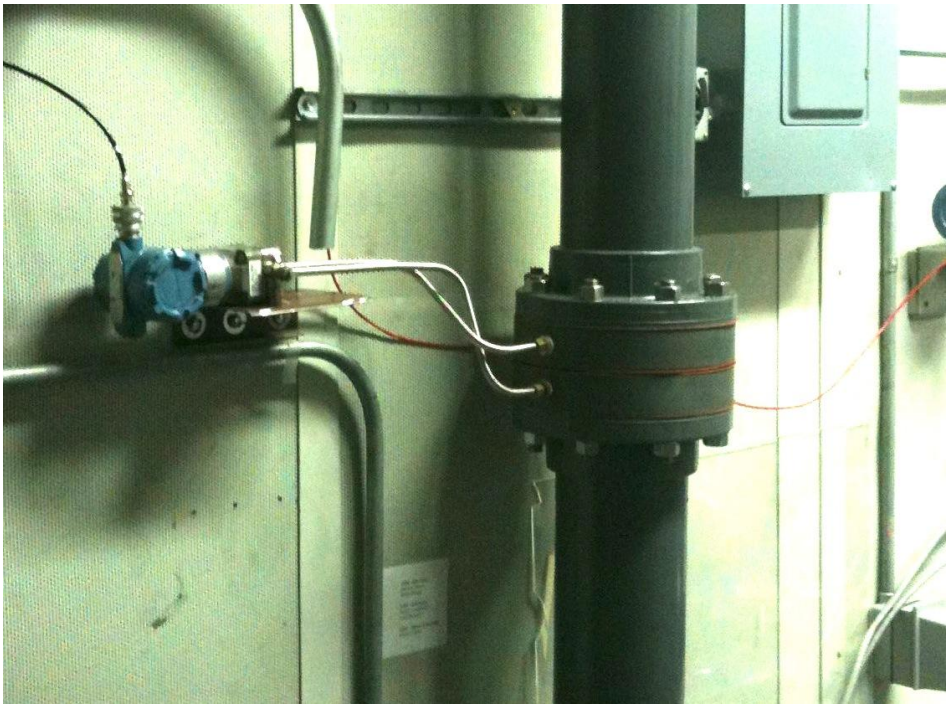

Figure 4.1 Orifice Flow Meter.

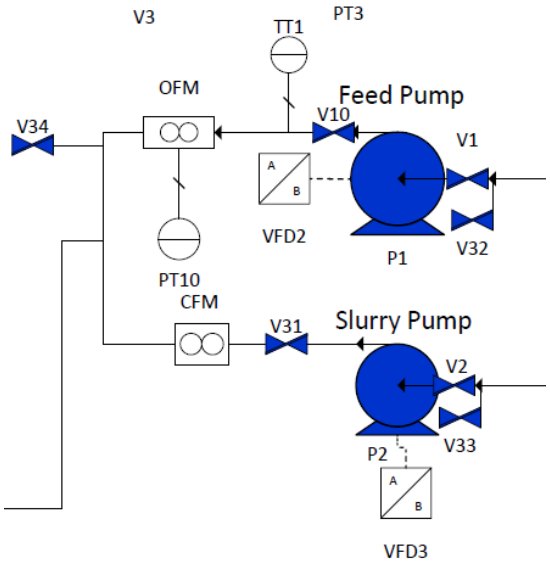

Figure 4.2 P&ID close up of auxiliary pumps and flow meters.

4.2 Coriolis Flow Meter

The Coriolis flow meter (CFM), shown in Figure 4.3, will return values of measured density and mass flow rate for the slurry pump (mixture). The CFM is placed at the exit of the slurry pump, before the mixing tee and in parallel with the OFM, as shown in Figure 4.2. The calibration curve for density was prepared using factory provided software and can be found in Appendix C.

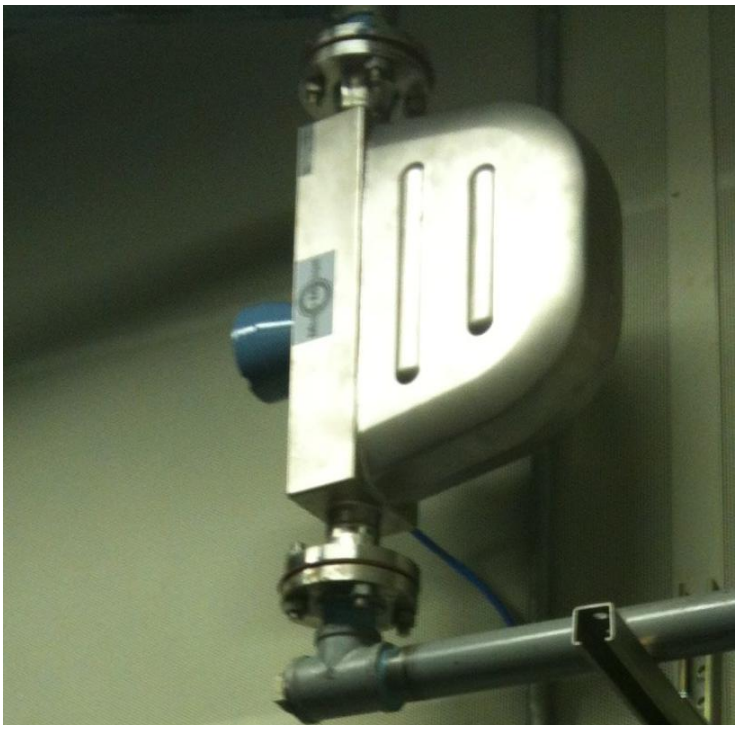

Figure 4.3 Coriolis Flow Meter.

The CFM will output mass flow rate and density of the slurry pump; with these two values we can also calculate the volume flow rate in the slurry pump to know the total

flow rate in the ESP. The volume flow rate and mass flow rate of the mix ($\dot{m}_m$) are related by the equation:

$$Q\ (gpm) = .2641 \frac{\dot{m}_m \left({}^{kg}/_{min} \right)}{\rho_{\ m} \left({}^{kg}/_{\text{liter}} \right)} \qquad 4.4$$

The mass flow rate of the mix refers to the total mass flow rate in the slurry pump (sand and water combined) and is the mass flow rate output by the CFM. The mass flow rate of the mix and density can also be used to determine the concentration of sand in the mixture. First, the mass flow rate of sand $\left(\frac{kg}{min}\right)$ can be found using the following equation:

$$\dot{m}_s = \frac{\dot{m}_m - \frac{m_m}{\rho_m}\rho_w}{(1 - \frac{\rho_w}{\rho_s})} \qquad 4.5$$

Where $\dot{m}_s$ is the mass flow rate of sand $\left(\frac{kg}{min}\right)$, ρ_s is the density of the sand as tested in the laboratory (Section 5.3) divided by the density of water at the given temperature, and ρ_m and ρ_w are the densities of the mixture (as measured by the CFM) and of water in $\frac{kg}{lit}$, respectively.

The concentration of sand $\left(\frac{grams}{liter}\right)$, passing through the ESP can be found with equation 4.6:

$$C = 1000\frac{\dot{m}_s}{3.785Q_{FP} + \frac{(\dot{m}_m - \dot{m}_s)}{\rho_w}} \qquad 4.6$$

C denotes the concentration of sand $\left(\frac{grams}{liter}\right)$, found by inserting the value for mass flow rate found with the CFM in equation 4.4 and Q_{FP} is the volume flow rate (gpm) of the feed pump as measured by the OFM using equations 4.1 to 4.3. For details on the development of equations 4.5 and 4.6, refer to Appendix D.

4.3 Pressure Transducers

Three pressure transducers will be used to monitor the pump and to generate performance curves. The difference between pressures of the transducers at the inlet and outlet of the ESP will be used to calculate the head of the pump. The head per stage can be determined by dividing the total head developed by the pump by the number of stages (3). Table 4.3 shows the description of each pressure transducer and the item number used in the P&ID. Each pressure transducer was calibrated in the laboratory using a dead weight tester. Individual calibration curves are found in Appendix C.

Table 4.3 Pressure transducers.

Item No.	Description
PT1	Pressure Transducer Outlet ESP
PT2	Pressure Transducer Seal Housing
PT3	Pressure Transducer Inlet ESP

4.4 Thermocouple

One thermocouple (TT1 in Figure 4.2) will be placed at the inlet of the ESP before the mixing tee. The thermocouple will be used to monitor the temperature of the water to protect the equipment and to estimate more accurate values of water density. The thermocouples are factory calibrated and the Labview software does the conversion automatically (see Section 4.10 for information on the Labview software).

4.5 Proximity Probes

To measure vibration, rotational speed and monitor pump movement, 13 proximity probes will be used. Proximity probes are a highly accurate instrument capable of measuring very small deviations in distance. A typical proximity probe will have a scale factor of around -200 $^{mV}/_{mil}$, and their linear range will start at around 10 mils from the target (3 V). It is important to note these studies are not interested in the total distance but in the displacement, thus the probes were not calibrated for distance. Table 4.4 lists the proximity probes used and their designated item number on the P&ID.

The proximity probe hardware consists of the probe, an extension cable and a proximitor. It is extremely important that the right combination of these be used to maintain the factory calibration, a certain model proximitor can only accept a specific model of probe and a specific total length (length of the probe cable and extension combined). The proximitors in use in these studies accept the 3300 XL 5 or 8 mm probes with a total length of 5 meters.

Table 4.4 Proximity probe item number and position.

Item No.	Description
PP1	Proximity Probe Shaft 1 X
PP2	Proximity Probe Shaft 1 Y
PP3	Proximity Probe Impeller 1 X
PP4	Proximity Probe Impeller 1 Y
PP5	Proximity Probe Shaft 2 X
PP6	Proximity Probe Shaft 2 Y
PP7	Proximity Probe Impeller 2 X
PP8	Proximity Probe Impeller 2 Y
PP9	Proximity Probe Shaft 3 X
PP10	Proximity Probe Shaft 3 Y
PP11	Proximity Probe Coupling X
PP12	Proximity Probe Coupling Y
PP13	Proximity Probe Coupling Z

The proximity probes have an output range of 0 to -17 V, since the DAQ system in use can only detect up to -10 V, the probe is installed at a distance where the output reading is 6.5 V. This ensures that the probe is in the middle of the range and can detect a displacement of up to approximately 17.5 mil in each direction.

4.6 Accelerometers

Two accelerometers will be placed on the casing of the pump; one will be placed near the inlet and the other near the exit. Each accelerometer can detect acceleration in three directions, these accelerometers will be used to monitor vibration and compare with the data acquired with the proximity probes. The accelerometers have a factory-calibrated output of 500 $^{mV}/_{g}$.

The accelerometer hardware consists of three piezoelectric elements, inside a small casing (Figure 4.4), that generate a voltage when deformed. Each element is placed ninety degrees from each other, thus giving acceleration in three dimensions (X, Y and Z). The accelerometer is connected to a conditioner with a factory provided cable. The conditioner is the device that provides power to the accelerometer and amplifies the voltage received from the accelerometer into a voltage compatible with the A/D converter (Section 4.9).

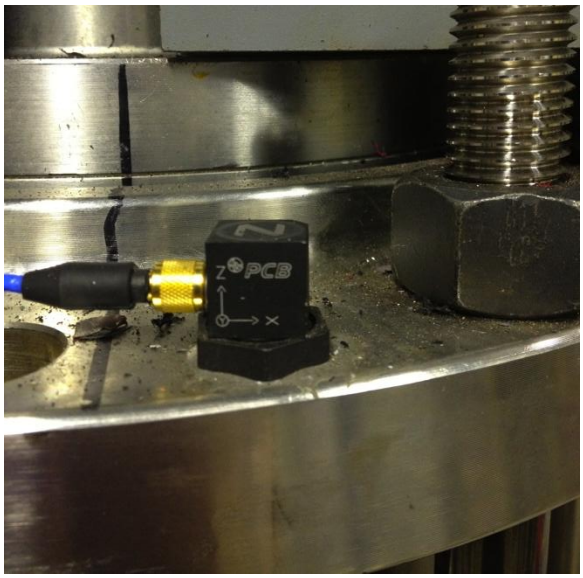

Figure 4.4 PCB Piezoelectric Tri-Axial accelerometer placed near the casing of the ESP.

4.7 Strain Gages

Two strain gages will be placed in the coupling shown in Figure 4.5; this coupling is hollow and was designed to deform enough, under the expected loads, to be detected by the strain gages.

The strain gages in use are Binsfield model BH10K, these strain gages are epoxied to the coupling; they are then connected to a wireless transmitter box and a battery pack (Figure 4.6), these transmitters and battery pack rotate with the shaft and send the information to the antenna which is connected to a receiver also connected to the A/D converter.

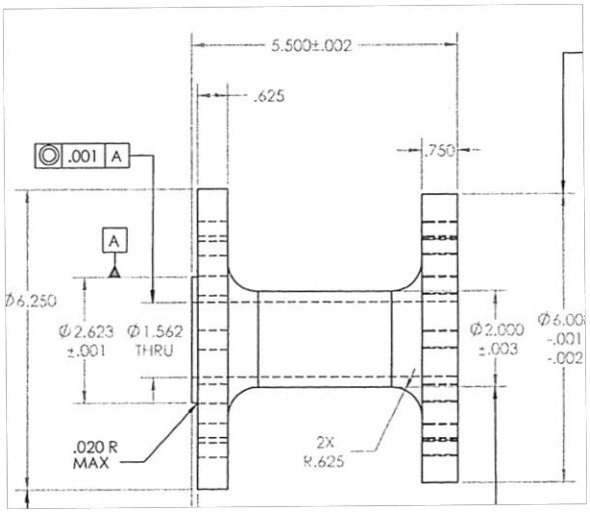

Figure 4.5 Coupling between ESP and motor used to carry strain gages to measure torque and thrust.

One strain gage (SG1) was positioned to detect axial strain and will be used to measure thrust, similarly another strain gage (SG2) is placed in the radial direction to detect torque, both calibration curves can be found in Appendix C.

Figure 4.6 Binsfield strain gage battery pack (left) and transmitter (right).

4.8 Level Sensors

To protect equipment and for monitoring purposes, level switches will be used as alarms for water level inside the tank and sand level inside the hopper. These switches are basic on/off switches that will turn on an alarm that signals when an undesired level has been reached or turn the equipment off when the hopper or tank is empty.

Five level switches are used for the experiment, two sand sensors and three water level sensors. The wiring diagram of the switches is found in the Instrumentation Wiring Diagrams in Appendix E. Both the water and the sand level are being fed by a power supply inside the test cell, the returning line from the sensors is connected to two resistances in series, the bigger resistance is to take the majority of the 18 V voltage drop, the remaining resistance is small enough that it can create a voltage drop large

enough to be read by the data acquisition device, where it is read as a Boolean (T/F) signal.

The water level sensors consist of a magnetic float, which can be switched between normally open (N/O) and normally closed (N/C) by turning the float over. Normally open means that the switch is at its open state when not triggered, normally close is at its closed state when not triggered; when the water or sand level rises above the switch's level, the switch is triggered and changes its position. Similarly the sand level sensor consists of a capacitor switch that changes its position when it detects material in close proximity, the sand switches can be changed from N/O to N/C by cutting a wire inside the instrument. The N/O or N/C position for each switch was chosen for convenience.

The high water (N/O) and medium water (N/O) level sensors will turn on a visible alarm in the Labview program and will turn on a light inside the test cell. The low water (N/O) level sensor will sound an alarm and shutdown the auxiliary pumps when triggered.

The medium level (N/O) sensor of the sand will turn on a visible alarm in the Labview program which indicates the operator that it is time to change the bag. The low level (N/C) sand auger will turn off the sand auger to prevent its damage.

4.9 Data Acquisition Hardware

The hardware used for control signal output and data acquisition for all instruments that do not require a high frequency response and/or simultaneous measurements is a National Instrument cRIO chassis with multiple modules. The 9205 module is a voltage-reading module able to read up to 32 single-ended channels, 16 differential input channels or a combination of both. Two 9265 modules with 4 output channels each are used for signal outputs for the VFDs and pinch valve and a 9213 is used for temperature. A detailed description of the connections inside the box and wiring can be found in the Instrumentation Wiring Diagrams in Appendix E.

To connect to the instruments, a special box was prepared with RS235 connectors for easy removal and modification. The box contains plugs for the instruments' cables where each instrument is connected, depending on the requirements of the instrument, to a power supply, 470 ohm resistance (to convert from 4-20 mA signal to the 0-10 V signal compatible with the A/D converter) and/or tied directly to another plug which connects to the A/D converter (if the instrument has its own power supply and a 0-10 V output). The RS235 connector coming out of the box and going to the instruments is connected using multi-pair, multi-shield cable to minimize noise from the equipment in the test cell.

For the instruments that require high frequency responses and/or simultaneous measurements such as the proximity probes and accelerometers a Measurement Computing USB 1616FS and USB 1208FS are used. These instruments both have

simultaneous sampling methods. The ten internal proximity probes, PP1-PP10, (Section 4.5) and the six accelerometers (Section 4.6) are connected to the USB1616FS, this allows for a high sample rate and simultaneous measurement necessary for making comparisons between instruments.

4.10 Data Acquisition Software

The software used to perform all the data measurements and controls is National Instruments Labview. Two different programs are used, one is used to control the equipment and collect the data from all the instruments connected to the cRio (Figure 4.7), the other is used to collect the data from the proximity probes and accelerometers (Figure 4.8).

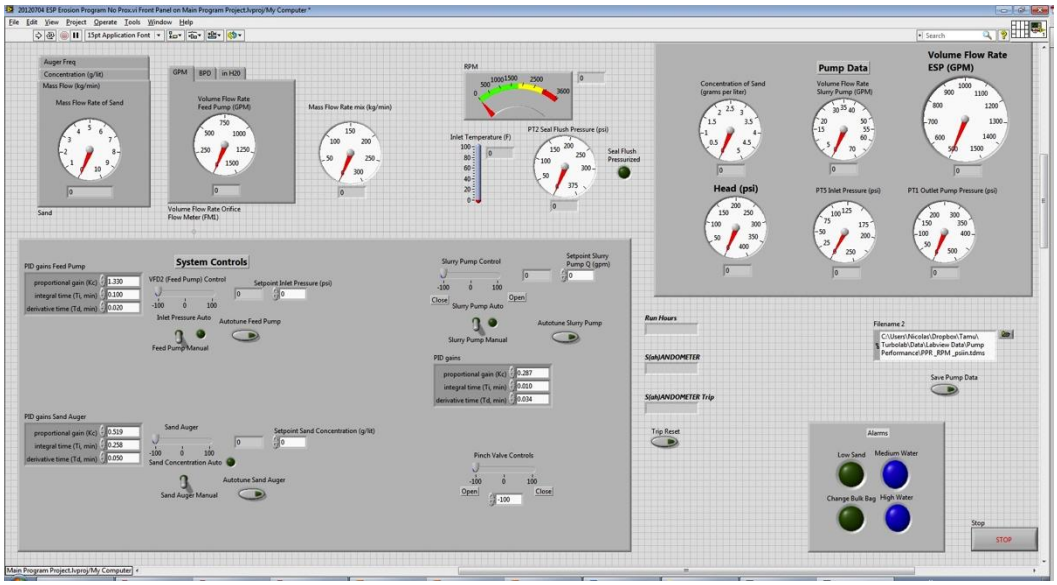

Figure 4.7 Labview monitoring and controls screenshot.

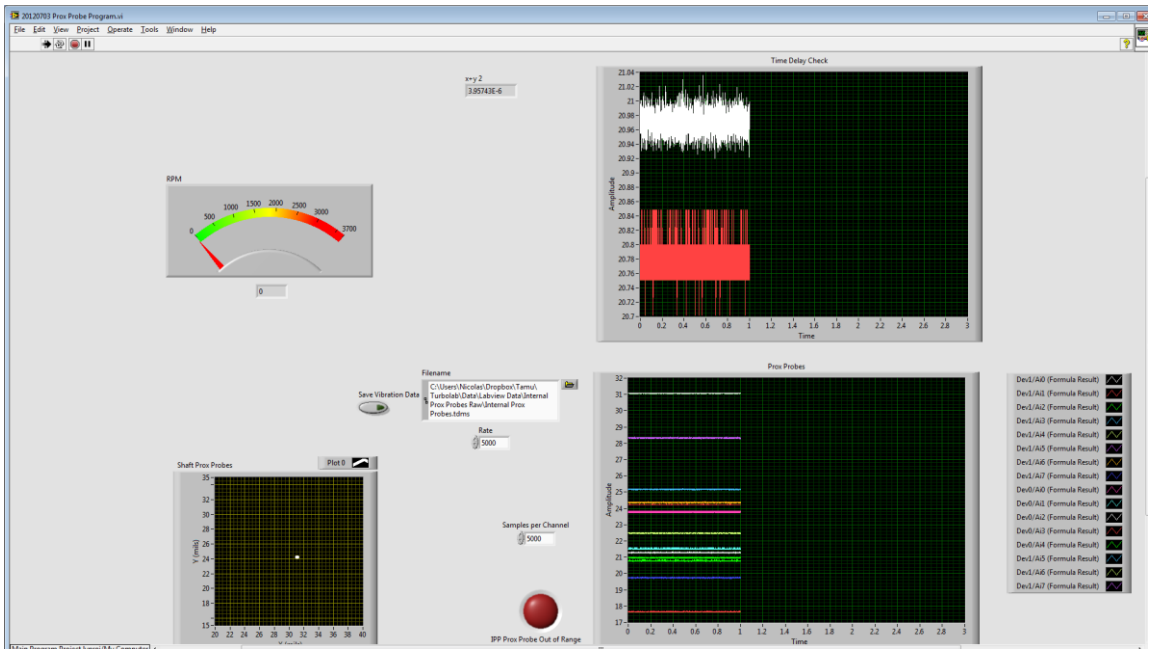

Figure 4.8 Labview vibration data monitoring screenshot.

The Labview Monitoring and Control program receives the signal from all the pressure transducers, CFM, level switches, and such, and converts it into useful data and sends signals to the VFDs and pinch valve to control them. In the case of the level switches, the program reads the voltage and compares it to a set threshold where it is converted into a Boolean signal (true or false) which turns on an alarm and/or shuts off equipment when triggered as shown in Section 4.8; the rest of the instruments' input signals, except for the thermocouple's (the thermocouple's signal is read and converted automatically into temperature by the software) are read as a value between 0 and 10 volts, this value is then transformed into usable data via the formulas obtained by the instrument manufacturer or by calibration in the laboratory (Appendix C). Another purpose of the Monitoring and Control program is to output signals that control equipment such as the pinch valve and VFDs. All equipment controlled by the computer is governed using a

signal of 4-20 mA. These signals can be controlled manually via a slider switch or automatically via a (Proportional Integral Derivative) PID controller.

The PID reads a signal and compares it to a set-point specified by the operator to obtain the error and adjusts the output signal (such as the speed of the VFD or pinch valve position) to correct it; the result is a real time feedback loop that if tuned properly will keep the desired variable within acceptable limits. Three different PID controllers are used in this program: one each for the feed pump, slurry pump and sand auger.

There are a number of variables used to manipulate the PID:

- The process variable is the variable to be controlled (pressure, sand concentration, etc.)
- The set-point is the value desired for the process variable.
- The gains are values that control the response of the controller to changes in the process variable or set-point.

The gains used in this program were found using the Labview auto-tuning process in combination with trial and error. Table 4.5 shows the parameters used for each PID, including gains, process variables and controller output.

Table 4.5 Gains used for each PID.

Process Variable	Controller Output	Gains	
Inlet Pressure	Feed Pump VFD	Kc	1.33
		Ti	.1
		Td	.02
Slurry Pump Flow Rate	Slurry Pump VFD	Kc	.287
		Ti	.01
		Td	.034
Sand Concentration	Sand Auger VFD	Kc	.287
		Ti	.010
		Td	.034

The Vibration Monitoring program (screenshot shown in Figure 4.8) is the program used to acquire all data from the proximity probes and accelerometers. The program shows three graphs: one is for the internal proximity probes (bottom right), another is for the accelerometers (top right) and the third one is an X-Y plot of the seal shaft probes (PP11-PP12) used to monitor the position of the shaft with respect to the seal in the Cartesian coordinate system (bottom left).

The sampling rate for the proximity probes and accelerometers can be changed by changing the value in the box labeled as Rate, the total number of samples per channel can be changed in the Samples per Channel IPP. The software will collect data for an amount of time equal to the number in the Samples per Channel box divided by the sampling rate (in seconds) before displaying the data and/or saving it, increasing the Samples box value will increase the amount of time it takes to display new data on the screen but will generate a longer sample of continuous data when saving.

The program also shows the rotational speed of the pump in RPMs. To measure the RPMs of the pump, the program uses one of the proximity probes measuring the distance to an impeller that has a notch, or phasor, cut on it. The phasor creates a sudden spike in the signal (Figure 4.9). The signal of one of these proximity probes is fed into the comparator shown in Figure 4.10, which outputs a true value when it surpasses a set trigger point, this creates a square wave and the frequency of this wave is then obtained by the software and converted into RPM. To prevent the software from reading an error when the pump is not running the frequency counter is put inside a case loop where it only runs when the amplitude (RMS minus DC) of the signal is above a certain level.

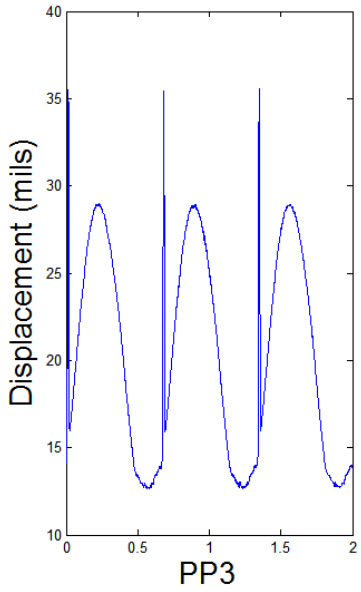

Figure 4.9 Spike read by PP3 created by the groove cut in the impeller.

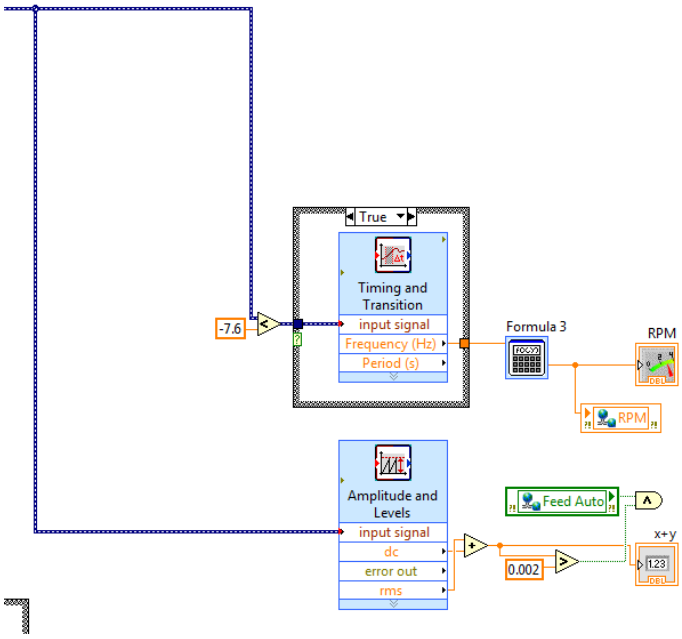

Figure 4.10 Block diagram of RPM counter. The two blue lines are the same signal coming from the proximity probe.

5. RESULTS

The results shown in this work will be strictly the baseline results to be used for comparison with the results obtained after running sand through the pump.

5.1 Pump Performance

To determine the pump curves the pump was run at the desired speed using the VFD drive. The pinch valve was then closed gradually to increase the pressure rise across the pump, saving the data on each step.

Initially, a choke with a 1 $^{13}/_{16}$" orifice was used, however, this restriction was too small and the range of flow rates achieved was around 450 to 1000 gpm, not enough to reach the BEP. The choke was then changed to a 2 ¼ ", with this choke, flow rates of up to 1300 gpm were reached but flow rates lower than 1000 gpm were unachievable. Since the pressure drop on the bigger orifice plate is smaller, the pressure drop that has to be undergone in the pinch valve to achieve the same head is larger, the hypothesis is that this large pressure drop would create suction inside the pinch valve which would close the valve shut at flow rates of about 1000 GPM, effectively dead-heading the pump. The

same phenomenon was also encountered with the smaller choke, but at much lower flow rates (450 GPM), the result being that the smaller choke would only run at the left end of the curve (low flow rates) while the bigger choke only ran at the right end of the curve.

The pump curve shown in Figure 5.1 contains data from tests with both chokes, displaying the whole range of flow rates possible. To avoid having to change chokes to perform pump curve tests in the future a different, more resilient rubber for the pinch valve would have to be used or the valve would need to be replaced for a larger valve or a different type valve. Another option is to place a gate valve to be used only when running the performance tests (which are run with no sand, eliminating concerns about erosion of the valve), this will allow for all flow rates desired to be reached by opening and closing the valve, as necessary.

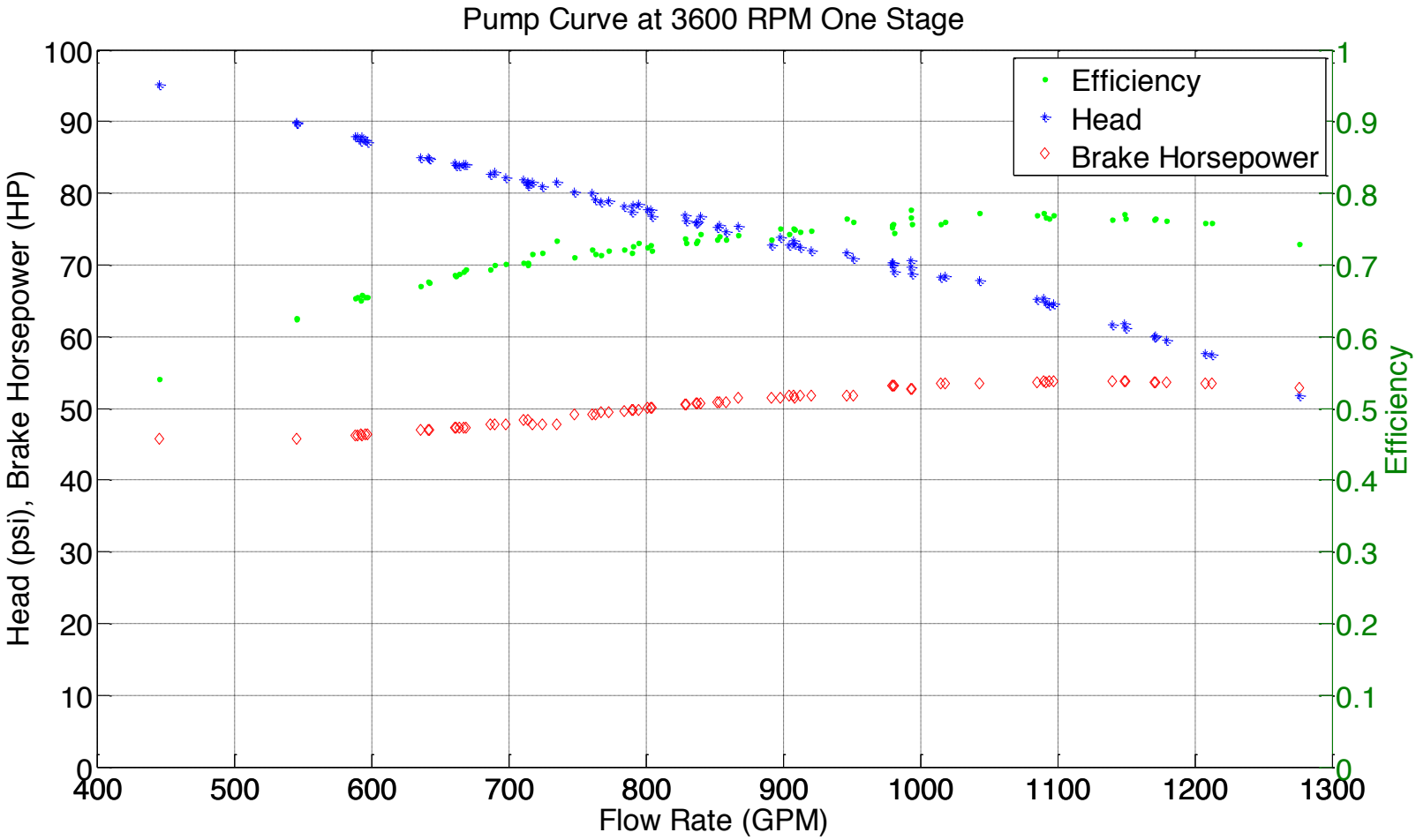

Figure 5.1 Pump curve for one stage ESP at 3600 RPM

Because of strain gages malfunction, accurate values for brake horsepower could not be measured. The brake horsepower was estimated by multiplying the efficiency times the electrical power; for simplicity, a constant value of 93.6% for the motor efficiency was used to calculate the BHP (Figure 3.8). The curve in Figure 5.1 shows the BEP to be at around 1,100 gpm (38,000 bpd), and the head rise per stage generated by the pump at this flow rate is about 65 psi (150 feet), a value 27% larger than the value in the manufacturer's catalog curve, the reason for this discrepancy is unknown. At BEP, the BHP is 55 HP per stage, a value 32% larger than the manufacturer's curve, the efficiency, at 77% is similar to the efficiency shown on the manufacturer's curve.

The left end of the curve shows that the pump is able to generate up to 95 psi (220 feet) per stage at around 450 GPM (16,000 BPD). The opposite end of the curve shows that at 50 psi (115 feet) per stage, the pump can move 1,300 GPM (45,000 BPD)

Appendix F shows a Matlab program that plots the pump curve, and compares it to the baseline data. This program can be used to compare different RPMs to the baseline 3600 RPM or to compare the pump curve of a worn out pump to the new one at 3600 RPM or a combination of both. This work will use the program to compare the pump curves at different RPM.

To create the program, the conjoined data (from the two chokes) was imported into Matlab using Program 2. The data was then plotted and fitted with a quadratic curve. The curve fit coefficients were then saved in the program. After removing values with high standard deviations, the data under study is then plotted in the same figure as the baseline curve; the values for mean percent change and maximum percent change between the two data sets (with respect to baseline) are then displayed.

Figure 5.2 shows the baseline curve at 3600 RPM with its curve fits superimposed, Table 5.1 shows the mean percent change and maximum difference of head, power and efficiency, since this plot compares the baseline curve with its own curve fit, the % change values are low, as expected.

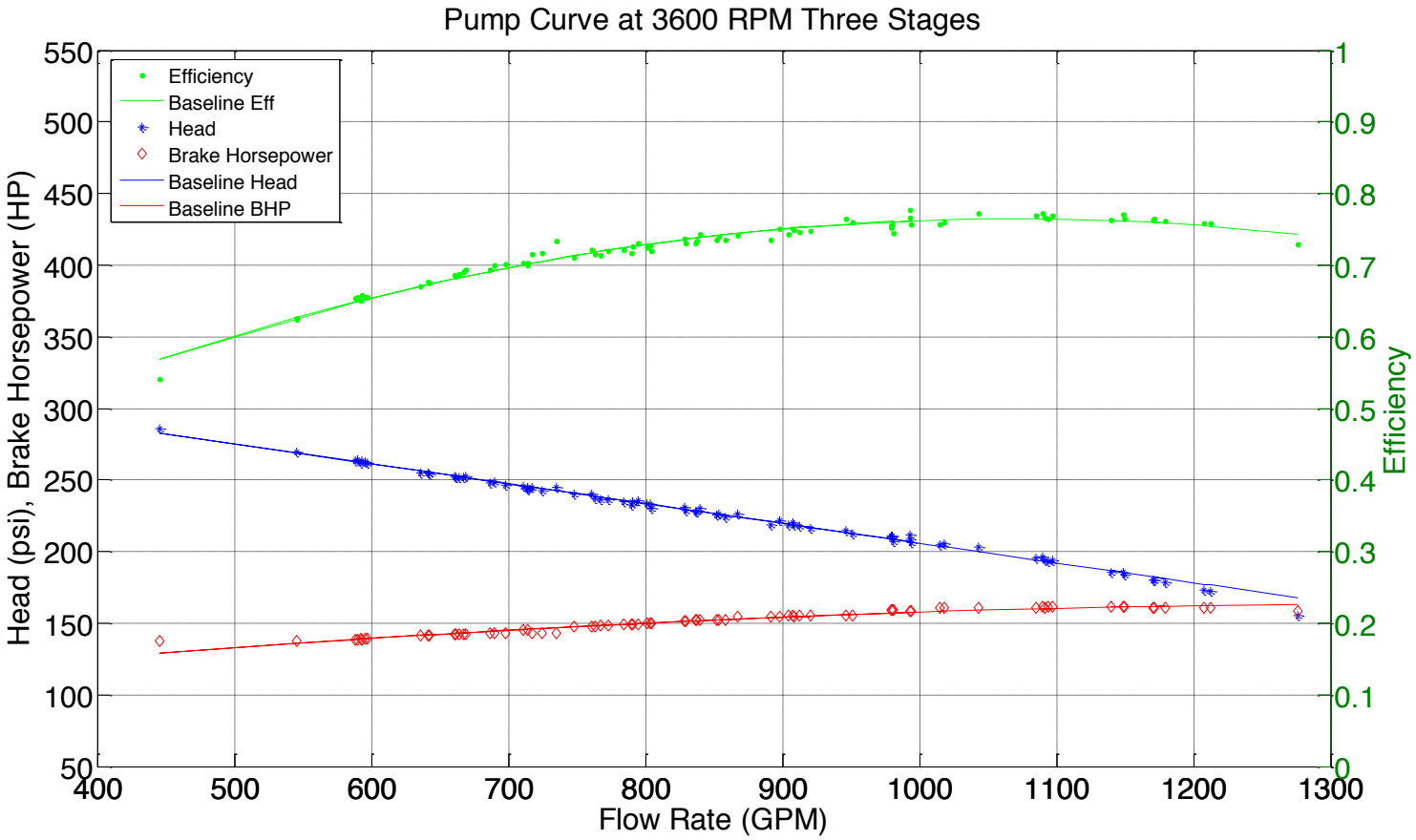

Figure 5.2 Baseline pump curve for three stages with its curve fits overlaid.

Table 5.1 Percent change between baseline pump curve and its curve fits, these values are as expected low and indicate an accurate fit. Positive values correspond to a negative change.

Parameter	Mean % Change	Max % Change
Head	0.17	7.92
Power	-.0036	2.85
Efficiency	-0.02	5.31

Table 5.2 shows the change in the performance of the pump for 2700, 3000, 3300 and 3600 RPM. The data used at 3600 RPM was taken at a different time than the baseline data, using the 2 ¼" (1000-1300 GPM at 3600 RPM) choke, the low percent change values indicate repeatability of results. The table shows that the head and power drop at a similar rate, consequently efficiency at different RPMs undergoes minimal change.

Table 5.2 Percent change relative to baseline pump curve and pump curves at 2700, 3000, 3300 and 3600 RPM. Low percentage change at 3600 RPM shows repeatability of results. Positive values correspond to a negative change.

RPM	Parameter	Mean % Change	Max % Change
3600	Head	2.32	7.24
	Power	1.65	4.52
	Efficiency	0.05	2.42
3300	Head	28.70	36.09
	Power	27.83	31.83
	Efficiency	0.69	2.88
3000	Head	72.09	88.85
	Power	68.99	76.29
	Efficiency	1.87	7.07
2700	Head	127.81	153.38
	Power	124.87	134.17
	Efficiency	1.25	8.37

Figure 5.3 shows the pump curve at 3300 RPM with the 2 ¼" choke, plotted with the baseline curve, in this plot the efficiency is seen to have a negative slope as opposed to nearly zero slope of the baseline, this indicates that the BEP will be found at the low end of the flow rates shown (possibly lower).

Figure 5.4 demonstrates the pump curve at 2700 RPM with the baseline curve superimposed. At 2700 RPM the negative slope of the efficiency can be seen more clearly than at 3300 RPM, while the baseline has a positive slope in this RPM range; these results indicate that the BEP of the 2700 RPM curve will be found at lower flow rates than those shown, while the BEP for the baseline will be found at higher flow rates than those shown.

It is recommended that performance tests at 3600 RPM be taken periodically and be data driven, that is, the frequency of the test should be increased if significant performance or vibration change is detected, at the discretion of the operator. Performance tests at different pump speeds should also be taken periodically, although not necessarily as frequently as the 3600 RPM tests.

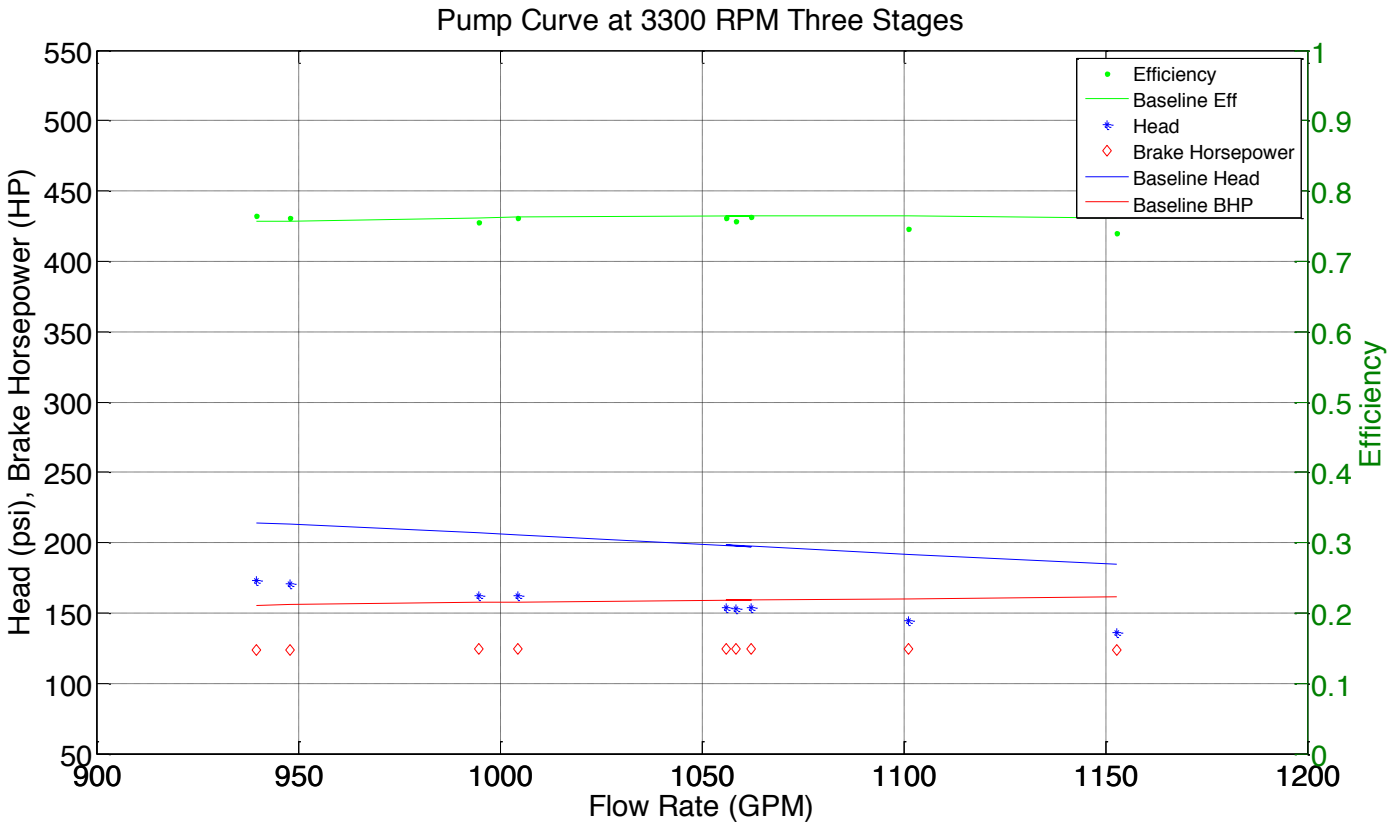

Figure 5.3 Pump curve for three stages of the ESP at 3300 RPM, the lines correspond to the baseline data (3600 RPM).

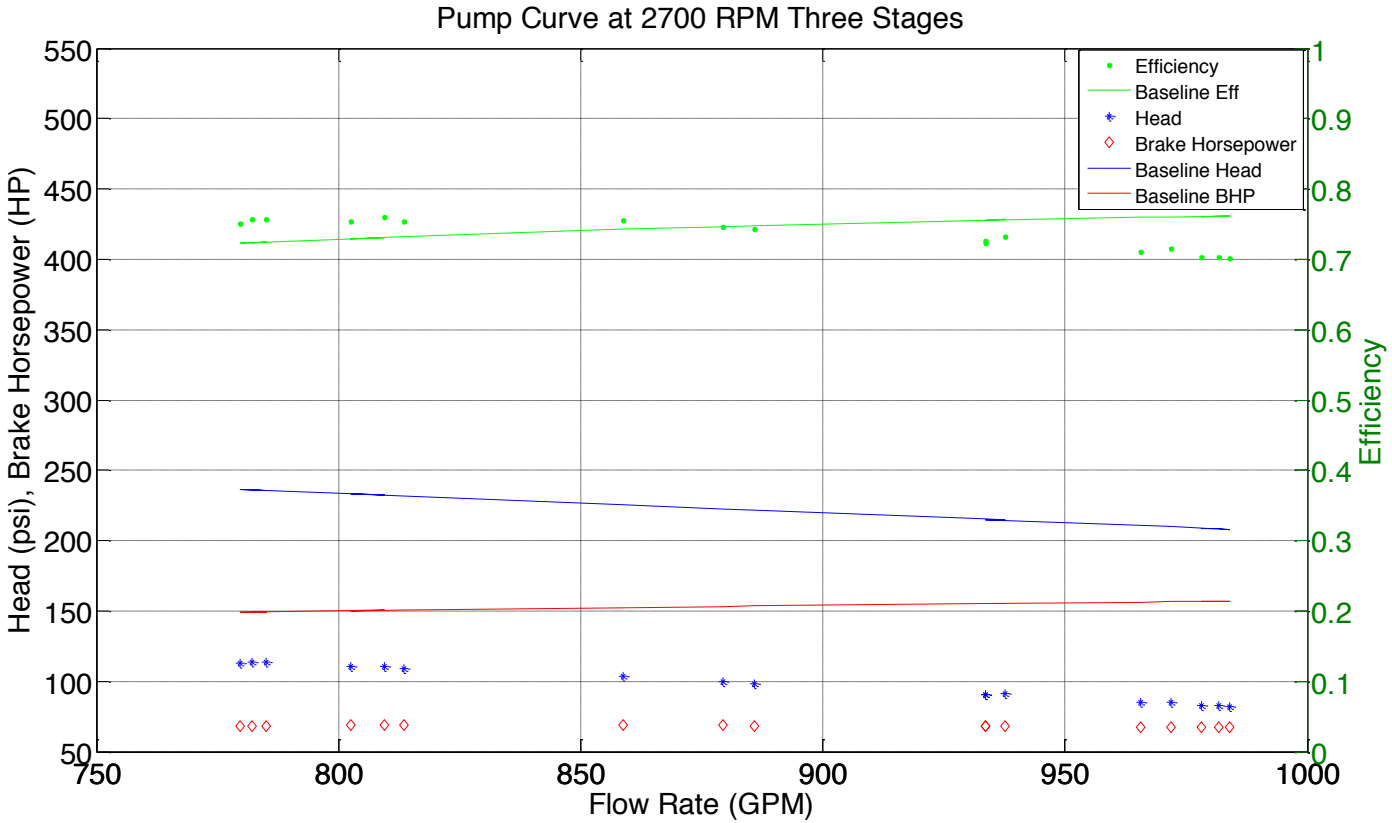

Figure 5.4 Pump curve for three stages of the ESP at 2700 RPM, the lines correspond to the baseline data (3600 RPM).

5.2 Vibration

The ten internal proximity probes are placed on the casing of the pump looking at the internal rotating components of the pump. The probes are set in 5 sections 90 degrees apart from each other (X and Y), as shown in Figure 5.5. The X proximity probes are labeled with odd numbers and the Y are labeled with even numbers. The numbering starts from bottom (first stage) to top. The first, third and fifth section are looking at the shaft, the second and fourth section are looking at the impeller.

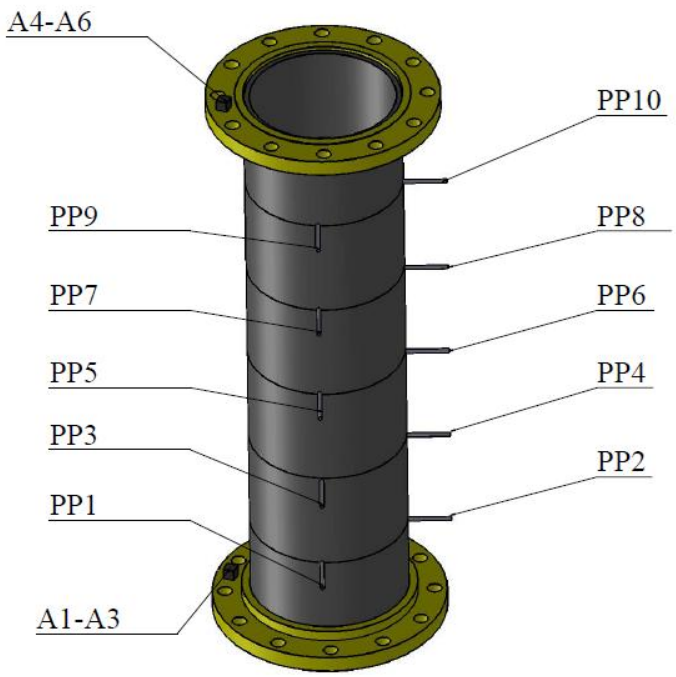

Figure 5.5 Position and nomenclature for proximity probes and accelerometer.

Runout refers to out of center rotation, in this work it will refer more specifically to the signal read on the proximity probe when rotating the shaft without any dynamic forces (vibration). Shaft runout could be caused by several factors including:

- Shaftness eccentricity (out of round)
- Surface scratches or imperfections
- Variations in electrical conductivity of material

The runout can be measured by performing a slow roll, rotating the pump as slow as possible to ensure that there is little dynamic shaft motion. In some situations, such as with horizontal rotating machinery, this result can be removed electronically from the data to compensate. For the ESP under study, however, the lack of a radial force, such as gravity, constraining the ESP's shaft when performing the slow roll, in combination with its large clearances in the bearings, makes it impossible to guarantee that the probe readouts during the slow roll do not include any dynamic motion, even at 90 RPM, the slowest speed achieved by the VFD. Nonetheless, the runout data was collected and the orbit of each proximity probe location is plotted in Figure 5.6. All probe locations show a circular or oval shape except for the second impeller which shows a figure eight shape; furthermore, the first impeller shows an unusually high displacement (16 mil); since the maximum diametrical clearance is 12 mil, this must be due to out of roundness of the impeller or the shaft not being in the center of it. The spikes seen in the orbit plots of the impellers are due to the phasors.

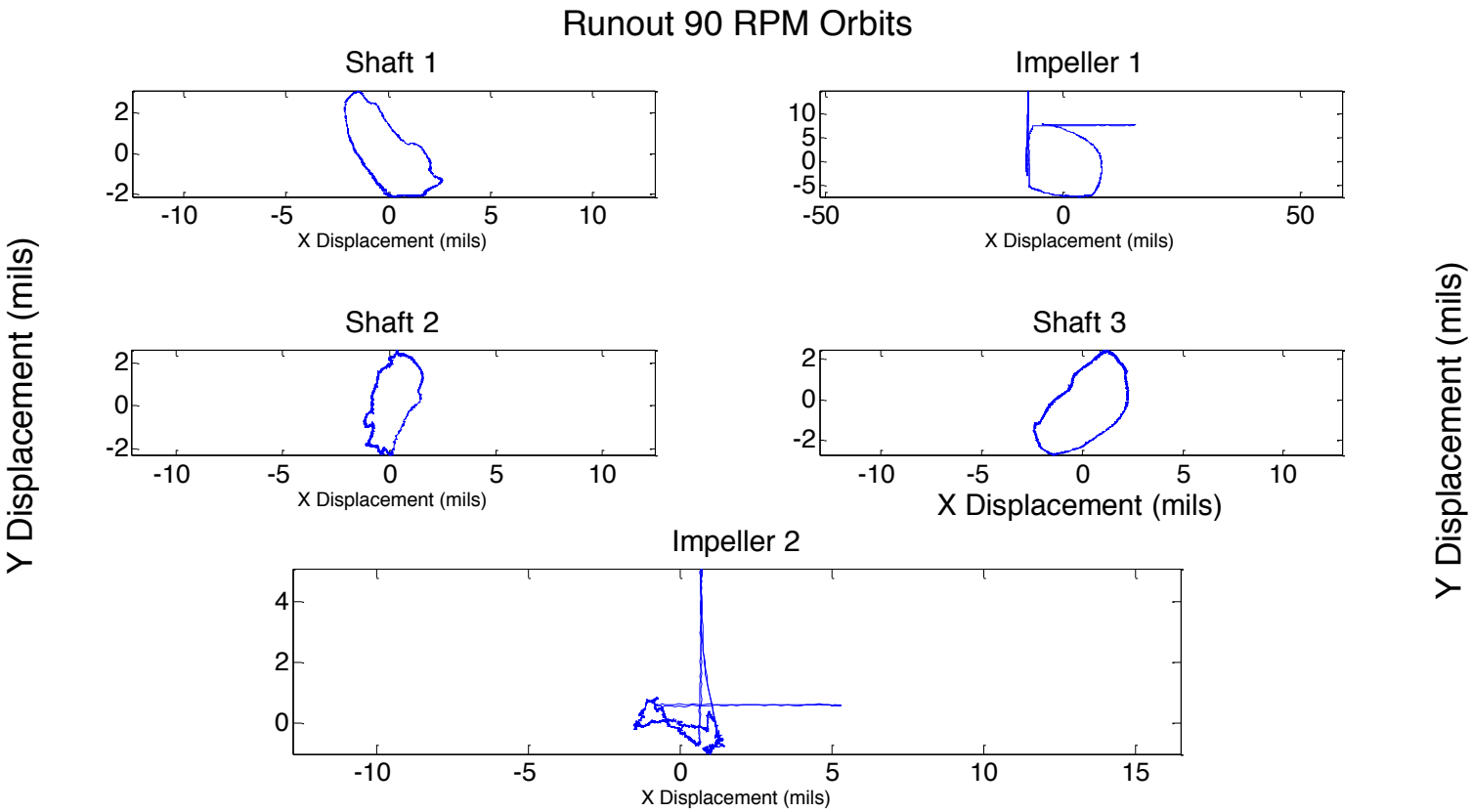

Figure 5.6 Orbits of different pump locations during slow roll (runout). The peak lines in both impellers correspond to the phasor, which is read once per revolution in each probe (X and Y).

Figure 5.7 shows the time domain plots of all proximity probes for the runout data. Apart from the phasors, the probes show very little surface imperfections, but the first impeller probes (PP3 and PP4) show a runout (probably due to eccentricity of the impeller) of about 16 mils peak to peak. Figure 5.8 shows the runout on the second impeller, this impeller shows a reasonable amount of imperfection, including an extra peak of about ½ mil that could be due to a scratch or machining imperfection, but the runout is almost negligible. Also of note is the phasor position relative to the wave in the x and y directions, in the x direction the phasor is leading the sine wave, in the y direction, the phasor appears to be lagging the wave, which indicates that there is an imperfection somewhere in the rotor (or bearings) that pushes the impeller away from the y probe before reaching the same distance as the x probe.

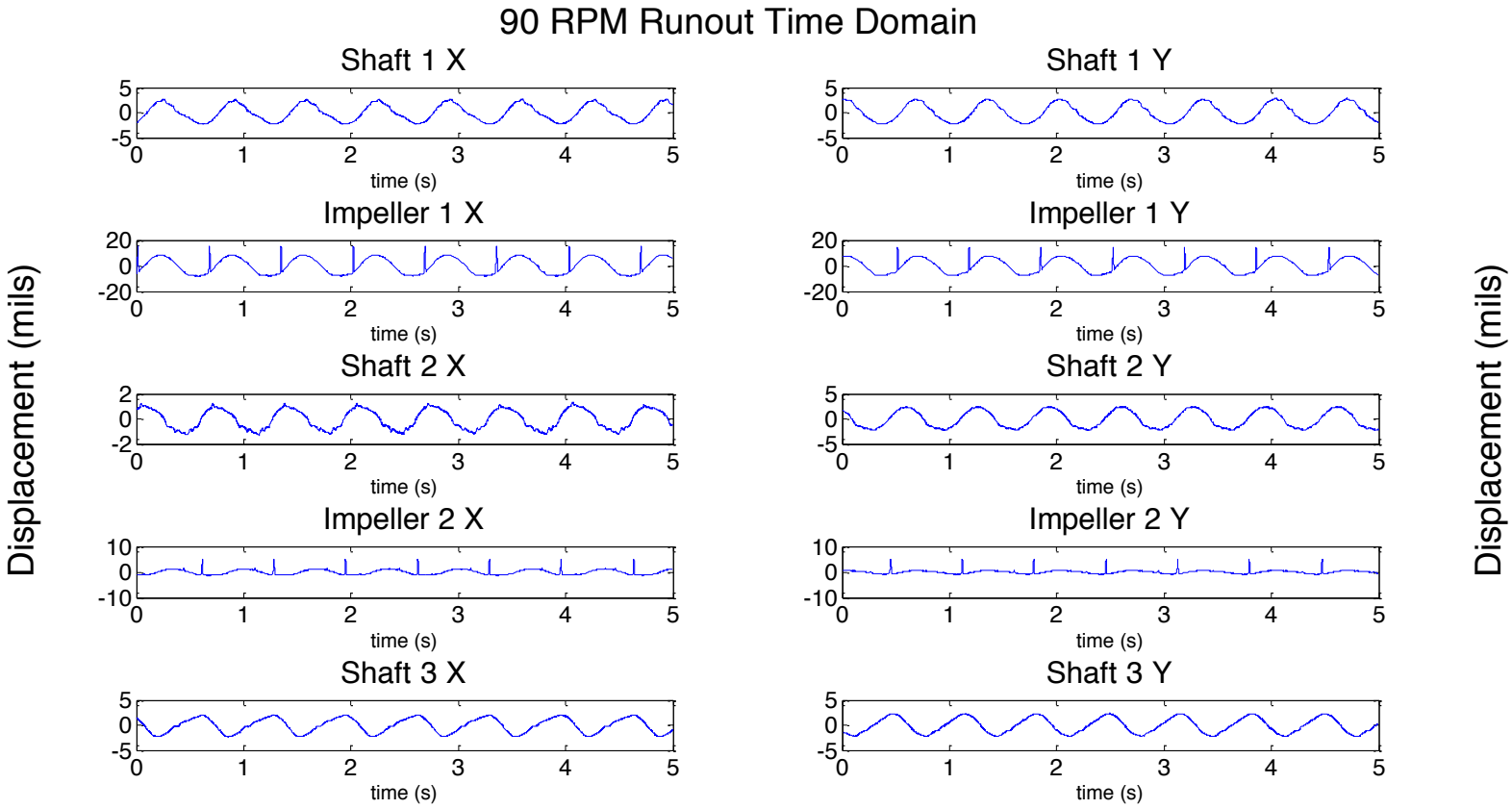

Figure 5.7 Time domain plot of proximity probe data at 90 RPM (runout).

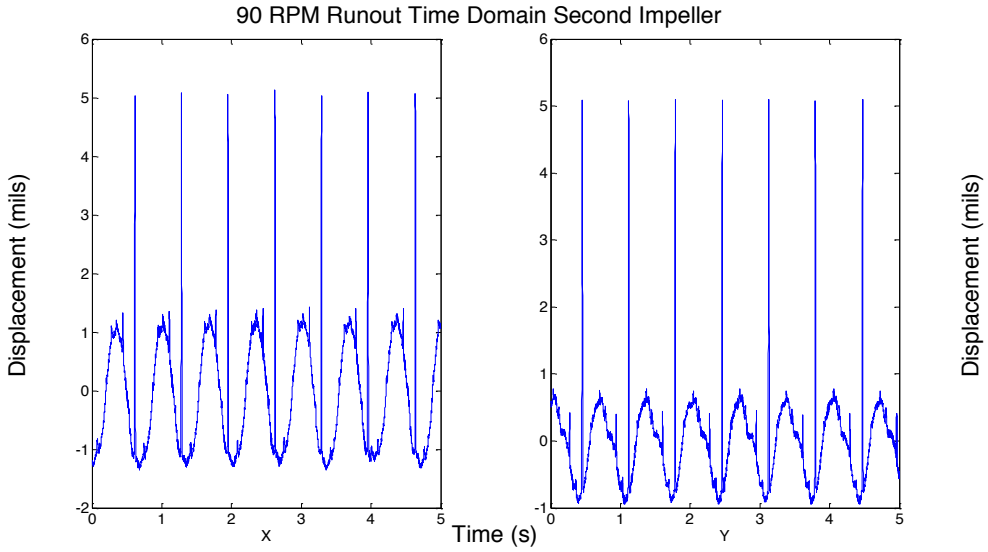

Figure 5.8 PP7 and PP8 runout

The orbits of the pump at 3600 RPM can be found in Figure 5.9. Except for the third shaft location all look to have circular shaped orbits; the third shaft location has an unrecognizable shape, which can be better understood by analyzing the frequency spectrum. Also of note is the shape of the second impeller, which was a figure eight at 90 RPM and is circular at 3600 RPM. The amplitudes of the orbits seem to be of similar size as the amplitudes of the runout.

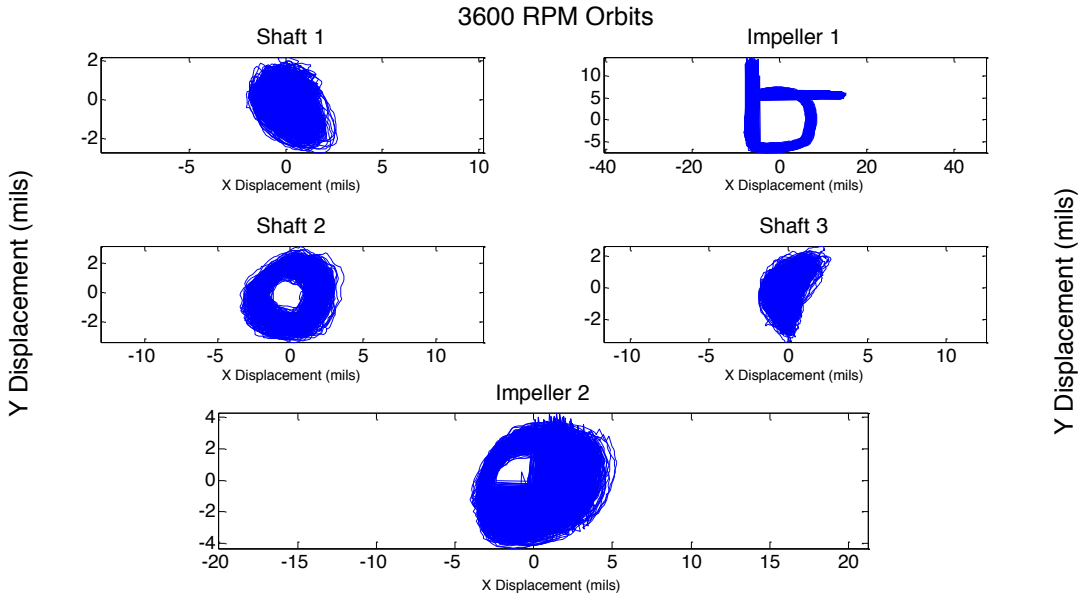

Figure 5.9 ESP Pump orbit for all proximity probe locations at 3600 RPM.

The time domain plots of the shaft and impeller locations can be found in Figure 5.10 and Figure 5.11, respectively, the x probes are in the first column and the y in the second. The plots show different vibration patterns on each location, but to better understand them, the frequency spectrum needs to be analyzed.

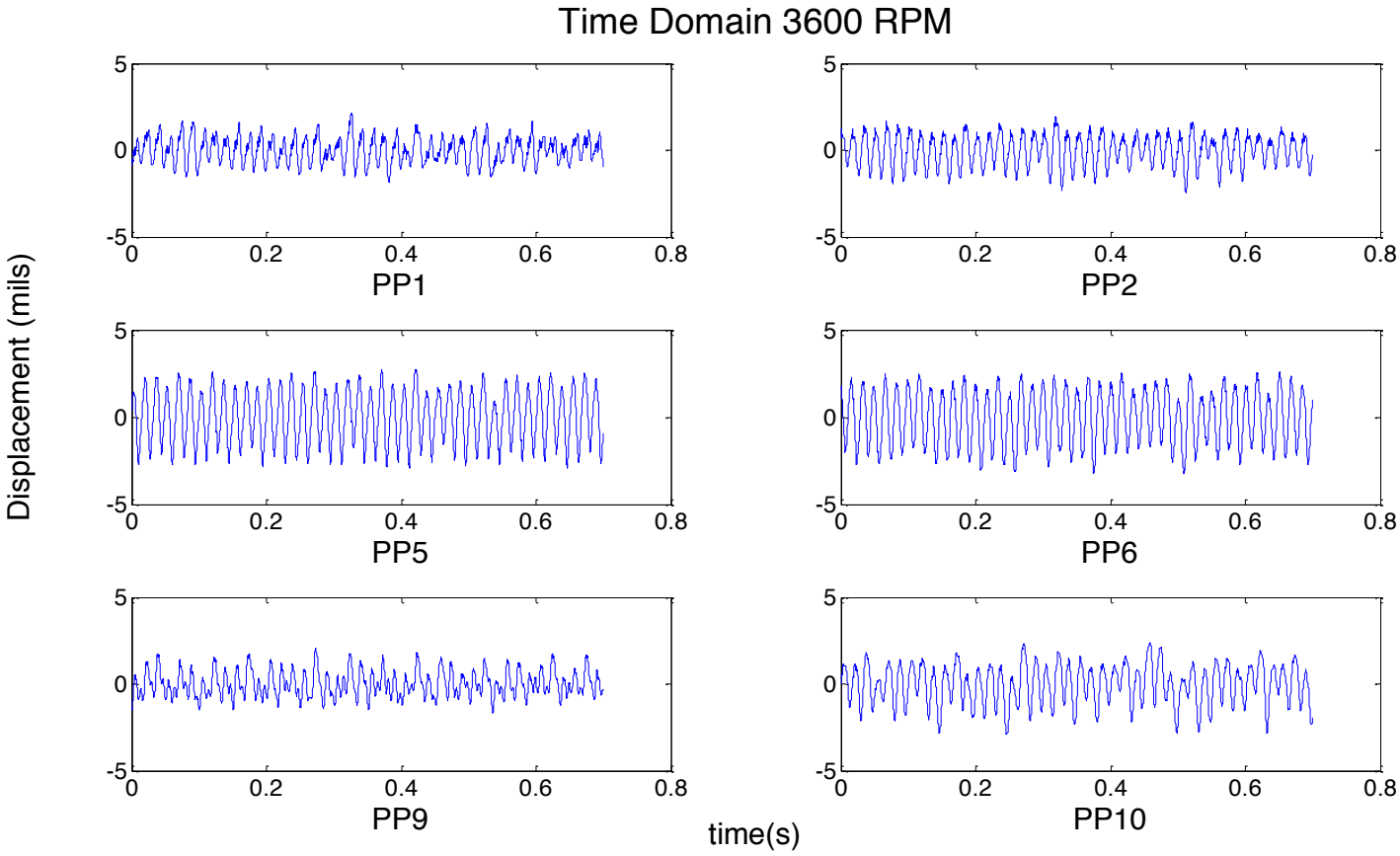

Figure 5.10 Time domain plot for shaft locations at 3600 RPM.

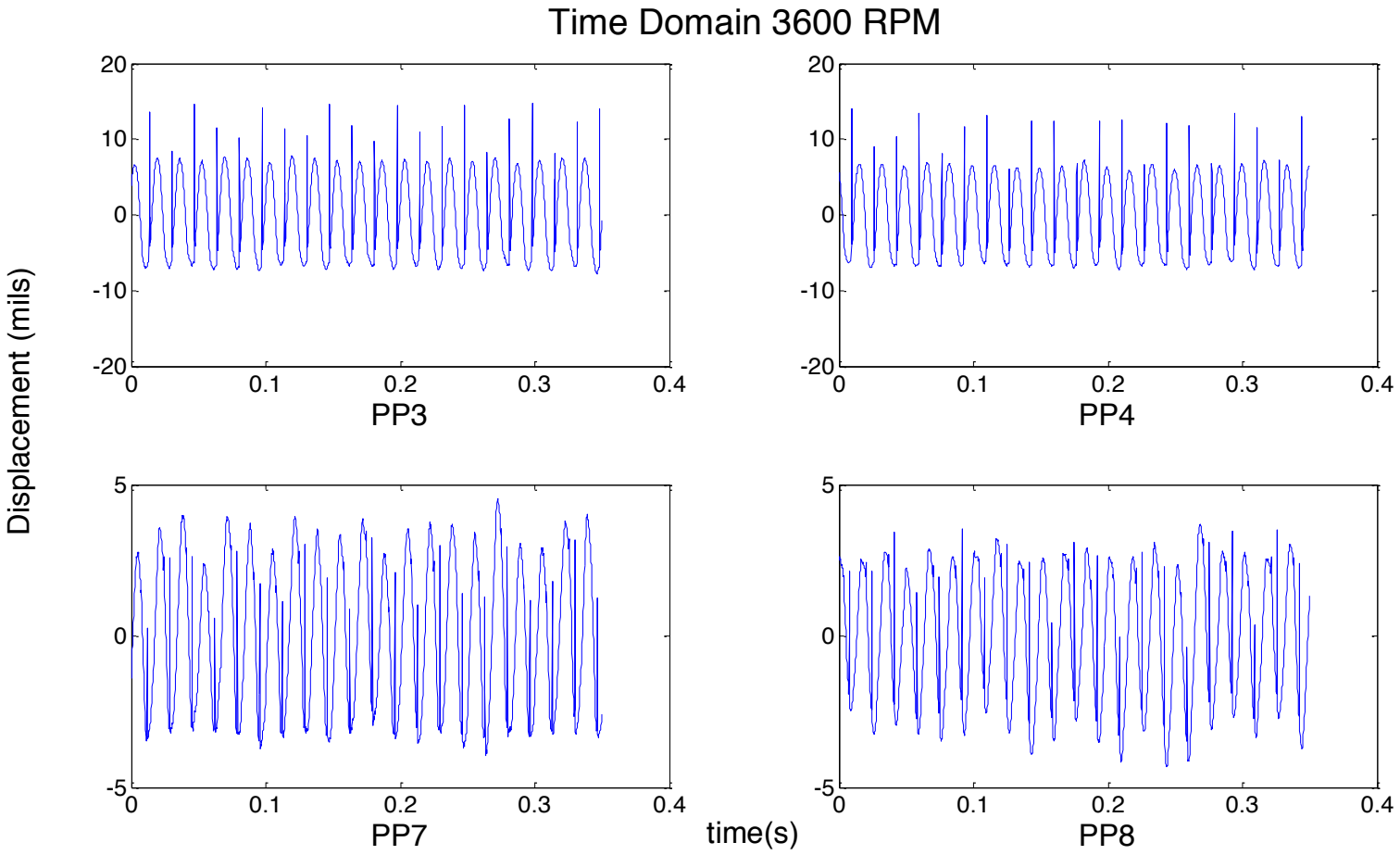

Figure 5.11 Time domain plot for impeller locations at 3600 RPM.

To obtain the frequency spectrum of the vibrations a Fast Fourier Transform (FFT) was performed on the data. The FFT is an efficient algorithm used to compute the Discrete Fourier Transform (DFT). The DFT and FFT transform a function from the time domain into the frequency domain, decomposing the signal into a Fourier series, a sum of a set of oscillating functions, sines and cosines, at different frequencies that describe a periodic signal. The FFT outputs values of peak to peak amplitudes plotted with respect to frequency; the noticeable peaks in the spectrum indicate a significant frequency component in the vibration data.

The frequency spectrums of all five locations at 3600 RPM is shown in Figure 5.12. All proximity probes show their highest peak frequency at the running speed (3600 RPM), as expected. The frequency spectrum also shows a significant peak at around 7000 RPM, this is the second harmonic (2X) of the rotating speed and is common in rotating machinery, but should be monitored.

Of note is the lack of a frequency peak at half the running speed (1/2X), this 1/2X peak is very common in two concentric cylinders rotation relative to each other and is commonly known as oil whirl. When there is fluid contained in an annular region between two cylinders where one cylinder is rotating inside another, the fluid film is set into motion; the fluid next to the rotor will have the same velocity as the surface of the

rotor while the fluid next to the bearing will have zero velocity. This velocity difference will create an average velocity profile slightly less than 1/2X, considering losses; this creates a precession of the shaft of about ½ the running speed. If this speed coincides with the critical speed of the pump, it could induce instability to the pump. The fact that the oil whirl phenomenon is not significantly present could be due to the relatively low viscosity of water as well as many other factors, including the vertical position of the shaft. The whirl phenomenon in this pump, or lack of it, merits further investigation.

The three probe locations closest to the exit of the pump show small peak amplitudes at around 1000 CPM, this peak's cause is unknown, but the possibility of it being whirl should not be discarded. Figure 5.14 shows a close up of the third shaft's frequency spectrum, the peak in discussion shows an amplitude of 0.25 mils peak to peak and merits further investigation and monitoring.

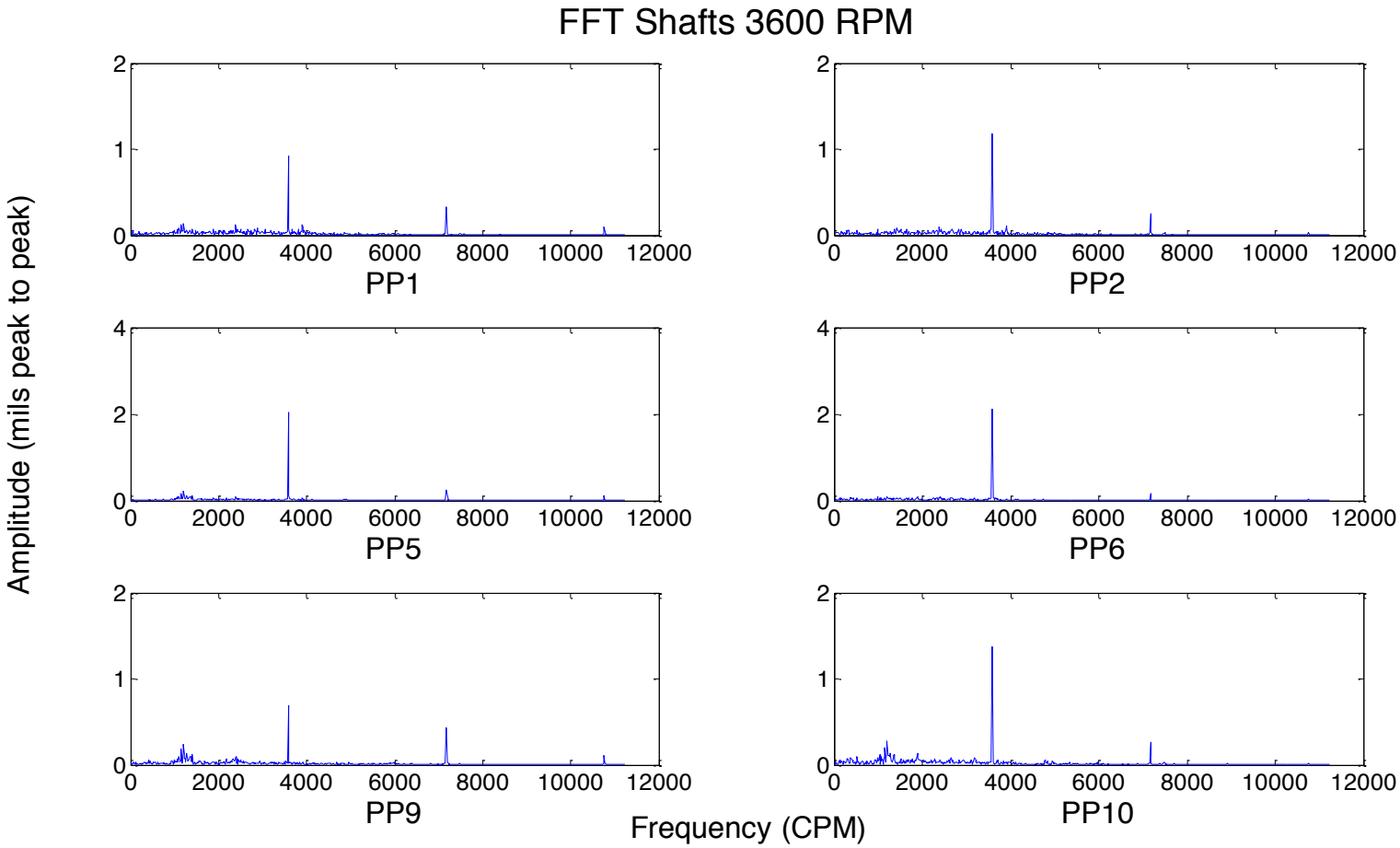

Figure 5.12 Frequency spectrum on shaft locations at 3600 RPM.

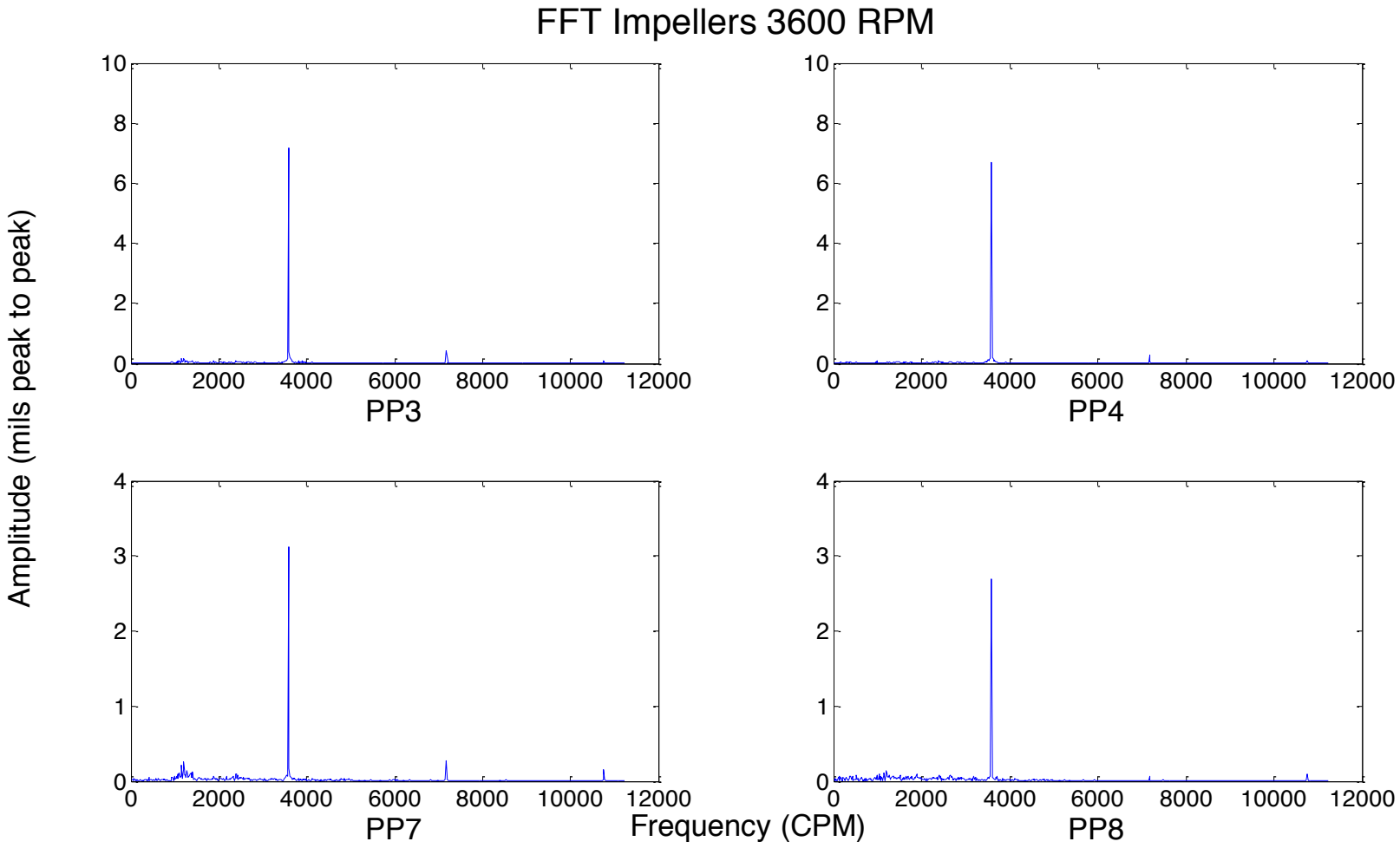

Figure 5.13 Frequency spectrum on impeller locations at 3600 RPM.

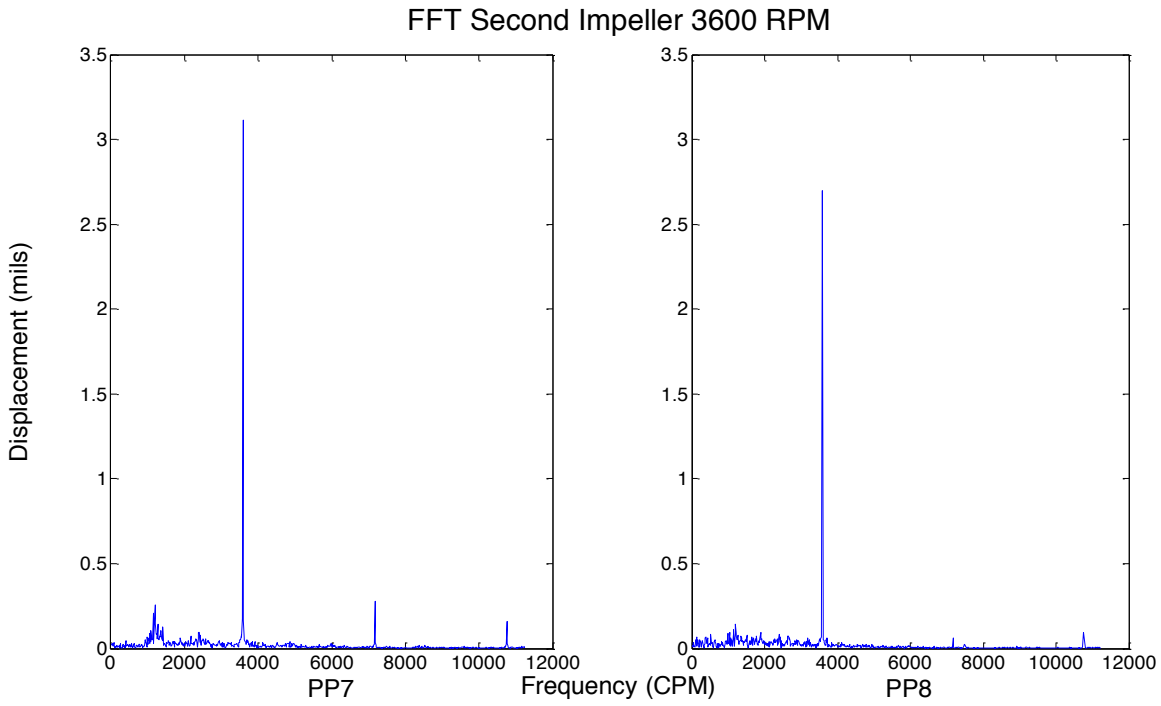

Figure 5.14 Shaft 3 frequency spectrum at 3600 RPM.

To find natural frequencies of the pump, mode shapes and other useful vibration data for a wide range of speeds, ramp down tests are commonly performed. The ramp down test consists of bringing the pump up to steady state at running speed, turning it off and saving the data whiles the pump coasts down to a stop. The data on the ramp down performed in the ESP was analyzed by dividing it into several sections of data and performing an FFT on each section. The frequency at which the maximum peak occurs can be approximated as the pump speed during that section of data, these results were then plotted in a three dimensional (pump speed, frequency and amplitude) graph in what is called a Waterfall plot. The program used for the Waterfall plots can be found in Appendix F.

Nothing unusual is noticed from the waterfall plot of the shaft locations, shown in Figure 5.15, the 1X and 2X of the rotating speed can be seen to increase normally with the rotating speed of the pump, as expected. Rotating the waterfall plot 90 degrees, creates a two dimensional plot where the maximum amplitude of the frequency spectrum is plotted vs. the running speed. As can be perceived in Figure 5.16, there is a noticeable increase in the peak amplitude at around 1100 RPM. This indicates that 1100 RPM could be a natural frequency of the system; this speed is dangerously close to the 1/2X that the oil whirl would occur, and if this is the case the whirl could go unstable and prove destructive to the pump. Also, running the pump at this speed for long periods of time will produce excess vibrations due to resonance, the phenomenon of the natural frequency and oil whirl on this pump should be studied further in order to better understand the pump.

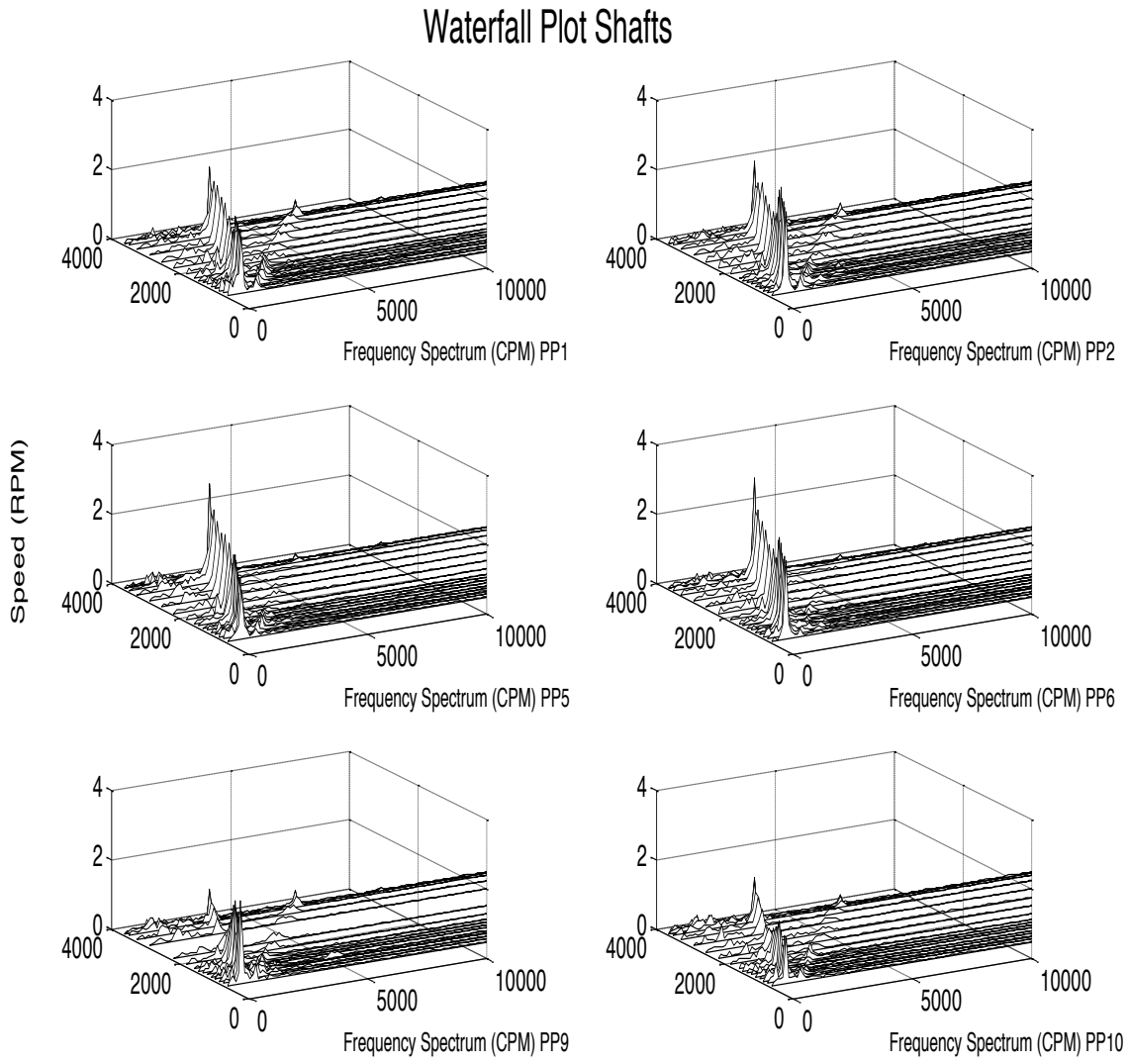

Figure 5.15 Waterfall plot for ramp down for all shaft locations, the top row corresponds to the first (inlet) shaft

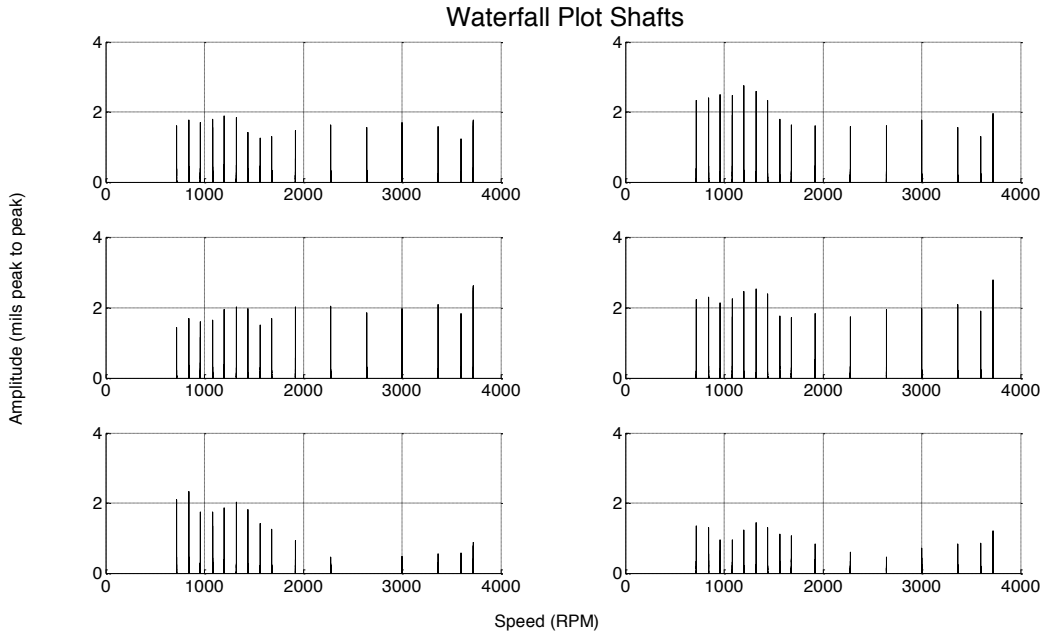

Figure 5.16 Maximum of amplitude of waterfall plot vs. pump speed for all shaft locations.

The waterfall plots for the impeller locations can be seen in Figure 5.17, these plots do not show anything at frequencies other than the running speed. The maximum of the amplitude plot for the impellers, shown in Figure 5.18, displays the same peak amplitude at 1100 RPM for the first impeller; but it is not as noticeable in the second impeller Y probe, and non-existent on the X probe. These results show that the pump needs further and more in-detail vibration analysis, including using the VFD to run at suspected resonant frequencies and/or using the VFD to create a more accurate waterfall plot by saving the data at a sequence of speeds instead of a ramp down.

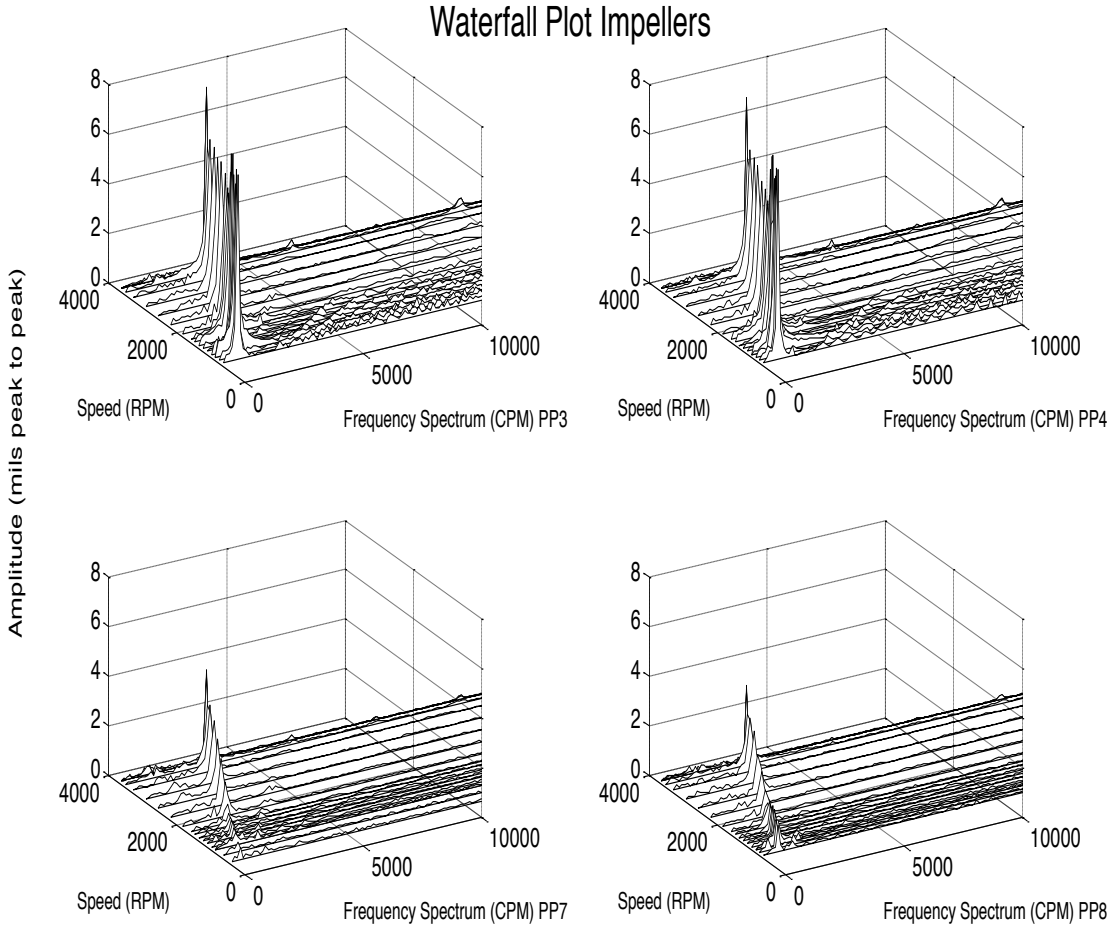

Figure 5.17 Waterfall plot for ramp down all impeller locations, top row is the first (bottom) impeller location.

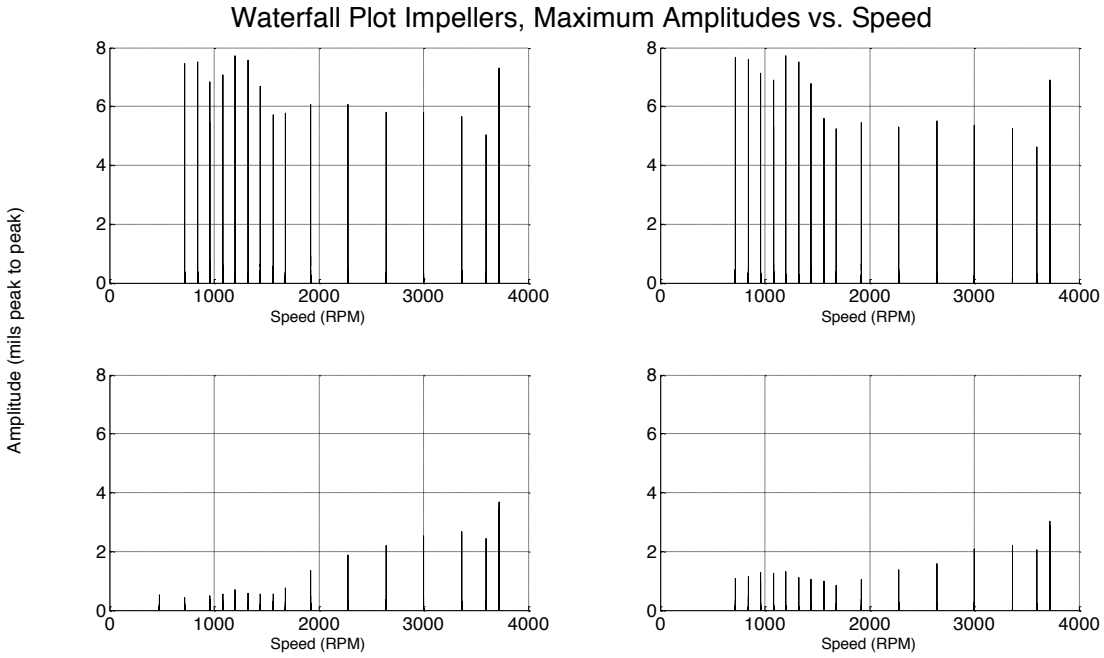

Figure 5.18 Maximum of amplitude of waterfall plot vs. pump speed for all shafts

The orbits of the shaft locations during the ramp down are plotted in Figure 5.19, each row corresponds to a shaft location (top row is first location) while pump velocity decreases from left to right. The plot shows the first two shaft locations to have a nearly circular orbit at high velocity and the orbits turning more elliptical as the speed decreases. The third impeller shows an unrecognizable pattern at high velocity turning into a more recognizable elliptical pattern as the pump speed decreases.

The same orbit plot, but for the impeller locations, can be seen in Figure 5.20. The plot shows almost no change for the first impeller, while the second impeller seems to have a smaller diameter orbit as it slows down.

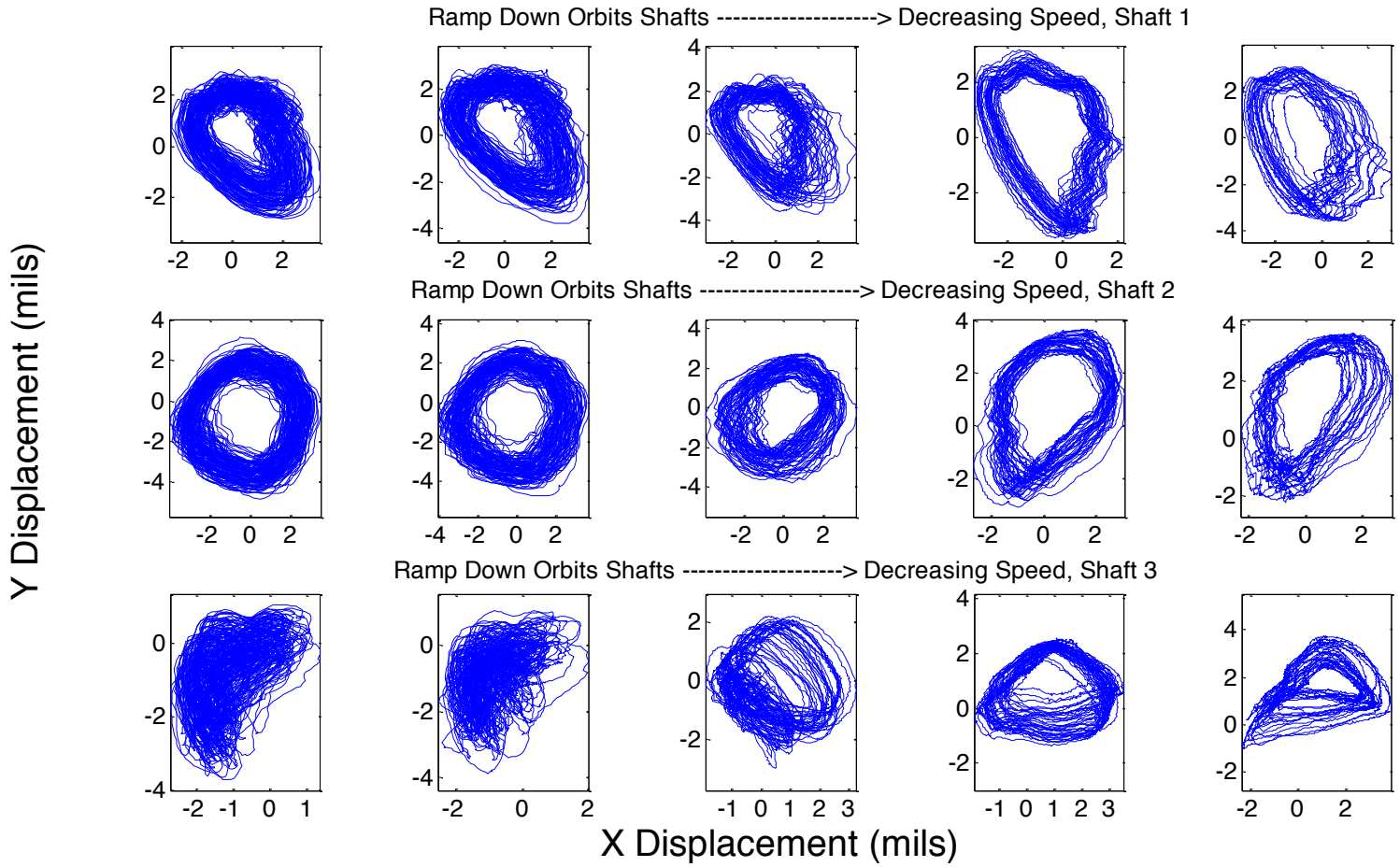

Figure 5.19 Orbit of the shaft locations with decreasing speed.

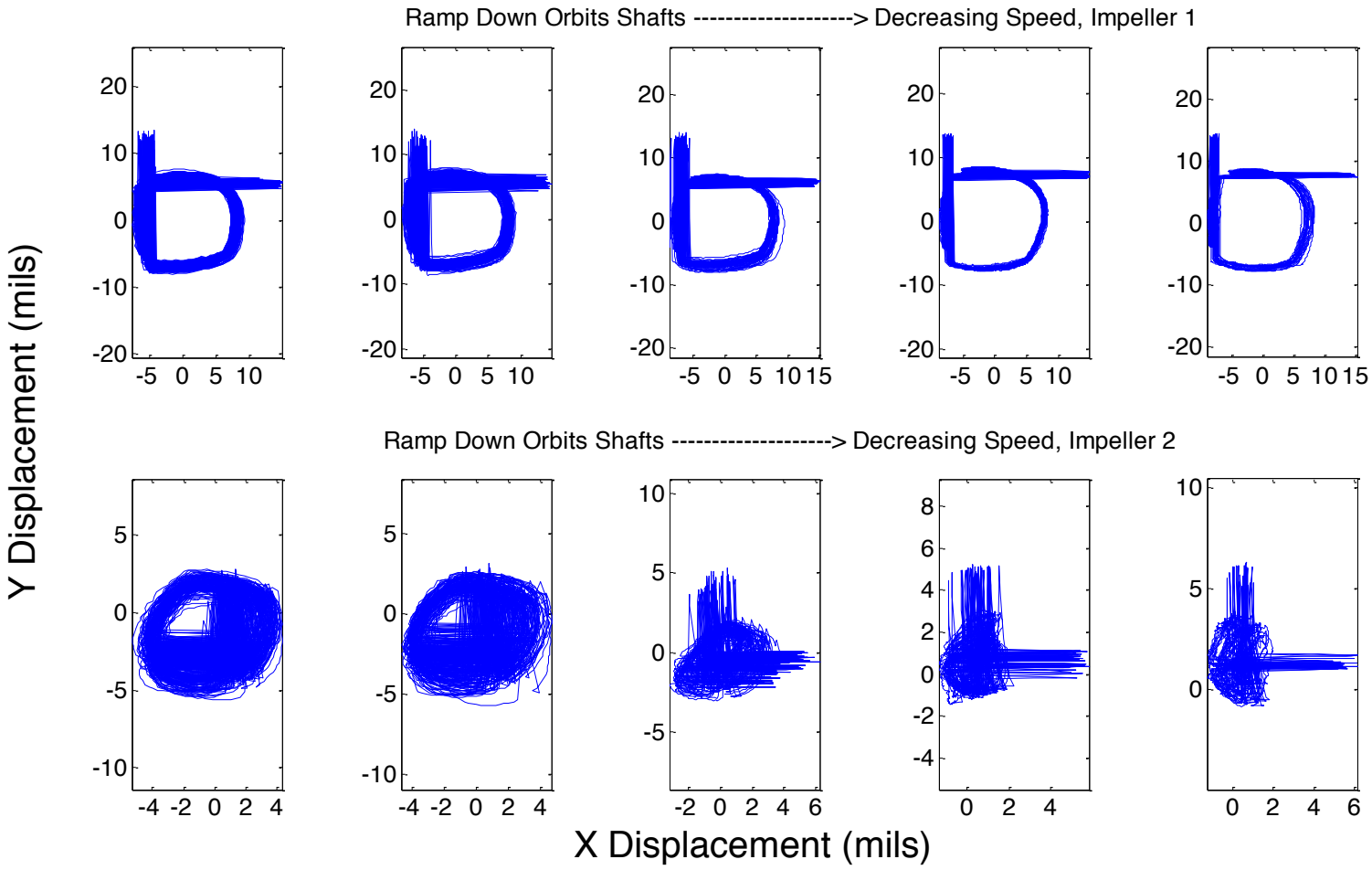

Figure 5.20 Orbit of the impeller locations with decreasing speed.

The accelerometers were used to determine the vibration in the casing of the pump. The x and y axes of the accelerometers do not coincide with the X and Y axis of the proximity probes, but can be related via the following formula:

$$X = x\cos\theta + y\sin\theta \quad 5.1$$

$$Y = y\cos\theta - x\sin\theta \quad 5.2$$

The angle (θ) for each accelerometer is shown in Table 5.3.

Table 5.3 Accelerometer angles relative to the proximity probe axes.

Accelerometer	Angle(θ)
Inlet	29°
Outlet	21°

The time domain data for accelerometers is impractical to analyze and an FFT needs to be performed in order to understand the casing vibration. The FFT for all axes of the first (inlet) accelerometer is shown in Figure 5.21, besides the running frequency the accelerometer shows a smaller peak frequency at around 1800 CPM (1/2x) in the x direction. This vibration is not noticeable in the x and y axes.

The outlet accelerometer, its frequency spectrum displayed in Figure 5.22 shows a noticeable peak at around 1500 CPM in all three axes, the excitation of this frequency is unknown and further investigation is needed to determine if this frequency is related to the 1100 CPM frequency found during the ramp down.

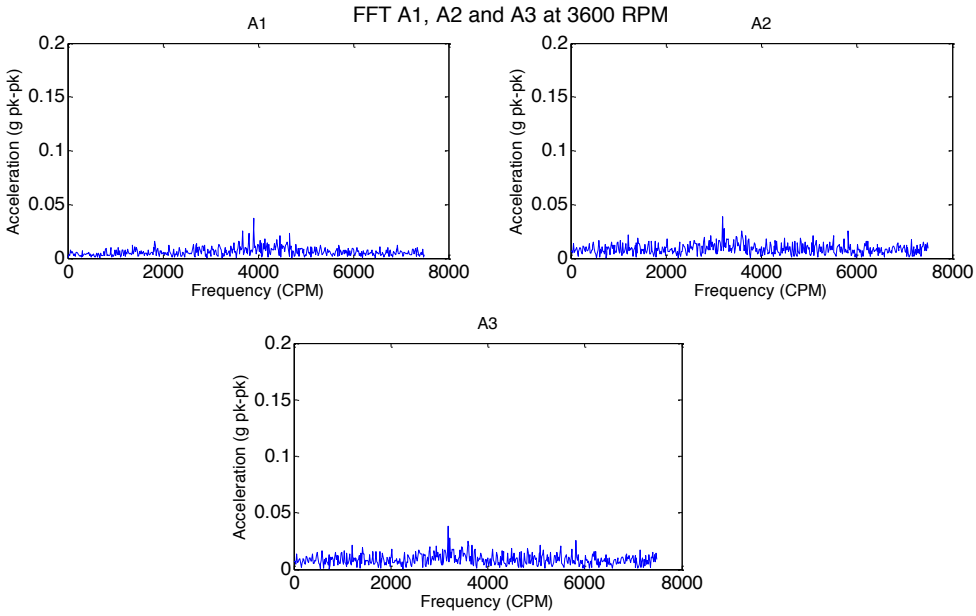

Figure 5.21 Frequency spectrum at 3600 RPM inlet flange accelerometer.

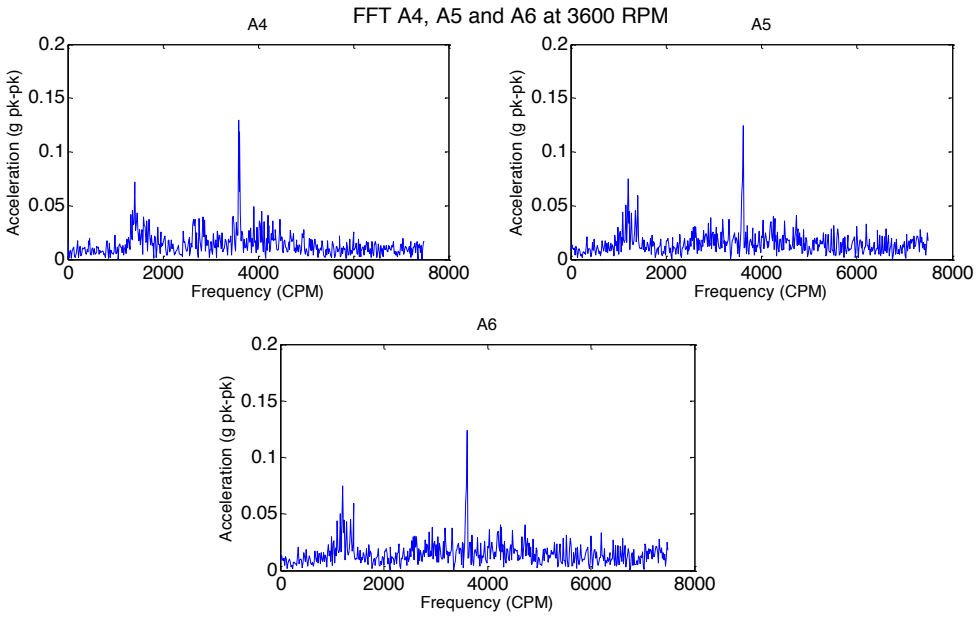

Figure 5.22 Frequency spectrum at 3600 RPM exit flange accelerometer.

To be able to compare the internal vibrations of the pump to the movement of the casing the data needs to be in the same units for the accelerometers and the proximity probes. To achieve this, the accelerometer data was transformed from acceleration to displacement. To transform from acceleration to displacement for a function $y = \sin(\omega t), \ddot{y} = \omega^2 \sin(\omega t)$ therefore the integral is found by dividing by ω^2, where ω is the frequency in $^{rad}/_{s}$, is shown in equation 5.3.

$$disp = \iint a \cdot dt = 3.864 * 10^5 \frac{a}{\omega^2} \qquad 5.3$$

The displacement is in mils, the acceleration is in g's and the constant is the transform between g's and mils per second square. The conversion is carried out in the frequency domain and Figure 5.23 and Figure 5.24 show the results; the high values for the low frequencies are a result of the division by a very small number squared and can be considered noise, and ignored.

Figure 5.23 shows no distinct frequency peaks along its spectrum, meaning that there is little vibration in the inlet part of the pump. The displacement frequency spectrum for the accelerometer in the outlet part of the casing is shown in Figure 5.24, on this location the spectrum shows a noticeable frequency of around 2 mils in all three axes and a distinct 1/2X frequency peak in the X and Y axes. To be able to relate both the internals of the pump to the casing a study of the relationship between the phase angles of the two could prove to be very valuable.

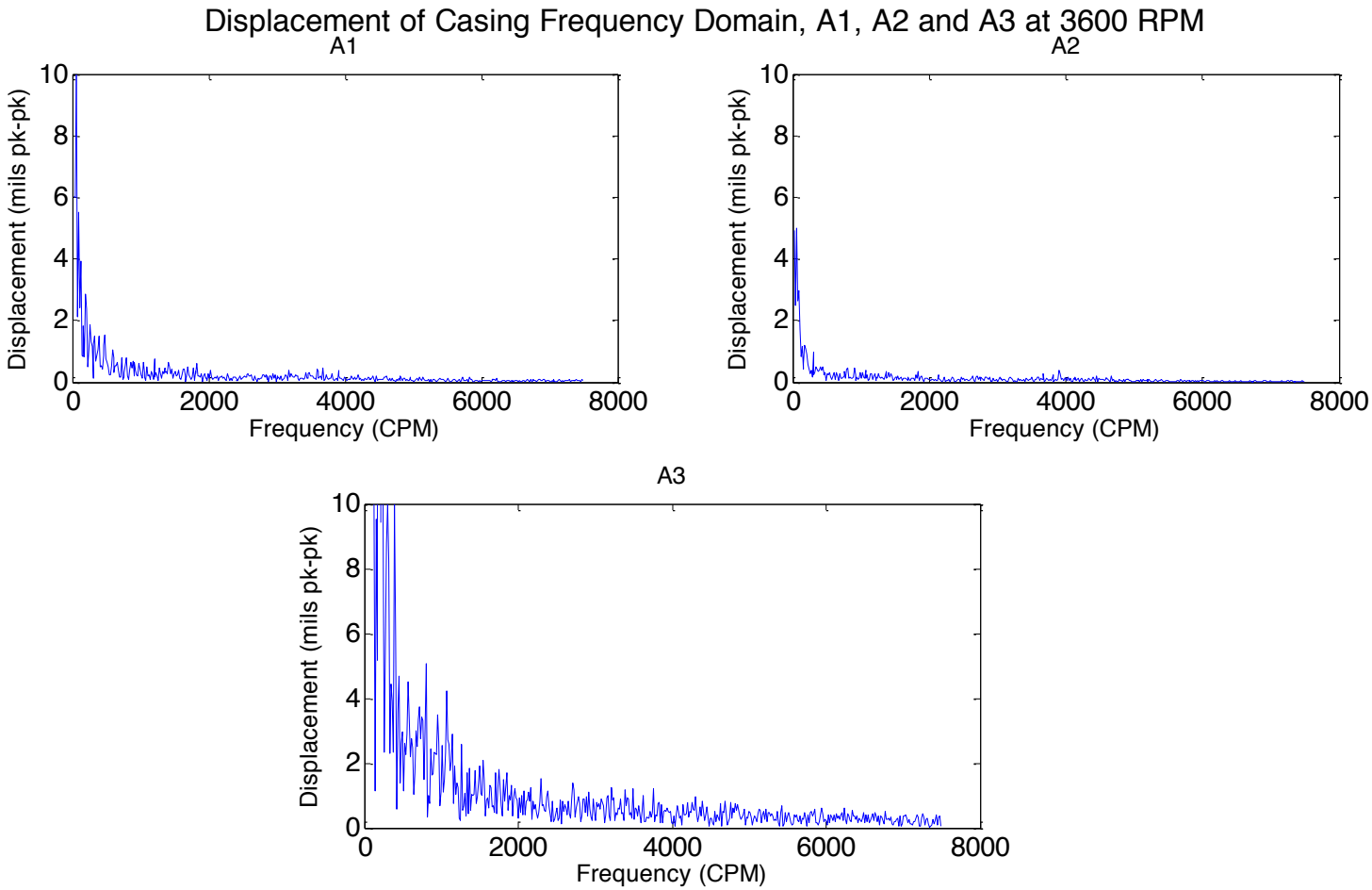

Figure 5.23 Frequency spectrum of displacement of inlet casing at 3600 RPM.

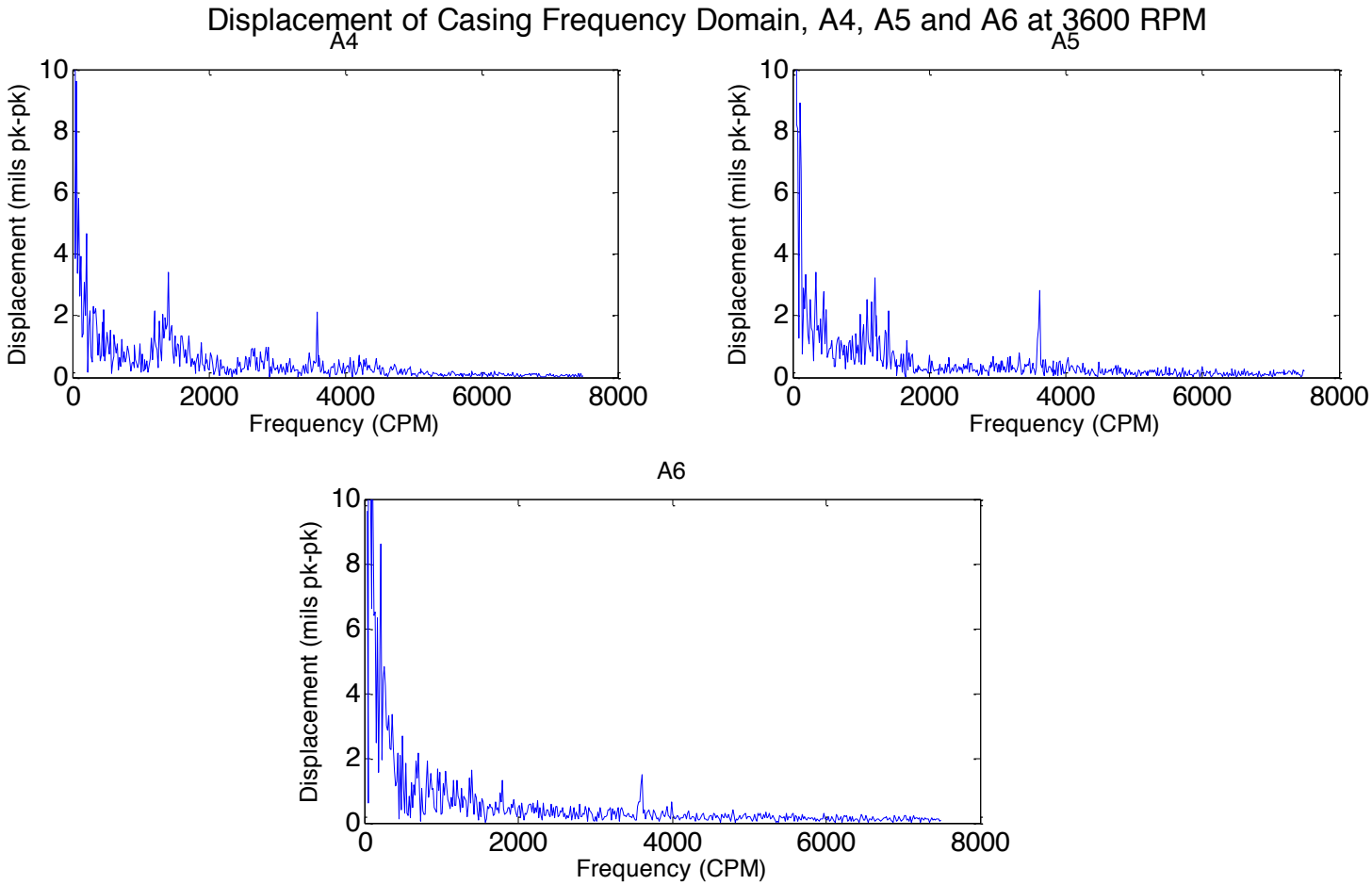

Figure 5.24 Frequency spectrum of displacement of outlet casing at 3600 RPM.

5.3 Sand Analysis

To make accurate estimates of flow rate and concentration of sand, the density of the sand was measured using a graduated cylinder. To avoid measuring the empty spaces in between the sand as part of the volume (bulk density), water was placed in the graduated cylinder and its volume and weight measured. Afterwards, sand was added to the graduated cylinder with water and the volume and weight again measured and noted. The weight and volume differences correspond to the weight and volume of the sand. The density of the sand was found to be 2.65, the results can be seen in Table 5.4. Since the sand density does not change with temperature but the water density does, the values for specific gravity of the sand used in this investigation will be the density of the sand measured divided by the density of the water at the given temperature.

Table 5.4 Density of sand measured in the laboratory.

Mass Sand (kg)	Volume Sand (mL)	Density (g/cc)	Uncertainty (g/cc)
0.281818182	107	2.633814783	0.0245
0.440909091	168	2.624458874	0.0156
0.345454545	130	2.657342657	0.0203
0.272727273	102	2.673796791	0.0259
Mean		2.647353277	
Standard Deviation		0.022409013	

The sieving results obtained for the first bag of sand used are shown in Table 5.5. The majority (89.9%) is between 70 and 100 mesh (5.9 and 8.3 mils), approximately 8% of the sample was found to be 120 mesh (5 mils).

Table 5.5 Sieve analysis of Sample 1.

Total Weight of Sample		1.29 lbs		
Mesh Size	Weight Sieve	Weight Sieve	Weight	Percent
50	0.81	0.82	0.01	**0.78%**
60	0.78	0.79	0.01	**0.78%**
70	0.78	1.12	0.34	**26.36%**
80	0.75	1.11	0.36	**27.91%**
100	0.75	1.21	0.46	**35.66%**
120	0.75	0.85	0.1	**7.75%**
Pan	0.83	0.84	0.01	**0.78%**
Total			1.29	100.00%

A picture of the sieved sand taken using the microscope and computer software is shown in Figure 5.25, the sand shown is 170 mesh (3.5 mils). Table 5.6 shows the eccentricity value per mesh size for unused sand, the same data is shown in the form of a bar chart in Figure 5.26.

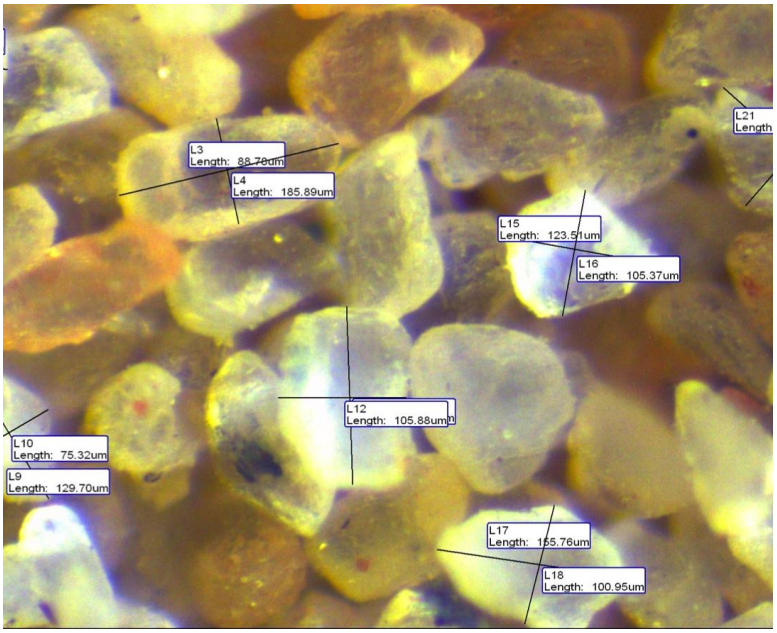

Figure 5.25 Sieved sand picture taken with the microscope software with the measurements used to calculate the eccentricity. The sand sample is 170 mesh.

Table 5.6 Average eccentricity and standard deviation for each mesh size.

Mesh	Size (mils)	Mean ε	σ
50	11.7	0.6810	0.1472
60	9.8	0.6683	0.1298
70	8.3	0.6809	0.0900
80	7	0.6217	0.1294
100	5.9	0.6621	0.0889
120	4.9	0.6787	0.1301
170	3.5	0.8011	0.1204
200	2.9	0.8016	0.0777
Pan	0	0.7607	0.0833
Total		0.706233	0.1254

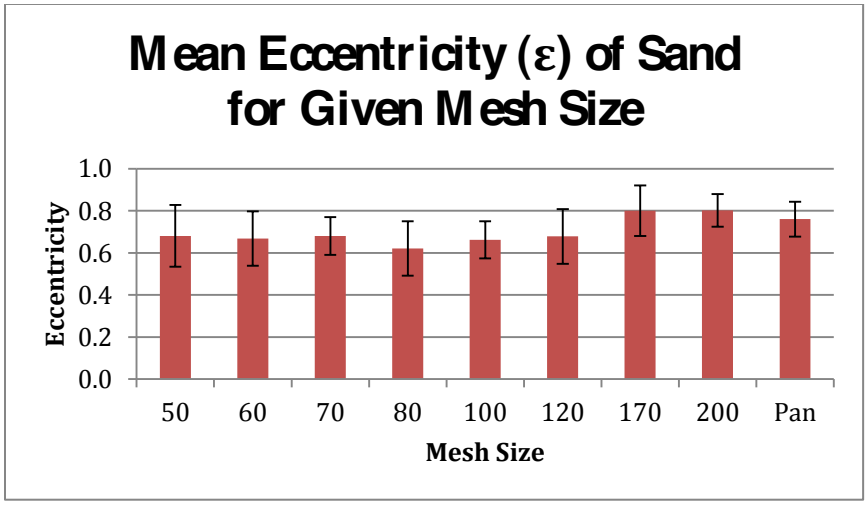

Figure 5.26 Mean eccentricity of sand for given mesh size.

6. UNCERTAINTY ANALYSIS

To estimate the error involved in the measurements due to instruments accuracies and errors, the Kline and McClintock uncertainty analysis is used. The Kline and McClintock analysis states that the error propagation on a measurement that depends on a number of individual variables, $R = f(a, b, c \ldots,)$, is given by the following formula:

$$U_R = \sqrt{\left(\frac{dR}{da}U_a\right)^2 + \left(\frac{dR}{db}U_b\right)^2 + \left(\frac{dR}{dc}U_c\right)^2 + \cdots} \qquad 6.1$$

Where U refers to the error of each variable and includes bias error and precision error. Bias error is a constant error in the measurement and if known should be removed from the measured value [8], instrument manufacturers will usually specify bias error limits. Precision error is a random error due to instrument resolution, imperfections of the measuring system, procedures and human error among others. Precision errors could be eliminated from the measured value by taking an infinite number of samples and averaging [8]. The values for the manufacturer stated error for each instrument used can be found in Table 6.1. The errors of the instruments not specified by the manufacturers were estimated as one half the amount of the smallest resolution capable of being read by the instrument.

Table 6.1 Uncertainty for instruments used in the experiment.

Instrument	Range	Error
Accelerometers	±10 g	10%
Coriolis Density Meter	.8 to 1.2 g/cc	±.001 g/cc
Coriolis Mass Flow Meter	-25 to 200 kg/min	±.1 %
Differential Pressure Transducer	0 to 400 in H_2O	±.12%
Graduated Cylinder	0 to 200 mL	.5 mL
Scale	0 to 20 lbs	.005 lbs
Pressure Transducer (250)	0 to 250 psi	±.08% span
Pressure Transducer (500 psi)	0 to 500 psi	±.08% span
Proximity Probes	10 to 90 mils	±6.5%
Thermocouple	-200 to 350°C	1 °C

6.1 Density of Water

The density of water is found using the following equation:

$$1 - \left(\frac{(T + 288.9414)}{508929.2 * (T + 68.12963)}\right)(T - 3.9863)^2$$

The uncertainty of the density of water increases with the temperature as shown in Figure 6.1, with a maximum uncertainty of .001 g/cc at 115 °F.

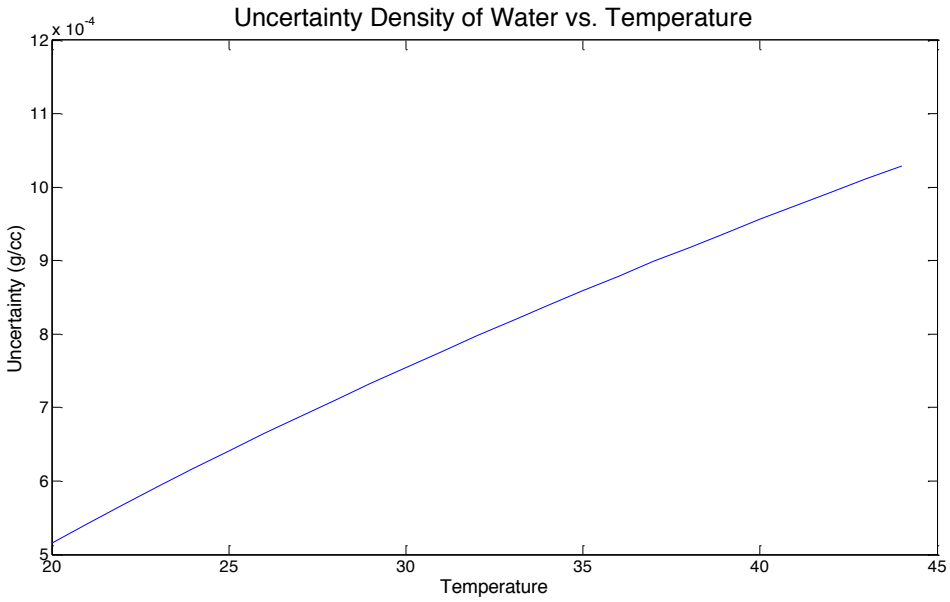

Figure 6.1 Uncertainty of water density measurement as a function of temperature.

6.2 Volume Flow Rate Feed Pump

The volumetric flow rate of the feed pump is calculated using equation 4.1.

$$Q_{FP} = 44.748 * d^2 * K * \sqrt{\Delta P_{OFM} / \rho_w} \qquad 4.1$$

The value of d is the orifice diameter, which is given and can be assumed to have an uncertainty of zero, K is a function of d, so it also has an uncertainty of zero. The uncertainty of the pressure difference is the error due to the differential pressure transmitter and is given in Table 6.1, and the uncertainty of the density of the water is shown in Figure 6.1. The uncertainty for the feed pump flow rate at BEP (1150 gpm) was found to be 1.33 gpm (.1 %).

6.3 Slurry Pump Volume Flow Rate

The slurry pump volume flow rate is calculated by the formula $Q = \frac{\dot{m}}{\rho}$, the uncertainty was calculated for a 40 gpm flow rate the pump run at during normal operating conditions is 0.05 gpm (.1%).

6.4 Hydraulic Power

The hydraulic power used $P = hQ/1714$, where h is the head in psi and Q is the sum of the slurry pump flow rate and the feed pump flow rate in gpm. The head is simply the difference between the outlet and inlet pressure and its uncertainty is a constant 0.45 psi. The uncertainty of the hydraulic power at BEP (115 HP) was calculated as 0.33 HP (.3 %).

6.5 Density of Sand

The density of sand was found using a graduated cylinder and a weighing scale. The formula for density is $\rho = {}^{m}/_{V}$, with the known error values of the scale and the cylinder the maximum error for the density of sand is found to be .0259 g/cc (6.8%).

6.6 Mass Flow Rate of Sand

The mass flow rate of sand is calculated using equation 4.5:

$$\dot{m}_s = \frac{\dot{m}_m - \frac{m_m}{\rho_m}\rho_w}{(1 - \frac{\rho_w}{\rho_s})} \qquad 4.5$$

The uncertainties of $\dot{m}_m$ and ρ_m are listed in Table 6.1 as .1% and .001 respectively. The uncertainty of sand is a function of temperature and can be seen in Figure 6.1 and the uncertainty of the density of the sand was calculated as .0259 g/cc. Given these numbers, at a flow rate of 55 gpm in the slurry pump, the uncertainty of the mass flow rate of sand is .43kg/min for a mass flow rate of approximately 4 kg/min (10%). The uncertainty of the mass flow rate of sand could be reduced by decreasing the mass flow rate of the slurry pump, which would effectively increase the mass flow rate of sand being measured; however, this option increases the chances of the sand settling in the pipe, which is undesired.

7. CONCLUSIONS

This work describes the design, operation and baseline testing of an Electrical Submersible Pump (ESP) erosion test rig in the Turbomachinery Laboratory. The erosion testing in this pump is done in an effort to "push the envelope" in machine life expectancy and performance. The final results of this investigation will take a long time to acquire and will be the subject of another student's thesis.

Due to depleted oil reservoirs around the world, oil companies are driving to find and extract oil from harder to reach places where environments are extreme and operation is costly. These extreme environments increase the cost of equipment changeover exponentially, hence the necessity to increase the equipment's lifespan. The project described will give oil companies, such as Shell, a tool to investigate the damages due to fine, un-filterable sands; not only on pumps, but a multitude of other equipment that requires it.

The study presented describes a test rig with the capability of introducing, measuring the concentration and separating sands as fine as 270 mesh (2 mil diameter). The rig provides enough flexibility to be used with a wide range of conditions and of equipment, including valves, seals, chokes and pumps. It can also be used in the future to investigate other types of pumps, not limited to ESPs.

This analysis described the running of the ESP with clean water and without the effects of sand erosion (0 run hours of sand). Performance data to generate pump curves was

taken and the pump's internal as well as external's vibration data was acquired and analyzed. The results found will be used in conjunction with the results found during and after erosion of the pump to draw conclusions that could help:

- Better understand the workings of an ESP and the erosion and abrasion effects on its performance and life expectancy.
- Recommend operating conditions or ranges to extend the life of the pump.
- Compare performance and vibration data to physical damage in the pump to allow the engineers to make inferences on the condition of the pump.
- Improve design of the pump.

The tested ESP's head generation and brake horsepower, when compared to the manufacturer's curves, was significantly higher, the reason for this merits further investigation. The efficiency of the pump, however, is similar to the efficiency specified by the manufacturer.

The vibration analysis indicates several trends such as the suspected resonant frequency at 1100 CPM. It also shows several traits that appear to be random and unexplained. The vibration data needs more detailed analysis and the pump should be modeled using software, such as XLTRC, to be able to draw conclusion about the behavior of the pump. The data from the accelerometers should be transformed, by integration, into velocity and displacement in an effort to obtain more useful and specific information, including possible correlations between the accelerometer and proximity probes. These correlations could help an engineer in the field make deductions on the internal

vibrations of a pump by analyzing the external (casing) accelerations. The unusually large runout on the first impeller should also be investigated further. Finally, the pump should be disassembled and the pump runout on each proximity probe location should be obtained using a lathe, the vibration data should then be retaken after assembly, and compared to the data prior to disassembly to correlate the runout or dynamic behavior to assembling variances. It is therefore recommended that the vibration data taken before, during and after erosion testing be analyzed by a student and a separate thesis be performed on the pump's rotor-dynamics.

This work has only skimmed the surface of the abundance of data and knowledge that could be gained during these experiments. The data and results obtained from these studies will help engineers make more educated decisions to extend the life of an ESP when running it deep-sea.

REFERENCES

[1] Takacs, G., "Electrical Submersible Pump Manual", First edition, Elsevier, Inc. 2009.

[2] Powers, M.L., "Effects of Speed Variation on Performance and Longevity of Electrical Submersible Pumps" SPE 14349, SPE Production Engineering, February 1987.

[3] Upchurch, E.R., "Analyzing Electric Submersible Pump Failures in the East Wilmington Field of California" 65th Annual Technical Conference and Exhibition of the Society of Petroleum Engineers, New Orleans, Louisiana, September 1990.

[4] Divine, D.L. Lannom, R.W. and Johnson, R.A., "Determining Pump Wear and Remaining Life from Electric Submersible Pump Test Curves" SPE 22399, Paper presented at the 1992 SPE Intl. Meeting on Petroleum Engineering, Beijing, China.

[5] Forder, A., Thew, M. and Harrison, D. "A Numerical Investigation of Solid Particle Erosion Experienced within Oilfield Control Valves". Elsevier Inc. 1997.

[6] True, M.E. and Weiner, P.D. "A Laboratory Evaluation of Sand Erosion of Oil and Gas Well Producing Equipment". Paper presented at the 1975 API Annual Meeting, Division of Production. Dallas, Texas.

[7] Tilly, G.P., "Sand Erosion of Metals and Plastics: A Brief Review". National Gas Turbine Establishment. Pyestock, Great Britain, July, 1969.

[8] Tavoularis, Stavros. "Measurement in Fluid Mechanics". First Edition, Cambridge University Press. 2005.

APPENDIX A

P&ID

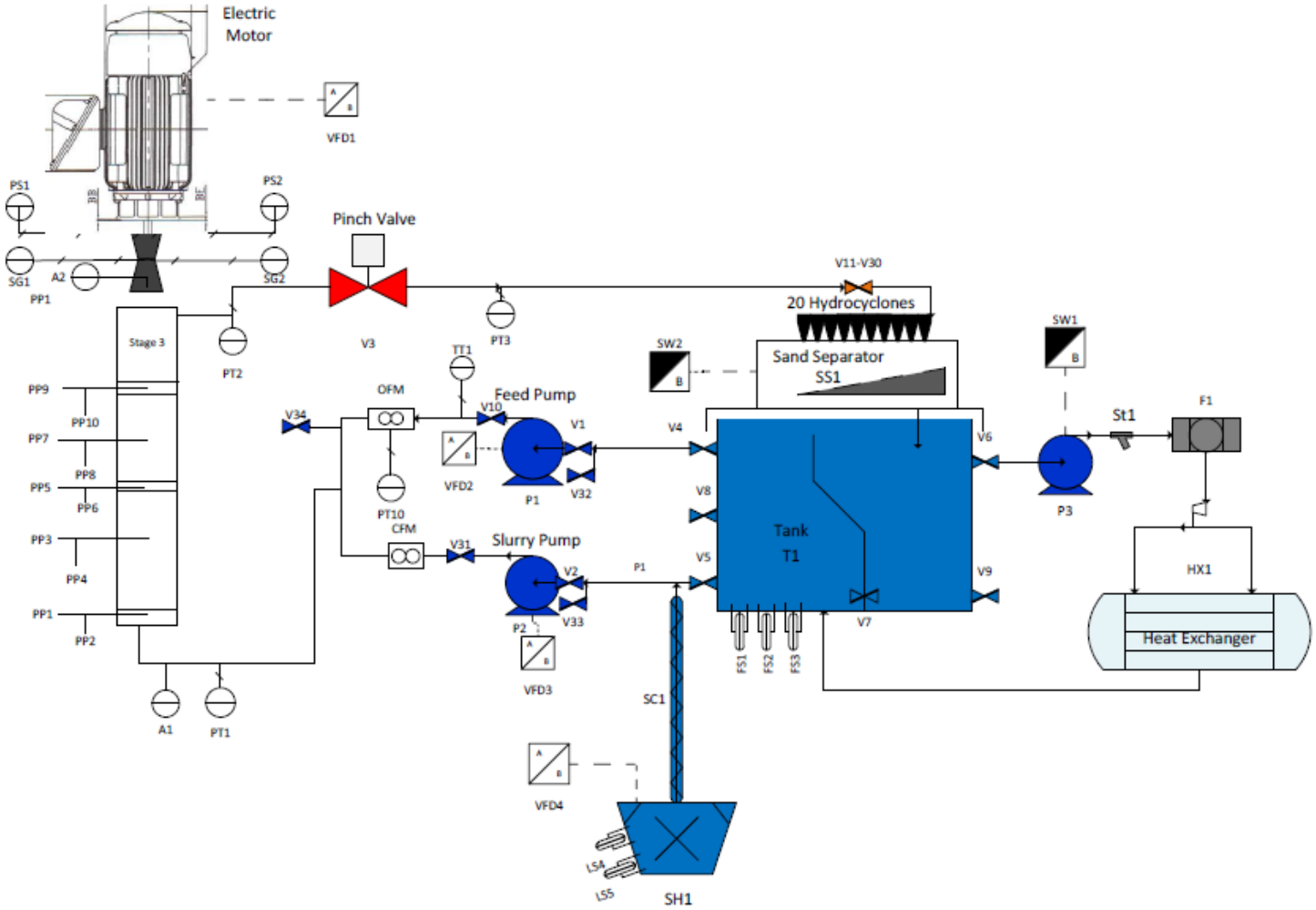
Electric Motor
VFD1
PS1
PS2
BB
BF
Pinch Valve
SG1
A2
SG2
PP1
V11-V30
20 Hydrocyclones
Stage 3
V3
PT3
SW2
Sand Separator
SS1
SW1
PT2
TT1
PP9
OFM
Feed Pump
V10
V1
V4
V6
St1
F1
PP10
V34
PP7
PP8
VFD2
P1
V32
V8
PP5
PP6
PT10
CFM
Tank
T1
P3
PP3
V31
Slurry Pump
V2
P1
V5
V9
HX1
PP4
PP1
P2
V33
V7
Heat Exchanger
PP2
FS1
FS2
FS3
VFD3
SC1
A1
PT1
VFD4
LS4
LS5
SH1

APPENDIX B

SEAL DRAWING

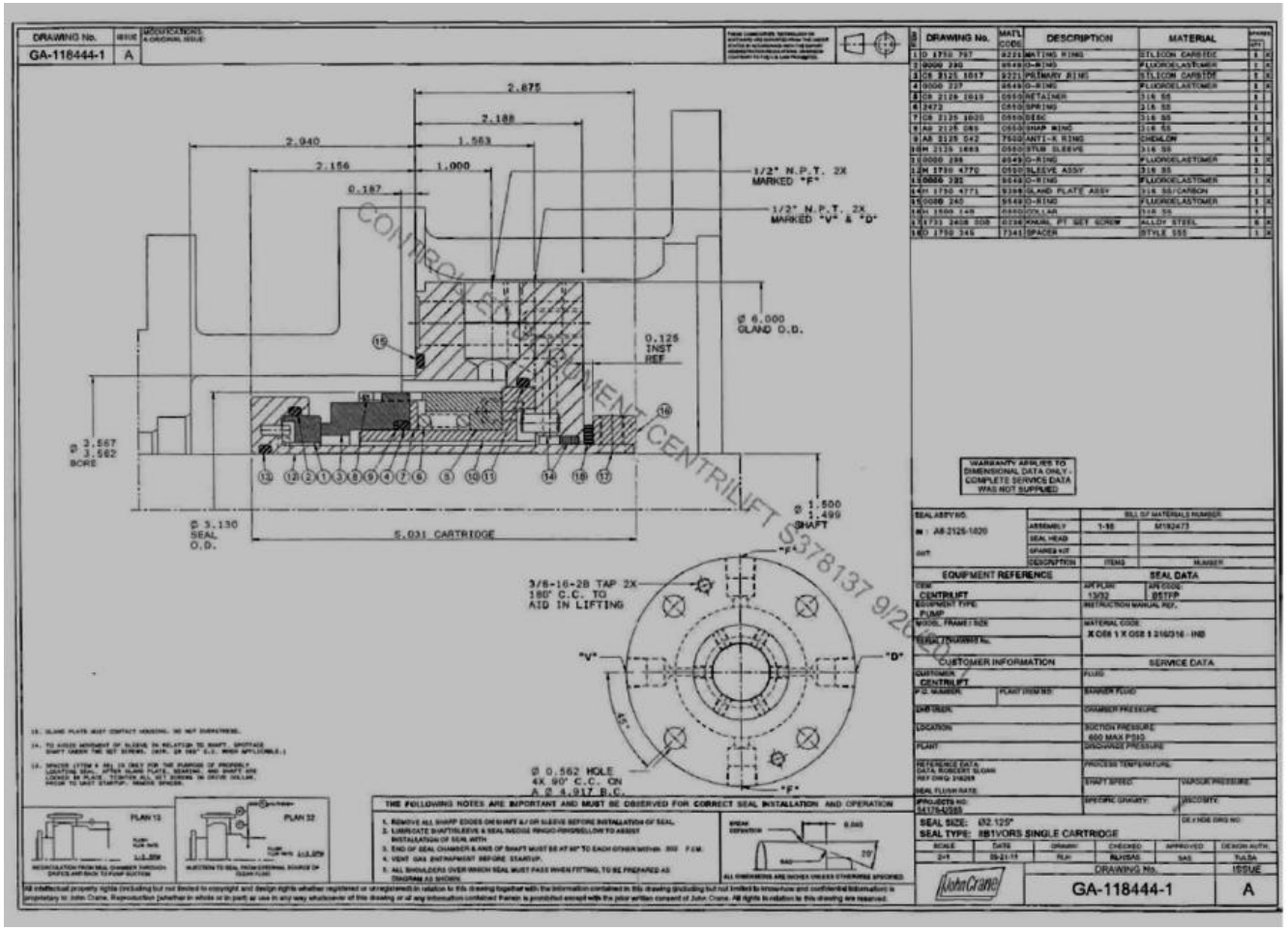

APPENDIX C

CALIBRATION CURVES

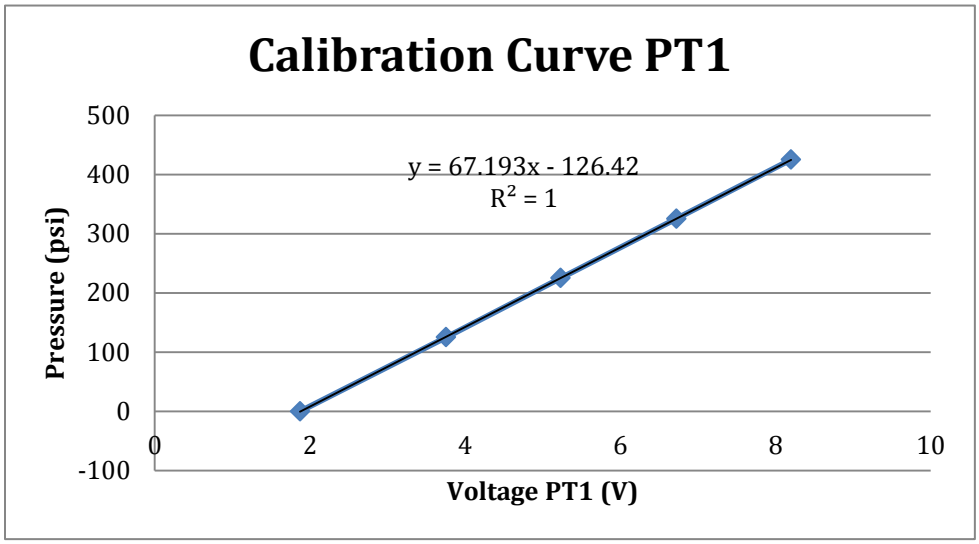

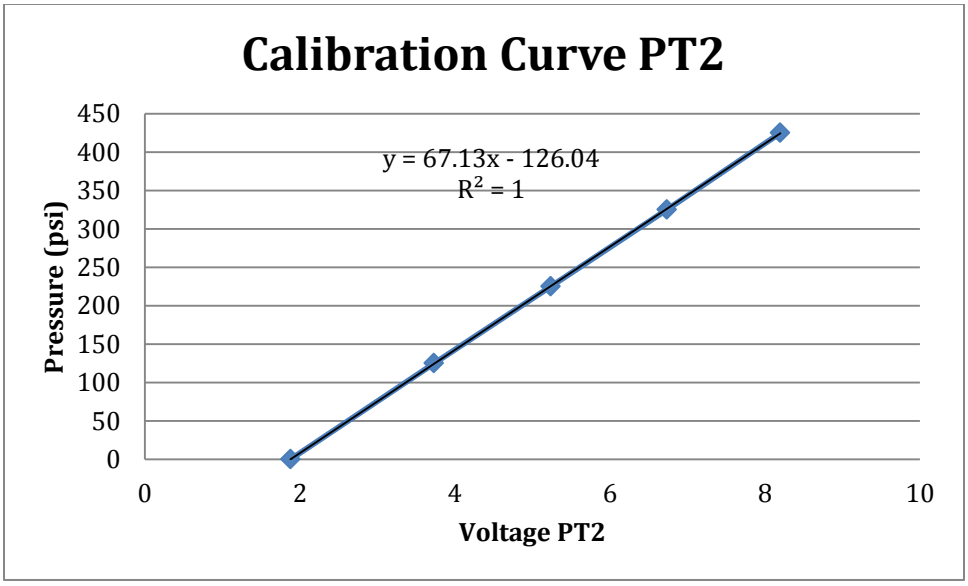

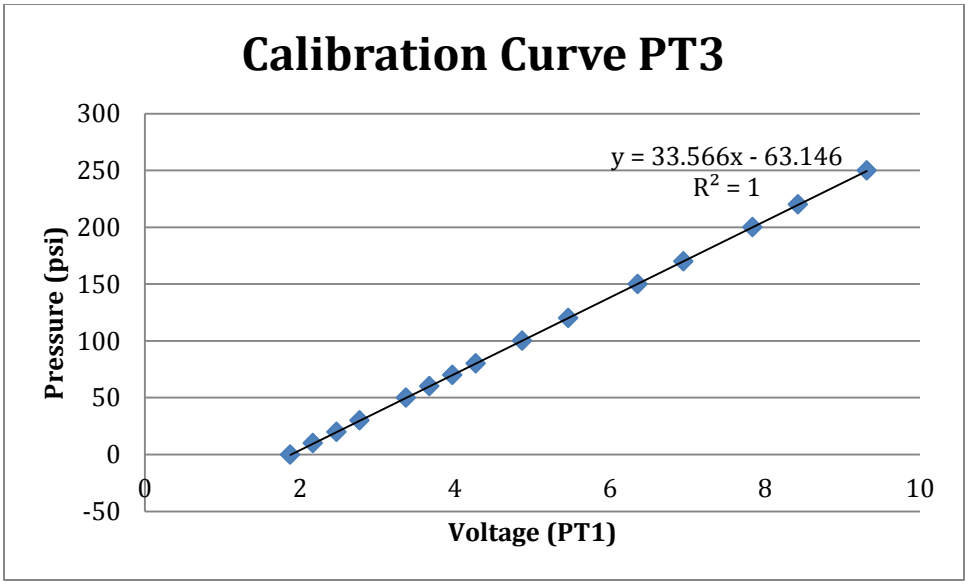
Calibration Curve PT3
y = 33.566x - 63.146
R² = 1
Pressure (psi)
300
250
200
150
100
50
0
-50
0
2
4
6
8
10
Voltage (PT1)

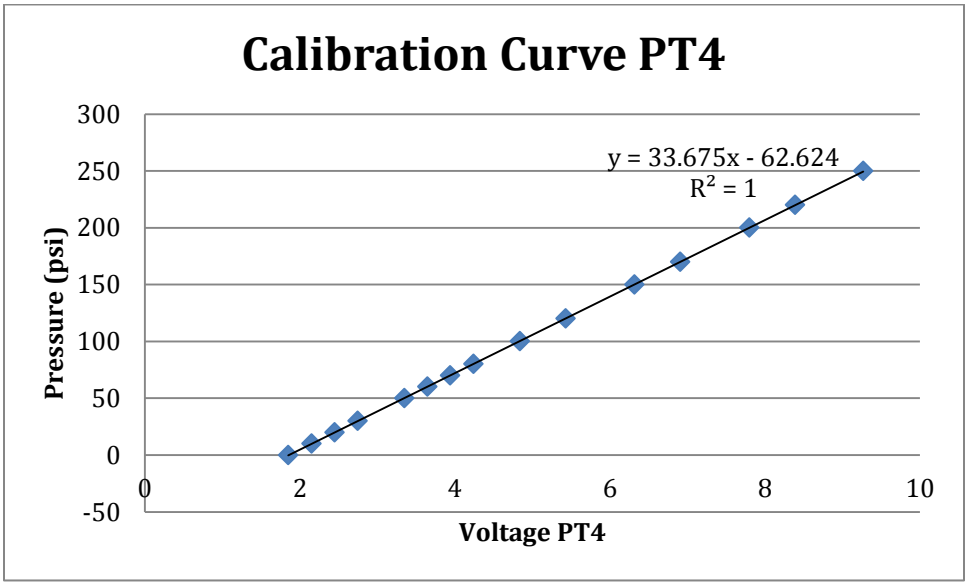
Calibration Curve PT4
y = 33.675x - 62.624
R² = 1
Pressure (psi)
300
250
200
150
100
50
0
-50
0
2
4
6
8
10
Voltage PT4

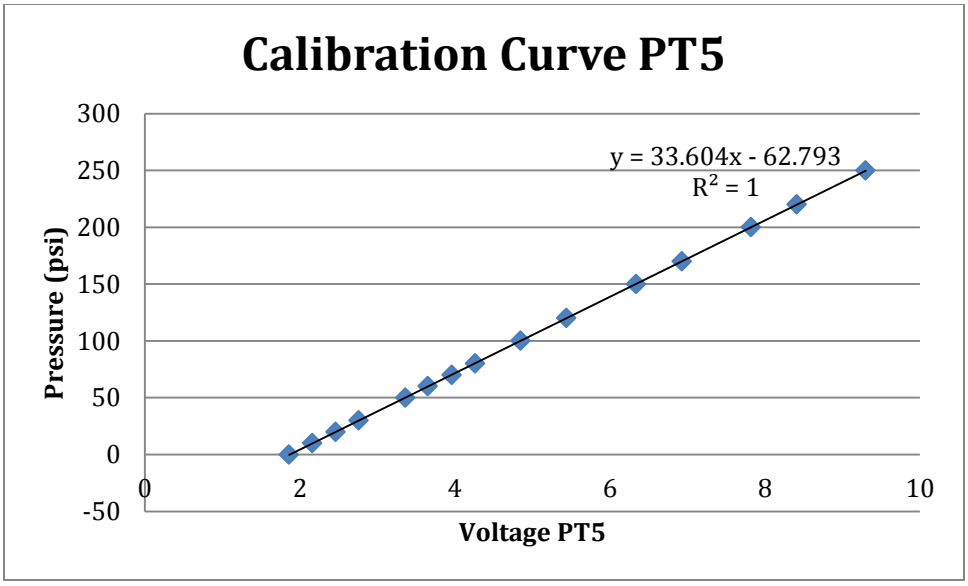
Calibration Curve PT5
y = 33.604x - 62.793
R² = 1
Pressure (psi)
300
250
200
150
100
50
0
-50
0
2
4
6
8
10
Voltage PT5

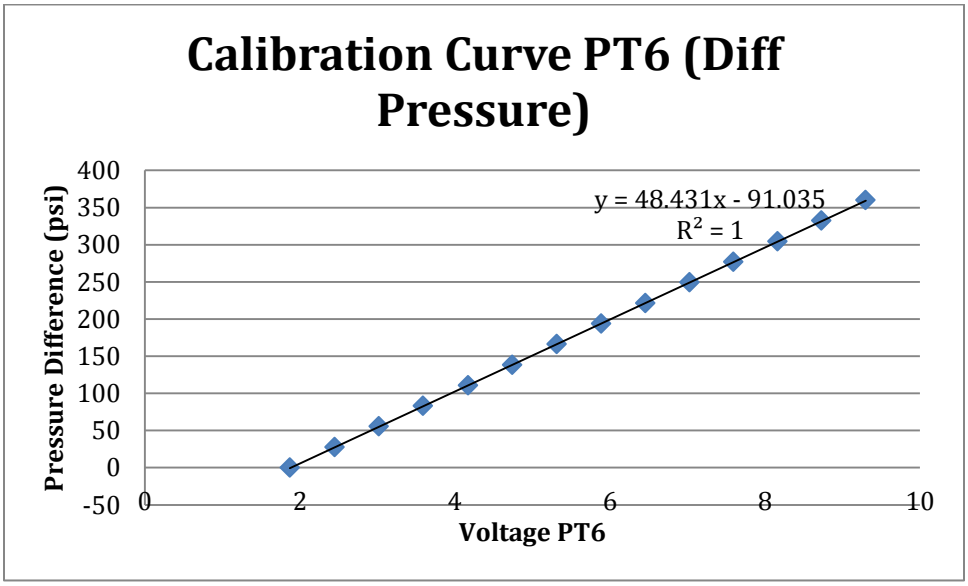
Calibration Curve PT6 (Diff Pressure)
y = 48.431x - 91.035
R² = 1
Pressure Difference (psi)
400
350
300
250
200
150
100
50
0
-50
0
2
4
6
8
10
Voltage PT6

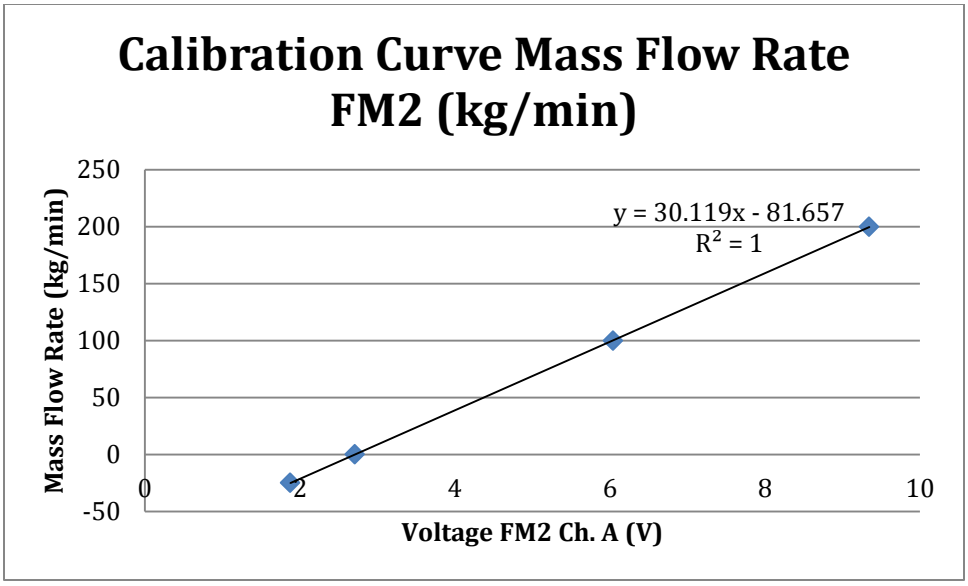
Calibration Curve Mass Flow Rate FM2 (kg/min)
Mass Flow Rate (kg/min)
250
200
150
100
50
0
-50
0
2
4
6
8
10
y = 30.119x - 81.657
R² = 1
Voltage FM2 Ch. A (V)

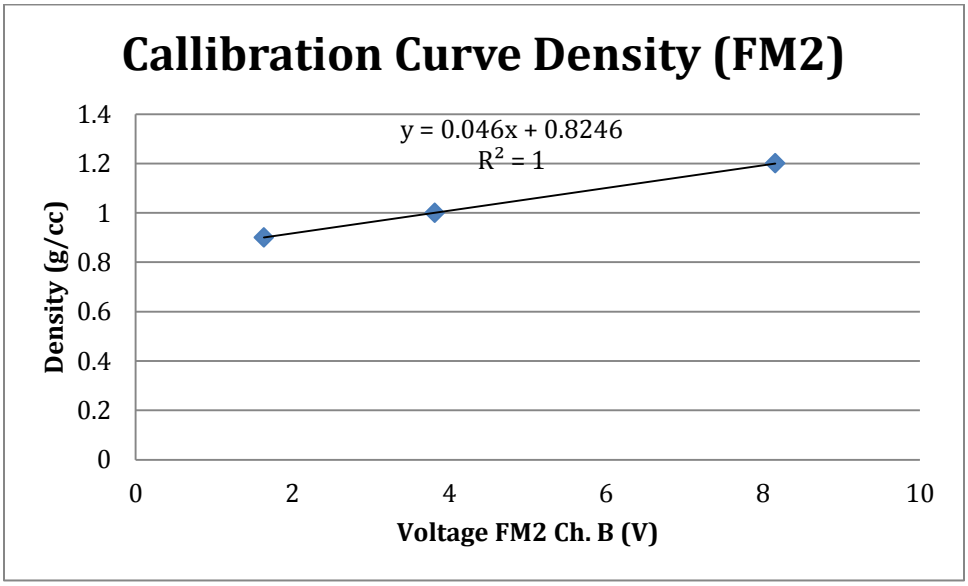
Callibration Curve Density (FM2)
Density (g/cc)
1.4
1.2
1
0.8
0.6
0.4
0.2
0
0
2
4
6
8
10
y = 0.046x + 0.8246
R² = 1
Voltage FM2 Ch. B (V)

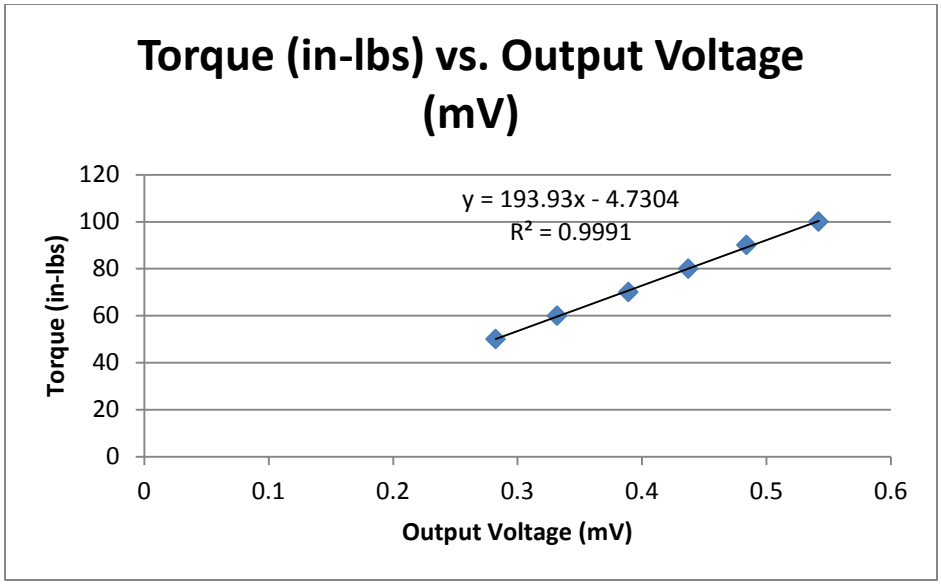
Torque (in-lbs) vs. Output Voltage (mV)
y = 193.93x - 4.7304
R² = 0.9991
Torque (in-lbs)
120
100
80
60
40
20
0
0
0.1
0.2
0.3
0.4
0.5
0.6
Output Voltage (mV)

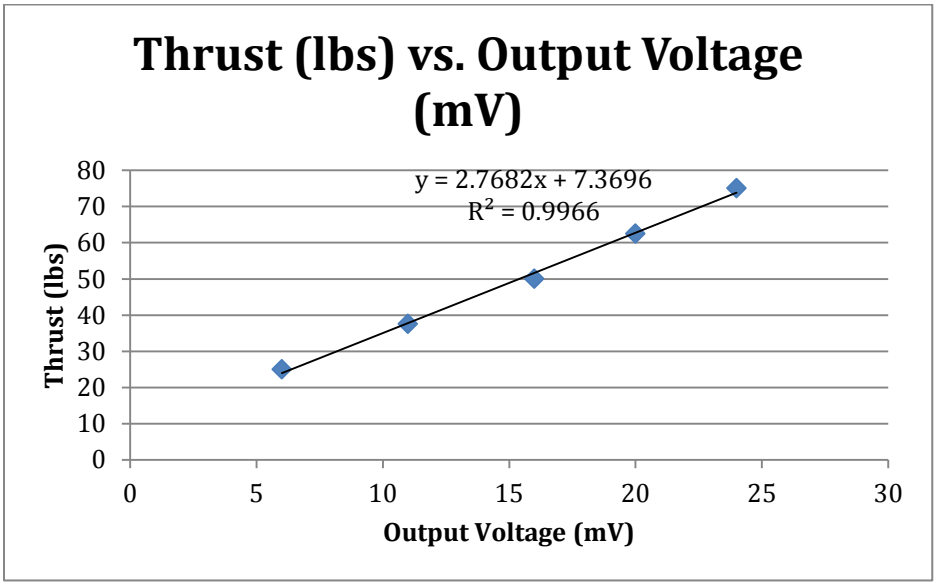
Thrust (lbs) vs. Output Voltage (mV)
y = 2.7682x + 7.3696
R² = 0.9966
Thrust (lbs)
80
70
60
50
40
30
20
10
0
0
5
10
15
20
25
30
Output Voltage (mV)

APPENDIX D

DEVELOPMENT OF SAND MASS FLOW RATE AND SAND CONCENTRATION EQUATIONS

The known values are ρ_m, $\dot{m}_m$, ρ_w, and ρ_s, where the subscript m is the mixture in the slurry pump (sand and water), w refers to the water in the slurry pump only, and s is the sand. With these values the mass flow rate of sand ($\dot{m}_s$) can be found and used to calculate the concentration.

The mass flow rate of the mixture is equal to the sum of the mass flow rate of the sand and the water: $\dot{m}_m = \dot{m}_s + \dot{m}_w$. Given that $\dot{m} = Q\rho$ and $Q_m = Q_s + Q_w$,

$$Q_m\rho_m = Q_s\rho_s + Q_w\rho_w$$

$$Q_m\rho_m = Q_s\rho_s + (Q_m - Q_s)\rho_w$$

$$Q_m\rho_m - Q_m\rho_w = \dot{m}_s - \dot{m}_s\frac{\rho_w}{\rho_s}$$

$$Q_m\rho_m - Q_m\rho_w = \dot{m}_s - \dot{m}_s\frac{\rho_w}{\rho_s}$$

$$\dot{m}_s = \frac{\dot{m}_m - \frac{\dot{m}_m}{\rho_m}\rho_w}{1 - \frac{\rho_w}{\rho_s}} \qquad 4.5$$

To calculate the concentration (g/lit): $C = {\dot{m}_s}/{Q_w}$ and $Q_w = Q_{FP} + (Q_m - Q_s)$, arranging for units:

$$C = 1000 \frac{\dot{m}_s}{3.785 Q_{FP} + \frac{(\dot{m}_m - \dot{m}_s)}{\rho_w}} \qquad 4.6$$

APPENDIX E

INSTRUMENTATION WIRING

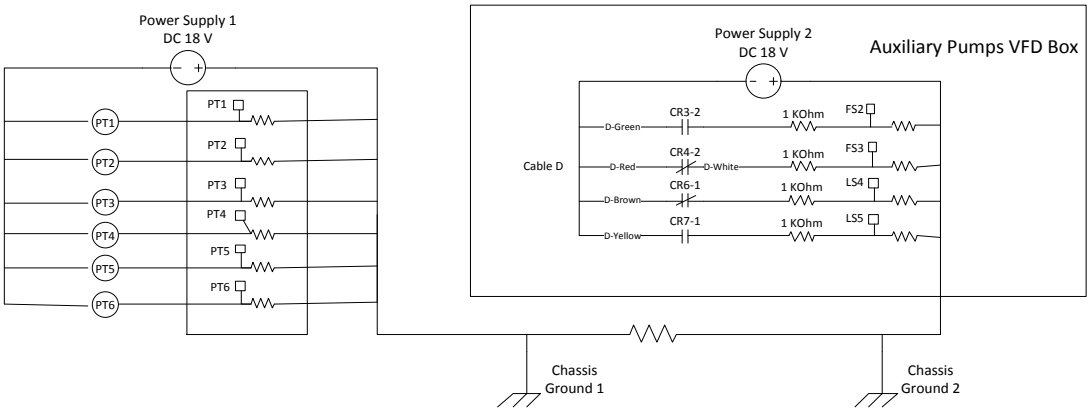

Figure E.1 Pressure transducers and level switches wiring diagram.

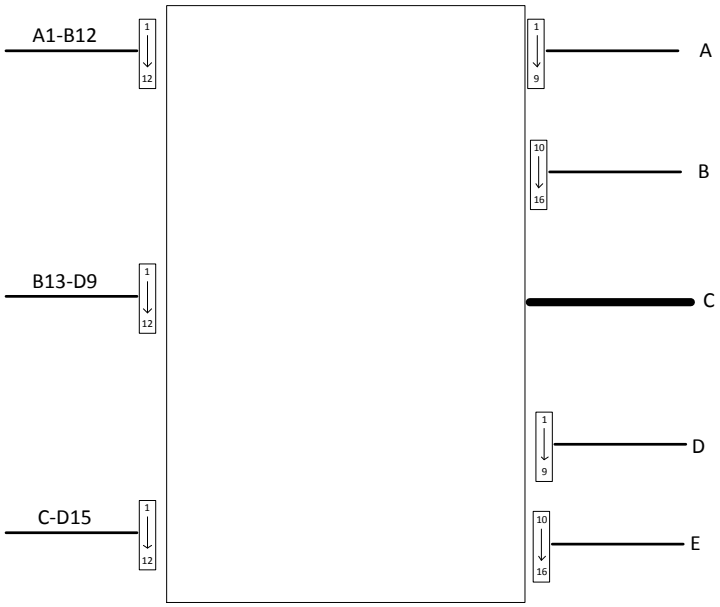

Figure E.2 Connections box cabling nomenclature (see Table E.1).

Table E.1 Connections box cable legend. Black lettering indicates first module single ended, red indicates first module differential, green indicates second module, yellow is third module and blue is not connected.

Number	Colors	Instrument	Instrument No.	NIQ Ch
A1	blue/black	Coriolis Flow Meter	FM2 (Mass FR)	Diff 0 (AI0,AI8)
A2	green/black	Coriolis Flow Meter	FM2 (Density)	Diff 1 (AI1,AI9)
A3	red/white	Pinch Valve Output	V3	Mod 2 AO 0 (0,1)
A4	brown/black			AI2
A5	yellow/black			AI10
A6	white/black			AI3
A7	red/black			AI11
A8	orange/black			AI4
A9	green/red			AI12
B-10	yellow/black	PT1 (Outlet Pressure)		AI5
B-11	red/black	PT2		AI13
B-12	blue/black	PT3		AI6
B-13	green/black	PT4		AI14
B-14	white/black	PT5 (Inlet Pressure)		AI7
B-15	brown/black			AI15
C	Coaxial	PT6 Diff Pressure Gauge (OFM)	FM1	Diff 21 (AI21,AI29)
D1	blue/black			AI16
D2	green/black	Tank Level Sensor (M)	FS2	AI24
D3	red/white	Tank Level Sensor (H)	FS3	AI17
D4	brown/black	Sand Level Sensor (L)	LS4	AI25
D5	yellow/black	Sand Level Sensor (M)	LS5	Diff 18 (AI18,AI26)
D6	white/black	VFD2 (Feed Pump) Output		Mod 3 AO0 (0,1)
D7	red/black	VFD2 (Feed Pump) Input		Diff 19 (Ai19,Ai27)
D8	orange/black	VFD3 (Slurry Pump) Output		Mod 3 AO1 (2,3)
D9	green/red	VFD3 (Slurry Pump) Input		Diff 20 (AI20,AI28)
E10	yellow/black	VFD4 output (Auger)	VFD4	Mod 2 AO1 (2,3)
E11	red/black	VFD4 input (Auger)	VFD4	Diff (AI22,AI30)
E12	blue/black			
E13	green/black			
E14	white/black			
E15	brown/black			

APPENDIX F

MATLAB PROGRAMS

Pump Curve Loading Data Program

```
clc
clear all
start=1
Sure=input('Are you sure this is the right data? (y/n)')

      %The columns in the file should be organized in the following
      %order ESP flow rate(m), ESP flow rate (dev), Head (m), Head
(dev),
      %Electrical Power (kW) with no columns after

    Last=input('What is the last row to be read?', 's');
   if isempty(Last)
       Last=150
  end
   PumpCurveData= xlsread('E:\Tamu\Turbolab\Data\Matlab\Pump
Curve\PumpCurveData1.xlsx','Untitled',['a2:e',num2str(Last)]);  %Select
file and data range
```

Pump Curve Program

```
clc
clear ImpData y
close all
start=1;
T=.0002;

RPM=input('What is the RPM of the test?');
if isempty(RPM)
  RPM=3600
end
Title=['Pump Curve at ', num2str(RPM), ' RPM']

l=length(PumpCurveData(:,1))
for n=l:-1:1
      if PumpCurveData(n,2)>12 || PumpCurveData(n,4)>10   %Delete all
rows with high standard deviations in head or flow
          PumpCurveData(n,:)=[];
      end
end
```

```
  ImpData(:,1)=PumpCurveData(:,1);                          %Flow Rate is
First Column
  ImpData(:,2)=PumpCurveData(:,3);                          %Head is Third
Column
  ImpData(:,3)=(PumpCurveData(:,5)*1.3)*.936;                  %Electrical
Power from the fifth column is changed to BHP
  ImpData(:,5)=(ImpData(:,1).*ImpData(:,2))/1714;           %Fluid
Horsepower is calculated from Head and Flow Rate
  ImpData(:,4)=ImpData(:,5)./ImpData(:,3);                  %Efficiency is
calculated using fluid HP and Electrical HP


  x=ImpData(:,1);
y(:,1)=ImpData(:,2);    %y1=head
y(:,2)=ImpData(:,3);    %y2=Brake Horsepower
y(:,3)=ImpData(:,4);    %y3=Efficiency



Sel=input('What do you want to plot? 1: Total Curve, 2: Per Stage
Curve');


 if Sel==1


figure (1)
set(gca,'FontSize',20);
[ax, h1, h2]=plotyy(x,y(:,1),x,y(:,3));
set(ax(2),'FontSize',20);
hold all
h3=plot(x,y(:,2));
set(get(ax(1),'Ylabel'),'String','Head (psi), Brake Horsepower
(HP)','FontSize',20);
set(ax(1),'XColor','black','YColor','black')

set(get(ax(2),'Ylabel'),'String','Efficiency','FontSize',20)

ylim(ax(2),[0 1]);
yl=get(gca,'YLim');
ylim(ax(1),[yl(1)/2 yl(2)*1.5]);
set(ax(2),'YTickMode','Auto');
set(ax(1),'YTickMode','Auto');
xlabel('Flow Rate (GPM)');
title([Title, ' Three Stages']);
set(h1,'LineStyle','*');
set(h2,'linestyle','.','MarkerEdgeColor','g');
set(h3,'linestyle','d','MarkerEdgeColor','r');
yl=get(gca,'YLim');
ylim(ax(1),[50 550]);
axes(ax(2))
```

```
leg=legend('Efficiency','Head','Brake Horsepower');
set(leg,'color','white');
grid(ax(1),'on')

  end

  if Sel==2

y(:,1)=y(:,1)/3;
y(:,2)=y(:,2)/3;

figure (1)
set(gca,'FontSize',20);
[ax, h1, h2]=plotyy(x,y(:,1),x,y(:,3));
set(ax(2),'FontSize',20);
hold all
h3=plot(x,y(:,2));
set(get(ax(1),'Ylabel'),'String','Head (psi), Brake Horsepower
(HP)','FontSize',20);
set(ax(1),'XColor','black','YColor','black')

set(get(ax(2),'Ylabel'),'String','Efficiency','FontSize',20)
ylim(ax(2),[0 1]);
yl=get(gca,'YLim');
ylim(ax(1),[yl(1)/2 yl(2)*1.5]);
set(ax(2),'YTickMode','Auto');
set(ax(1),'YTickMode','Auto');
xlabel('Flow Rate (GPM)');
title([Title, ' One Stage']);
set(h1,'LineStyle','*');
set(h2,'linestyle','.','MarkerEdgeColor','g');
set(h3,'linestyle','d','MarkerEdgeColor','r');
set(ax(1),'YLimMode','Auto')
yl=get(gca,'YLim');
ylim(ax(1),[0 100]);
axes(ax(2))
leg=legend('Efficiency','Head','Brake Horsepower');
set(leg,'color','white');
grid(ax(1),'on')



end
set([ax(1) ax(2)], 'XTickMode', 'Auto');
xlim([ax(2)],'auto');
xlim([ax(1)],'auto');
```

Pump Curve Comparison Program

```
clc
```

```
clear ImpData y Phead PEff PElPow x Difhead DifEff DifElPow
close all
start=1;
T=.0002;

% This program provides a way to compare the any obtained pump curve to
a
% pump curve obtained when the pump was brand new.  The results
obtained
% will be in percent difference with respect to baseline.


%Load data using the Load_data_from_excel_file in the same folder.



RPM=input('What is the RPM of the test?');
if isempty(RPM)
  RPM=3600
end
Title=['Pump Curve at ', num2str(RPM), ' RPM']


l=length(PumpCurveData(:,1));
for n=l:-1:1
      if PumpCurveData(n,2)>12 || PumpCurveData(n,4)>10   %Delete all
rows with high standard deviations in head or flow
          PumpCurveData(n,:)=[];
      end
end

  ImpData(:,1)=PumpCurveData(:,1);                        %Flow Rate is
First Column
  ImpData(:,2)=PumpCurveData(:,3);                        %Head is Third
Column
  ImpData(:,3)=PumpCurveData(:,5)*1.3*.936;                   %Electrical
Power from the fifth column is changed to BHP
  ImpData(:,5)=(ImpData(:,1).*ImpData(:,2))/1714;         %Fluid
Horsepower is calculated from Head and Flow Rate
  ImpData(:,4)=ImpData(:,5)./ImpData(:,3);                %Efficiency is
calculated using fluid HP and Electrical HP


x=ImpData(:,1);
y(:,1)=ImpData(:,2);    %y1=head
y(:,2)=ImpData(:,3);    %y2=Electrical Power
y(:,3)=ImpData(:,4);    %y3=Efficiency


figure (1)
set(gca,'FontSize',20);
```

```
[ax, h1, h2]=plotyy(x,y(:,1),x,y(:,3));
set(ax(2),'FontSize',20)
hold all
h3=plot(x,y(:,2));
set(get(ax(1),'Ylabel'),'String','Head (psi), Brake Horsepower
(HP)','FontSize',20);
set(ax(1),'XColor','black','YColor','black')

set(get(ax(2),'Ylabel'),'String','Efficiency','FontSize',20)
ylim(ax(2),[0 1]);
yl=get(gca,'YLim');
ylim(ax(1),[50 550]);
set(ax(2),'YTickMode','Auto');
set(ax(1),'YTickMode','Auto');
xlabel('Flow Rate (GPM)');
title([Title, ' Three Stages']);
set(h1,'LineStyle','*');
set(h2,'linestyle','.','MarkerEdgeColor','g');
set(h3,'linestyle','d','MarkerEdgeColor','r');



headfit=fit(x,y(:,1),'poly2');
ElPowfit=fit(x,y(:,2),'poly2');
Efffit=fit(x,y(:,3),'poly2');







chead= [8.377e-007    -0.1398   344.9];  % Baseline Coefficient values
of curve fit for head (taken from first test)
cElPow=[ -3.655e-005   0.104  90.13];
cEfffit=[-5.054e-007   0.001079   0.1888];

for i=1:length(x)
    Phead(i)=(chead(1)*(x(i))^2)+(chead(2)*(x(i)))+chead(3);
    Difhead(i)=((Phead(i)-y(i,1))/(y(i,1)))*100;
    PElPow(i)=(cElPow(1)*(x(i))^2)+(cElPow(2)*(x(i)))+cElPow(3);
    DifElPow(i)=((PElPow(i)-y(i,2))/(y(i,2)))*100;
    PEff(i)=(cEfffit(1)*(x(i))^2)+(cEfffit(2)*(x(i)))+cEfffit(3);
    DifEff(i)=((PEff(i)-y(i,3))/(y(i,3)))*100;

end
percdifferencehead=mean(Difhead);       %Difference between the current
pump curve and the baseline curve in Percent
maxdifferencehead=max(Difhead);
percdifferenceElPow=mean(DifElPow);      %Difference between the
current pump curve and the baseline curve in Percent
maxdifferenceElPow=max(DifElPow);
```

```
percdifferenceEff=mean(DifEff);        %Difference between the current
pump curve and the baseline curve in Percent
maxdifferenceEff=max(DifEff);

figure (1)
hold all
plot(x,Phead, 'b-')
plot(x,PElPow, 'r-')
set(ax(1),'YLimMode','Auto')
yl=get(gca,'YLim');
ylim(ax(1),[50 550]);
axes(ax(2))
hold all
plot(x,PEff, 'g-')
leg=legend('Efficiency','Baseline Eff','Head','Brake
Horsepower','Baseline Head','Baseline BHP');
set(leg,'FontSize',14)
set(leg,'color','white')
set([ax(1) ax(2)], 'XTickMode', 'Auto');
xlim([ax(2)],'auto');
xlim([ax(1)],'auto');
%Create matrix with Percent Difference and Max Difference
Diff(1,1)=percdifferencehead;
Diff(1,2)=maxdifferencehead;
Diff(2,1)=percdifferenceElPow;
Diff(2,2)=maxdifferenceElPow;
Diff(3,1)=percdifferenceEff;
Diff(3,2)=maxdifferenceEff;

grid(ax(1),'on')
```

Accelerometer Program

```
%Plot fft and/or time domain in pairs of prox probes
clc
clear x fft l acctodisp
close all
T=.0002

RPMq=input('What is the RPM?','s');
    if strcmp(RPMq,'0')||isempty(RPMq)
        RPMq=RPM;
    end
    RPM=RPMq
Sure=input('Have you loaded the correct data to the Data file?', 's');
SF=input(['Is ',num2str(1/(1000*T)),'kHz your sampling frequency?'],
's');
if strcmp(SF,'n')
        T=str2num(input('What is the sampling rate (in seconds)?','s'))
end
```

```
Plt=input(['What do you want to plot? 1: Time domain, 2: FFT, 3
Displacement FFT'], 's');
l=1000
lfft=500
File='.fig'

if isempty(Sure)||strcmp(Sure,'y')||strcmp(Sure,'Y')


  if str2num(Plt)== 1
for j=12:3:15  %Plot Accelerometers in time domain
    figure(j-11)
    subplot(2,2,[1 3]); plot(Data(1:l,1),Data(1:l,j));
    title(['A',num2str(j-11)],'FontSize',16);
    ylabel('Acceleration (g)','FontSize',16);    xlabel('time
(s)','FontSize',16);
    subplot(2,2,2); plot(Data(1:l,1),Data(1:l,j+1));
    title(['A',num2str(j-10)],'FontSize',16)
    ylabel('Acceleration (g)','FontSize',16);    xlabel('time
(s)','FontSize',16);
    subplot(2,2,4); plot(Data(1:l,1),Data(1:l,j+2));
    title(['A',num2str(j-9)],'FontSize',16)
    ylabel('Acceleration (g)','FontSize',16);    xlabel('time
(s)','FontSize',16);

    [ax4,h3]=suplabel( ['Time Domain A',num2str(j-11),', A',num2str(j-
10), ' and A',num2str(j-9),' at ', num2str(RPM), ' RPM'],'t');
    set(h3,'FontSize',20);
    pos1=get(h11,'OuterPosition');
    pos3=get(h33,'OuterPosition');
    set(h33,'OuterPosition',[(pos3(1)+(pos3(3)-pos1(3))/2)
(pos3(2)+(pos3(4)-pos1(4))/2) pos1(3) pos1(4)]);
    end
  end
  if str2num(Plt)==2
    for m=2:17  %Do fft
        x=Data(:,m);
    [y,f, ang]=fft_data(x,T);  %Perform FFT
    fft(:,1)=f;
    fft(:,m)=y;
    end

    for j=12:3:15  %Plot Accelerometers
    figure(j-1)
    h11=subplot(2,2,1); plot(fft(2:lfft,1),fft(2:lfft,j));
    title(['A',num2str(j-11)],'FontSize',16);
    ylabel('Acceleration (g pk-pk)','FontSize',16);
xlabel(['Frequency (CPM)'],'FontSize',16);
    h22=subplot(2,2,2); plot(fft(2:lfft,1),fft(2:lfft,j+1));
    title(['A',num2str(j-10)],'FontSize',16);
    ylabel('Acceleration (g pk-pk)','FontSize',16);
xlabel(['Frequency (CPM)'],'FontSize',16);
    h33=subplot(2,2,[3 4]); plot(fft(2:lfft,1),fft(2:lfft,j+1));
```

```
    title(['A',num2str(j-9)],'FontSize',16);
    ylabel('Acceleration (g pk-pk)','FontSize',16);
xlabel(['Frequency (CPM)'],'FontSize',16);
    [ax4,h3]=suplabel( ['FFT A',num2str(j-11),', A',num2str(j-10), '
and A',num2str(j-9),' at ', num2str(RPM), ' RPM'],'t');
    hh=[h11 h22 h33];
    set(hh,'ylim',[0 .2])
    set(h3,'FontSize',20);

    pos1=get(h11,'OuterPosition');
    pos3=get(h33,'OuterPosition');
    set(h33,'OuterPosition',[(pos3(1)+(pos3(3)-pos1(3))/2)
(pos3(2)+(pos3(4)-pos1(4))/2) pos1(3) pos1(4)]);
    end
  end

  if str2num(Plt)==3
    for j=12:3:15  %Plot Accelerometers
        x=Data(:,m);
    [y,f, ang]=fft_data(x,T);  %Perform FFT
    fft(:,1)=f;
    fft(:,2)=y;
    fft(:,3)=ang;
    acctodisp(:,1)=fft(:,1);
    acctodisp(:,m)=fft(:,m)*386400./(2*pi*acctodisp(:,1));




    figure(j-1)
    h11=subplot(2,2,1); plot(acctodisp(3:lfft,1),acctodisp(3:lfft,j));
    title(['A',num2str(j-11)],'FontSize',16);
    ylabel('Displacement (mils pk-pk)','FontSize',16);
xlabel(['Frequency (CPM)'],'FontSize',16);
    h22=subplot(2,2,2);
plot(acctodisp(3:lfft,1),acctodisp(3:lfft,j+1));
    title(['A',num2str(j-10)],'FontSize',16);
    ylabel('Displacement (mils pk-pk)','FontSize',16);
xlabel(['Frequency (CPM)'],'FontSize',16);
    h33=subplot(2,2,[3 4]);
plot(acctodisp(3:lfft,1),acctodisp(3:lfft,j+2));
    title(['A',num2str(j-9)],'FontSize',16);
    ylabel('Displacement (mils pk-pk)','FontSize',16);
xlabel(['Frequency (CPM)'],'FontSize',16);
    [ax4,h3]=suplabel( ['Displacement of Casing Frequency Domain,
A',num2str(j-11),', A',num2str(j-10), ' and A',num2str(j-9),' at ',
num2str(RPM), ' RPM'],'t');

    set(h3,'FontSize',20);
    linkaxes([h11 h22 h33],'y');
    set(h11, 'ylim', [0 10]);
```

```
    pos1=get(h11,'OuterPosition');
    pos3=get(h33,'OuterPosition');
    set(h33,'OuterPosition',[(pos3(1)+(pos3(3)-pos1(3))/2)
(pos3(2)+(pos3(4)-pos1(4))/2) pos1(3) pos1(4)]);

%     saveas(figure(j-1),[['FFT A',num2str(j-11),', A',num2str(j-10), '
and A',num2str(j-9),' at ', num2str(RPM), ' RPM'] File])
    end
  end

end
```

FFT Program

```
function [y,f, ang]=fft_data(x,T)
clear f
%   Function to perform FFT analysis on discrete signal x sampled at
time T


y=fft(x); len=length(x);

%   Form a frequency scale:
fmax=1/T; f=linspace(0,fmax,len);
%   Discard second half of points:
f(floor(len/2):len)=[]; y(floor(len/2):len)=[];
ang = angle(y);
%   Adjust amplitude
y=abs(y*2/length(x));
f=f*60;


if(nargout == 2)
    ang = [];
end
```

Impeller Prox Probe Program

```
%Plot fft and/or time domain in pairs of prox probes
clc
clear x fft l h
close all
T=.0002

Titleq=input('Type the title (0 or enter for same)','s');
    if strcmp(Titleq,'0')||isempty(Titleq)
```

```
        Titleq=Title
    end
    Title=Titleq
Sure=input('Have you loaded the correct data to the Data file?', 's');
SF=input(['Is ',num2str(1/(1000*T)),'kHz your sampling frequency?'],
's');
if strcmp(SF,'n')
        T=str2num(input('What is the sampling rate (in seconds)?','s'))
end
Plt=input(['What do you want to plot? 1: Time domain, 2: FFT'], 's');
l=1750
lfft=750
disc=19999
start=1

x(:,:)=Data(start:disc,:);

if isempty(Sure)||strcmp(Sure,'y')||strcmp(Sure,'Y')



  if str2num(Plt)== 1

    figure(1)
    h(1)=subplot(2,2,1); plot(Data(1:l,1),Data(1:l,4),'b-');
xlabel('PP3','FontSize',20);

    h(2)=subplot(2,2,2); plot(Data(1:l,1),Data(1:l,5),'b-');
xlabel(['PP4'],'FontSize',20);

    h(3)=subplot(2,2,3); plot(Data(1:l,1),Data(1:l,8),'b-');
xlabel(['PP7'],'FontSize',20);

    h(4)=subplot(2,2,4); plot(Data(1:l,1),Data(1:l,9),'b-');
xlabel(['PP8'],'FontSize',20);
     set(h,'FontSize',16)
    [ax1,h1]=suplabel('time(s)');
    [ax2,h2]=suplabel('Displacement (mils)', 'y');
    [ax4,h3]=suplabel( ['Time Domain ' Title],'t');
    set(h3,'FontSize',24);
    set(h1,'FontSize',20);
    set(h2,'FontSize',20);




  end
  if str2num(Plt)==2
    for m=2:11  %Do fft
        x=Data(:,m);
    [y,f, ang]=fft_data(x,T);  %Perform FFT
```

```
    fft(:,1)=f;
    fft(:,m)=y;
    end

     %Plot Internal Proximity Probes
     figure(1)
    h(1)=subplot(2,2,1); plot(fft(2:lfft,1),fft(2:lfft,4));
xlabel('PP3','FontSize',20);
    h(2)=subplot(2,2,2); plot(fft(2:lfft,1),fft(2:lfft,5));
xlabel(['PP4'],'FontSize',20);
    h(3)=subplot(2,2,3); plot(fft(2:lfft,1),fft(2:lfft,8));
xlabel(['PP7'],'FontSize',20);
    h(4)=subplot(2,2,4); plot(fft(2:lfft,1),fft(2:lfft,9));
xlabel(['PP8'],'FontSize',20);
       [ax1,h1]=suplabel('Frequency (CPM)');
    [ax2,h2]=suplabel('Amplitude (mils peak to peak)','y');
    [ax4,h3]=suplabel( ['FFT Impellers ' Title,],'t');
    set(h3,'FontSize',24);
    set(h2,'FontSize',20);
    set(h1,'FontSize',20);
    set(h,'FontSize',16)

%     saveas(figure(j-1),[Title, ' FFT PP',num2str(j-1), ' and
PP',num2str(j), File])

  end

for j=1:2:3
    lim1=get(h(j),'ylim');
    lim2=get(h(j+1),'ylim');
    maxy=max(lim1,lim2);
    linkaxes([h(j) h(j+1)],'y');
    set(h(j), 'ylim', maxy);
end

end
```

Shaft Prox Probe Program

```
%Plot fft and/or time domain in pairs of prox probes
clc
clear x fft l h
close all
T=.0002

Titleq=input('Type the title (0 or enter for same)','s');
    if strcmp(Titleq,'0')||isempty(Titleq)
        Titleq=Title
    end
    Title=Titleq
```

```
Sure=input('Have you loaded the correct data to the Data file?', 's');
SF=input(['Is ',num2str(1/(1000*T)),'kHz your sampling frequency?'],
's');
if strcmp(SF,'n')
        T=str2num(input('What is the sampling rate (in seconds)?','s'))
end
Plt=input(['What do you want to plot? 1: Time domain, 2: FFT'], 's');
l=3500
lfft=750
File='.emf'

if isempty(Sure)||strcmp(Sure,'y')||strcmp(Sure,'Y')

    for j=2:11
        Data(:,j)=Data(:,j)-mean(Data(:,j));
    end

  if str2num(Plt)== 1

    figure(1)
    h(1)=subplot(3,2,1); plot(Data(1:l,1),Data(1:l,2));
xlabel('PP1','FontSize',20);
    h(2)=subplot(3,2,2); plot(Data(1:l,1),Data(1:l,3));
xlabel(['PP2'],'FontSize',20);
    h(3)=subplot(3,2,3); plot(Data(1:l,1),Data(1:l,6));
xlabel(['PP5'],'FontSize',20);
    h(4)=subplot(3,2,4); plot(Data(1:l,1),Data(1:l,7));
xlabel(['PP6'],'FontSize',20);
    h(5)=subplot(3,2,5); plot(Data(1:l,1),Data(1:l,10));
xlabel(['PP9'],'FontSize',20);
    h(6)=subplot(3,2,6); plot(Data(1:l,1),Data(1:l,11));
xlabel(['PP10'],'FontSize',20);
    set(h,'FontSize',16)
    [ax1,h1]=suplabel('time(s)');
    [ax2,h2]=suplabel('Displacement (mils)', 'y');
    [ax4,h3]=suplabel( ['Time Domain ' Title],'t');
    set(h3,'FontSize',24);
    set(h1,'FontSize',20);
    set(h2,'FontSize',20);


%     saveas(figure(j-1),[Title, ' Time Domain PP',num2str(j-1), ' and
PP',num2str(j), File])

  end
  if str2num(Plt)==2
    for m=2:11  %Do fft
        x=Data(:,m);
    [y,f, ang]=fft_data(x,T);  %Perform FFT
    fft(:,1)=f;
    fft(:,m)=y;
    end
```

```
     %Plot Internal Proximity Probes
     figure(1)
    h(1)=subplot(3,2,1); plot(fft(1:lfft,1),fft(1:lfft,2));
xlabel('PP1','FontSize',20);
    h(2)=subplot(3,2,2); plot(fft(1:lfft,1),fft(1:lfft,3));
xlabel(['PP2'],'FontSize',20);
    h(3)=subplot(3,2,3); plot(fft(1:lfft,1),fft(1:lfft,6));
xlabel(['PP5'],'FontSize',20);
    h(4)=subplot(3,2,4); plot(fft(1:lfft,1),fft(1:lfft,7));
xlabel(['PP6'],'FontSize',20);
    h(5)=subplot(3,2,5); plot(fft(1:lfft,1),fft(1:lfft,10));
xlabel(['PP9'],'FontSize',20);
    h(6)=subplot(3,2,6); plot(fft(1:lfft,1),fft(1:lfft,11));
xlabel(['PP10'],'FontSize',20);
    [ax1,h1]=suplabel('Frequency (CPM)');
    [ax2,h2]=suplabel('Amplitude (mils peak to peak)','y');
    [ax4,h3]=suplabel( ['FFT Shafts ' Title,],'t');
    set(h3,'FontSize',24);
    set(h2,'FontSize',20);
    set(h1,'FontSize',20);
    set(h,'FontSize',16)

%     saveas(figure(j-1),[Title, ' FFT PP',num2str(j-1), ' and
PP',num2str(j), File])

  end

for j=1:2:5
    lim1=get(h(j),'ylim');
    lim2=get(h(j+1),'ylim');
    maxy=max(lim1,lim2);
    linkaxes([h(j) h(j+1)],'y');
    set(h(j), 'ylim', maxy);
end
```

Impellers Waterfall Program

```
clc
clear X x Y Z j fft deriv Sync delta a M lfft I Index XX YY ZZ
set(0,'defaultaxesfontsize',16);
set(0,'defaulttextfontsize',18);
close all
delta=2500
start=1 %Starting point
disc=start+delta-1  %Adjust to disconinuity in data
enda=50000/delta
lfft=300
Title=['Ramp Down Maximum Amplitude ', num2str(delta*.0002), ' Sec
Increments'] %Set title of Graph
```

```
File='.fig';

Plt=input('What do you want to plot?, 1: Regular Waterfall, 2: Maximum
Amplitude','s');

for j=2:11 %Set columns to be plotted
delta=2500
start=1 %Starting point
disc=start+delta-1  %Adjust to disconinuity in data
enda=50000/delta
    for a=1:enda
l=disc-start; %Number of points to be plotted
T=.0002; %Sampling Period
clear fft x
x(:,:)=Data(start:disc,:); %Make sure Data variable is correct


    if j>=2 && j<=11
    [y,f, ang]=fft_data(x(:,j),T);  %Perform FFT
    fft(:,1)=f(2:length(f));
    fft(2:length(f),j)=y(2:length(f));
    [YYY I]=max(fft(1:length(fft),j));
    Index=fft(I,1);
    X(a,1:lfft)=fft(1:lfft,1); Y(a,1:lfft)=Index;
Z(a,1:lfft)=fft(1:lfft,j);
    XX{j}=[X]; YY{j}=[Y]; ZZ{j}=[Z];
    end
    start=start+delta;
    disc=disc+delta;
end

end

    w(1)=figure(1);
for j=2:11
    if j==4||j==5||j==8||j==9
       if  j==4
           ax(j)=subplot(2,2,1);
       elseif j==5
           ax(j)=subplot(2,2,2);
       elseif j==8
           ax(j)=subplot(2,2,3);
       elseif j==9
           ax(j)=subplot(2,2,4);

       end

    w1=waterfall(XX{j},YY{j},ZZ{j});
    xlabel(['Frequency Spectrum (CPM) PP',num2str(j-1)],'FontSize',14);
    ylabel('Speed (RPM)','FontSize',14);
    set(w1,'edgecolor','k');
```

```
    ylim(ax(j),[0 4000]); xlim(ax(j), [0 10000]);
     zlim(ax(j),[0 8]);

    if strcmp(Plt,'1')
    view(ax(j),-30,30);
 elseif strcmp(Plt,'2')
     view(ax(j),90,0);
     end
 end
    end
```

```
    [ax2,h2]=suplabel('Amplitude (mils peak to peak)','y');
        [ax4,h3]=suplabel( 'Waterfall Plot Impellers');
    set(h3,'FontSize',24);
```

Shaft Waterfall Program

```
clc
clear X x Y Z j fft deriv Sync delta a M lfft I Index XX YY ZZ
set(0,'defaultaxesfontsize',16);
set(0,'defaulttextfontsize',18);
close all
delta=2500
start=1 %Starting point
disc=start+delta-1  %Adjust to disconinuity in data
enda=50000/delta
lfft=300
Title=['Ramp Down Maximum Amplitude ', num2str(delta*.0002), ' Sec
Increments'] %Set title of Graph
File='.fig';

Plt=input('What do you want to plot?, 1: Regular Waterfall, 2: Maximum
Amplitude','s');

for j=2:11 %Set columns to be plotted
delta=2500
start=1 %Starting point
disc=start+delta-1  %Adjust to disconinuity in data
enda=50000/delta
    for a=1:enda
l=disc-start; %Number of points to be plotted
T=.0002; %Sampling Period
```

```
clear fft x
x(:,:)=Data(start:disc,:); %Make sure Data variable is correct


    if j>=2 && j<=11
    [y,f, ang]=fft_data(x(:,j),T);  %Perform FFT
    fft(:,1)=f(2:length(f));
    fft(2:length(f),j)=y(2:length(f));
    [YYY I]=max(fft(1:length(fft),j));
    Index=fft(I,1);
    X(a,1:lfft)=fft(1:lfft,1); Y(a,1:lfft)=Index;
Z(a,1:lfft)=fft(1:lfft,j);
    XX{j}=[X]; YY{j}=[Y]; ZZ{j}=[Z];
    end
    start=start+delta;
    disc=disc+delta;
end

end

    w(1)=figure(1);
for j=2:11
    if j==2||j==3||j==6||j==7||j==10||j==11
       if  j==2
           ax(j)=subplot(3,2,1);
       elseif j==3
           ax(j)=subplot(3,2,2);
       elseif j==6
           ax(j)=subplot(3,2,3);
       elseif j==7
           ax(j)=subplot(3,2,4);
       elseif j==10
           ax(j)=subplot(3,2,5);
       elseif j==11
           ax(j)=subplot(3,2,6);
       end

    w1=waterfall(XX{j},YY{j},ZZ{j});
    xlabel(['Frequency Spectrum (CPM) PP',num2str(j-1)],'FontSize',14);
    set(w1,'edgecolor','k');



    ylim(ax(j),[0 4000]); xlim(ax(j), [0 10000]);
%     ylim(ax(j+1),[0 4000]); xlim(ax(j+1), [0 10000])
    if j==4
    zlim(ax(j),[0 8]);
%     zlim(ax(j+1),[0 8]); ;
    else
    zlim(ax(j),[0 4]);
%     zlim(ax(j+1),[0 4]);
    end
```

```
 if strcmp(Plt,'1')

    view(ax(j),-30,30)
 elseif strcmp(Plt,'2')
     view(ax(j),90,0)
 end
    end
end
%     view (ax(j+1),0,60)

%     saveas(figure(j-1),[Title, 'Waterfall PP',num2str(j-1), ' and
PP',num2str(j), File])

if strcmp (Plt,'1')
    [ax2,h2]=suplabel('Speed (RPM)','y');
    [ax4,h3]=suplabel( 'Waterfall Plot Shafts');
    set(h3,'FontSize',24);
elseif strcmp (Plt,'2')
    [ax2,h2]=suplabel('Amplitude (mils peak to peak)','y');
     [ax3,h3]=suplabel('Speed (RPM)','x');
    [ax4,h3]=suplabel( 'Waterfall Plot Shafts');
    set(h3,'FontSize',24);
end
% n=n+1;



% for j=2:11
% figure (j-1)
% plot(Sync(:,1),Sync(:,j))
% xlabel('frequency (RPM)')
% ylabel('RMS Displacement (mils)')
% title ([Title, ' FFT PP ', num2str(j-1)])
% saveas(figure(j-1),[Title, ' FFT PP ', num2str(j-1),'.fig'])
% end
```

APPENDIX G

RECOMMENDATIONS

This section is dedicated to the exposure of ideas that could help make the project easier to run, more accurate or more efficient.

In order to get more accurate results on the pump performance curves, the strain gages need to be fixed. The transmitter and battery packs of the strain gages need to be secured to the coupling in a manner that they stay balanced.

The low water level switch is currently connected to VFD2 and VFD3 via a relay that switches the auxiliary (slurry and feed) pumps off. If there is a loss of water in the loop and the level triggers the switch both auxiliary pumps will be shut off and an audible alarm will sound inside the test cell, however there are currently no signal telling the computer that the low level switch was triggered, therefore it is possible that, if the situation is unnoticed by the operator, the ESP could continue running dry; since the ESP is lubricated by water, if ran dry for long enough, the pump will be destroyed. It is therefore recommended that the low water level signal be connected to the computer and that either an analog output be added from the computer to VFD1 or an E-Stop signal be connected from the level switch or the computer to VFD1.

It is also recommended that an electrical power input from the VFD1 be connected to the DAQ. This, to avoid having to take the power readings by hand, the input is already existing and connected to the computer controlling the MVP test rig. The current setup

on the MVP test rig uses an Ethernet connection, several options for receiving this signal include:

- Splitting the current Ethernet line for both computers
- Finding an analog output out of the VFD1.
- Connect via network to the MVP test rig computer.
- Set up a program in Labview on the MVP test rig computer that outputs the power value (if the channel is available) and connect the output to one of the free inputs on the ESP test rig.

APPENDIX H

TEST PROCEDURES

ESP Erosion Test Procedures

For: Shell Inc.

TABLE OF CONTENTS

1 PURPOSE

1.1 To perform sand erosion testing on an Electric Submersible Pump (ESP) by circulating a light sand slurry (<.1% by volume) through it. The aforementioned pump will be cantilevered from a custom made platform inside the laboratory to maintain the pump vertically.

1.2 To assess and determine the amount of damage sustained by the pump using various methods which include:

- Pump performance and vibration analysis and comparisons to baseline operations.
- Visual inspection of the pump and its components including, impellers, diffusers, housing, shaft, bearings and seals.

1.3 To suggest and evaluate design enhancements and recommend best practices for pump handling and ideal operation to maximize pump life.

2 HSE REQUIREMENTS

2.1 All equipment operation/maintenance and pump assembly, disassembly, and cleaning activities in this document must be carried out by properly trained personnel; using appropriate personal protective equipment, tools and procedures.

2.2 When the pump is running, access to the erosion center shall be restricted. Barriers and signage shall be placed around the entrances to the erosion center to keep all unauthorized personnel away.

2.3 Flange guards must be placed around all flanges with expected pressures > 100 psig.

2.4 Only personnel trained and certified for forklift operations shall operate forklift.

2.5 All OSHA rules and regulations shall be followed strictly.

3 TEST PARAMETERS/METHODOLOGY

3.1 The test program will consist of daily 8-12 hour runs.

3.2 Periodic performance tests will be made to develop pump curves to compare to baseline and determine degradation. For directions on performance tests follow procedures on section 7.

3.3 The total test time per pump will be determined by pump performance degradation and/or pump destruction (this is expected to be anywhere from 300 to more than 500 hours).

3.4 After noticeable degradation in pump performance (parameters used to determine degradation and its threshold values to be determined prior to testing) the pump will be disassembled and inspected by authorized and trained personnel using procedures detailed in section 8.

3.5 Fixed pump parameters such as flow rate and/or head will be determined prior to the start of the testing and will not be changed for the duration of the testing unless otherwise ordered by authorized Shell personnel.

3.5.1 The flow rate or head of the pump will be controlled automatically using Labview software to control the setting of the pinch valve.

3.6 Sand concentration will be determined prior to the start of the testing and will not be changed for the duration of the testing unless otherwise ordered by authorized Shell personnel.

3.6.1 The sand concentration will be controlled automatically using Labview software. The software will determine the speed of the sand auger using a real-time control feedback loop.

4 TEST CONFIGURATION

4.1 Checkups:

4.1.1 Calculation for number of valves (V11-V30) open on separator:

1. To determine the number of valves that should be open for the separators the following formula should be followed, where N is the number of valves open, rounded to the larger integer:

$$N = \frac{Q}{65} \quad 1$$

4.1.2 Complete System Startup Checklist (Page 170), check all valves, switches and breakers are in their required position, checkmark all boxes and sign the document.

4.1.3 Check tank water level:

- if Low: fill with water
- if High: open drain valve V8 until the High Water Level sensor in Labview turns off.

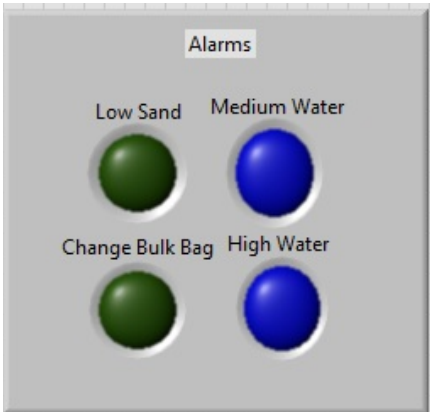

Figure 4.1 Labview Alarms*

5 PROCEDURES

5.1 Prior to start-up.

5.1.1 Load hopper with sand:

1. Pick up the bag frame using the forklift.
2. Place the frame on top of the bag and hook the four loops on each top corner of the bag to the hooks on the frame.
3. Drive the forklift to a position in front of the hopper, keeping the bag as close to the floor as possible.

Ensure that no person is inside the yellow box around the forklift, hopper and sand bag before elevating the bag.

4. Once in position elevate the bag and slowly drop on top of the hopper where the static blade will rip the bag and allow the flow of sand.
5. Slightly elevate the bag to ensure proper flow of sand.

5.1.2 Load empty bags on frames

1. If there is a full bag on the frame, unhook the four loops from the corners of the frame and remove the full bag by picking it up with the forklift, from the bottom pallet. Place the full bag on its designated space.
2. Place an empty pallet on the bottom of the frame.
3. Unfold and place the empty bag on the frame, hooking the four loops on the top corners
4. Move the frame in position to receive the wet sand from the separators.
5. Repeat with the spare cart, if necessary.

5.1.3 Visual Inspection

1. Ensure System Startup Checklist is complete (Section 4.1.2).
2. Visually inspect all piping, hoses, flanges, valves, instrumentation and tank for damage. Watch for wet spots on the item or on the floor and/or dirty spots that could indicate a leak or any other sign of abnormal activity.
3. Inspect all cables and electronics to ensure they are properly connected.

5.2 Start-up

5.2.1 Confirm the seal flush pump is on and that it is pressurized.

5.2.2 Ensure there is nobody in the lab room where the pump is located.

5.2.3 Move all slide indicators to zero and make sure the buttons are on Manual Figure 5.1).

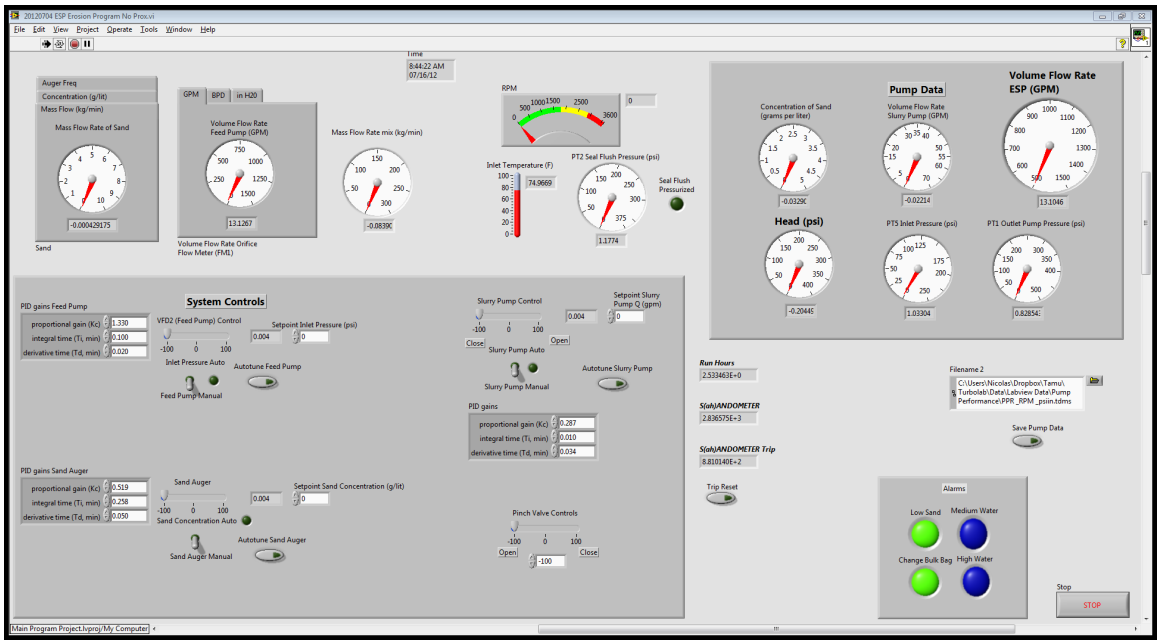

Figure 5.1 Labview System Controls

5.2.4 Click Start on the Labview Program (white arrow top left).

5.2.5 Set the desired flow rate for the slurry pump and set the switch to auto.

5.2.6 Wait for the flow rate to increase to its desired value.

5.2.7 Set inlet pressure:

1. To set the inlet pressure type the quantity desired (psi), in the Labview program in the box titled Inlet Pressure, shown in Figure 5.1.
2. Click on the Feed Pump Auto switch to turn on the feed pump.
3. The sudden increase in pressure will decrease the flow rate on the slurry pump until the PID can react.

5.2.8 Wait for the slurry pump flow rate and inlet pressure to settle to their desired values.

5.2.9 Turn on the ESP by hitting RUN on the Yaskawa VFD control, shown in Figure 5.2.

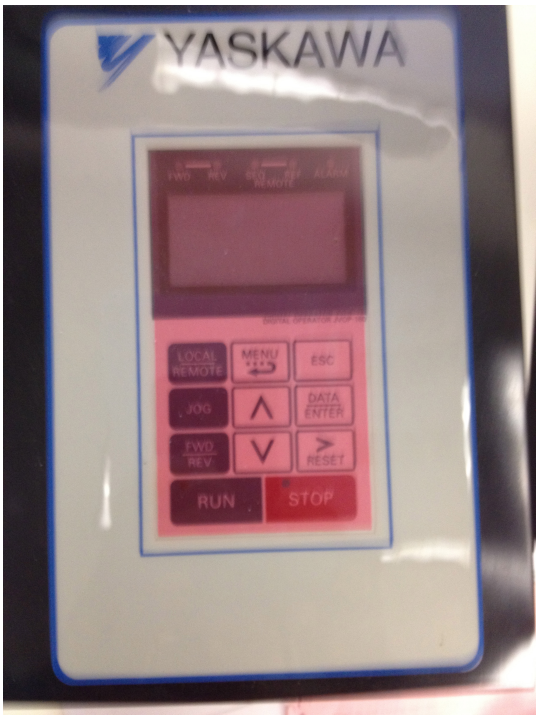

Figure 5.2 Yaskawa VFD Control

5.2.10 Set flow rate:

1. To set the flow rate, close the pinch valve until the desired value is reached.

5.2.11 Set sand concentration

1. To start the sand auger, turn on SW4.
2. To set the sand concentration, type the quantity required, in g/lit, in the Labview program in the box titled Sand Concentration, in the control shown in Figure 5.1.
3. Click on the Sand Auger Auto switch.

5.2.12 Monitor the Labview controls and replace full and empty sand bags as necessary (see Sections 5.1.1 and 5.1.2).

5.3 Testing

5.3.1 When required, save data by typing in the file name and clicking on the Save button in the Labview program.

5.3.2 Always pay close attention to the instruments in Labview and the test cell.

1. If any unusual sign is found, but not imminent danger to life or property, save data, shut down using regular shut down procedure 6.1.1 and report.
2. If something unusual occurs that could risk injury or property, hit the E-stop button immediately and complete shut down by following emergency shutdown procedure 6.1.2.

MAKE SURE THERE IS NO IMMINENT DANGER BEFORE STEPPING INTO THE LAB.

5.3.3 In case of alarms:

- If the high water alarm is activated, save data (if necessary) and shut down using regular shut down procedure 6.1.1. Make sure it is safe to enter the lab before entering to investigate the cause.
- If the medium water alarm is activated and there is no sign of water loss start the refill process on the tank, this process can be done while the system is running as long as an authorized person stays on the computer.
- If the low water alarm is activated and the system is not automatically shut down, hit the E-stop button and follow emergency shutdown procedures 6.1.2.
- If the medium sand alarm is activated, notify the person in charge of refilling the hopper. To refill the hopper, procedure 5.1.1 should be followed.
- If the low sand alarm is activated and the system is not automatically shut down, hit the E-stop and follow emergency shutdown procedures 6.1.2.

6 SHUT DOWN

Shutdown and Emergency Shutdown procedures should be well known and understood by any and all operators before running the system.

6.1.1 Regular shut down

1. Save data, if necessary.
2. Set the Sand Concentration to zero on the slider (Figure 5.1), switch the Sand Auger to manual.
3. Wait one minute for the sand to clean out of the pump.
4. Hit the STOP button on the Yaskawa VFD control (Figure 5.2).
5. Set the inlet pressure to zero on the slider (Figure 5.1) and switch the Feed Pump to manual to shut it off.
6. Set the slurry pump flow rate to zero on the slider (Figure 5.1) and switch the Slurry Pump to manual to shut it off.
7. Stop and Exit the Labview program.
8. Ensure that the pump has stopped spinning and turn the seal flush pump off and close the valve.
9. Follow Shutdown Checklist to ensure all appropriate valves, switches and breakers are off.
10. Perform a visual inspection of the areas.
11. Install the hopper cover.

6.1.2 Emergency shut down

1. Hit SW3 and SW4 (E-stop buttons labeled WATER and SAND) shown in Figure 6.1.

Figure 6.1 Auxiliary Pump and Sand Auger E-Stops

2. Hit the E-Stop button located on the wall or the stop button on the Yaskawa VFD drive.
3. Make sure there is no imminent danger.
4. Turn all sliders to the zero position on the Labview program (Figure 5.1) and put all controls on the manual position.
5. Click the stop button on Labview and report.

7 PERFORMANCE TESTING

7.1.1 Set the sand concentration to zero.

7.1.2 If not running already, start the system normally, per Section 5.2, maintaining the sand concentration at zero.

7.1.3 While keeping the Pinch Valve control on manual, set the pinch valve (V3) value to 100 (fully open) and save.

7.1.4 Increase the pinch valve (V3) slider value until the desired decrease is seen in the flow rate and save.

7.1.5 Repeat step 7.1.4 until the pump stalls.

7.1.6 Re-open the pinch valve quickly after the pump stalls.

8 ASSEMBLY AND INSTALLATION OF PUMP

Refer to Bill of Materials in Page 169.

8.1 Check the inventory of the parts as per BOM.

8.2 Install O-RINGS [16] to DIFFUSERS [24].

8.3 Attach the shaft extension tool to FLANGE [32].

8.4 Install INTAKE S/A [31].

8.5 Install O-RING [30 & 14] on the INTAKE S/A [31].

8.6 Straighten the SHAFT [7].

8.7 Install SLEEVE [5] and RETAINER RING [4] on the SHAFT [7].

8.8 If the retainer ring edges protrude, file.

8.9 Install the SHAFT [7] to INTAKE & FLANGE assembly.

8.10 Fasten the lock screw on the SHAFT [7] for the proper shaft extension.

8.11 Install first IMPELLER [21].

8.12 Install TAPERLOCK BUSHING [25] and KEY [26].

8.13 Fasten TAPERLOCK BUSHING [25] to the SHAFT [7] using CAPSCREW [28] and LOCK WASHER [29] (remove to get started if necessary, remember to put back).

8.14 Install KEY [6] and SPACER SLEEVE [27 & 5].

8.15 Install DIFFUSER [24] (hold back the diffuser to install the next impeller).

8.16 Install SPACER SLEEVE [23 & 22].

8.17 Repeat step 8.10 to 8.15 for the second stage.

8.18 Repeated step 8.10 and 8.11 for the third stage.

8.19 Install UPTHRUST PLATE [19].

8.20 Fasten TAPERLOCK BUSHING [25] to the SHAFT [7] using CAPSCREW [28] and LOCKWASHER [29].

8.21 Install SPACER SLEEVE [18 & 5].

8.22 Install RETAINER RING [4].

8.23 Install third DIFFUSER [24].

8.24 Make sure proximity probes in all the diffusers are aligned.

8.25 Install HOUSING [20].

8.26 Install O-RING [14] on HEAD ADAPTER [13].

8.27 Install HEAD ADAPTER [13].

8.28 Install FLANGE [12] against HEAD ADAPTER [13].

8.29 Install RODs [17] and screw them to the FLANGE [3].

8.30 Tighter NUTs [10] on the FLANGE [12].

8.31 Install O-RING [11] to HEAD S/A [3].

8.32 Install SLEEVE [5] and RETAINER RING [4] on the SHAFT [7].

8.33 Install HEAD S/A [3] on HEAD ADAPTER [13].

8.34 Tighten CAPSCREW [8] and LOCKWASHER [9].

8.35 Install MECHANICAL SEAL [2].

8.36 Screw DISCHARGE WELDMENT [33].

INSTRUMENT LIST

Instrument List			
Item No.	***Description***	***Manufacturer***	***Service***
A1	Accelerometer Inlet X	PCB	0-10 V
A2	Accelerometer Inlet Y	PCB	0-10 V
A3	Accelerometer Inlet Z	PCB	0-10 V
A4	Accelerometer Outlet X	PCB	0-10 V
A5	Accelerometer Outlet Y	PCB	0-10 V
A6	Accelerometer Outlet Z	PCB	0-10 V
PP1	Proximity Probe Shaft 1 X	Bently Nevada	0-10 V
PP2	Proximity Probe Shaft 1 Y	Bently Nevada	0-10 V
PP3	Proximity Probe Impeller 1 X	Bently Nevada	0-10 V
PP4	Proximity Probe Impeller 1 Y	Bently Nevada	0-10 V
PP5	Proximity Probe Shaft 2 X	Bently Nevada	0-10 V
PP6	Proximity Probe Shaft 2 Y	Bently Nevada	0-10 V
PP7	Proximity Probe Impeller 2 X	Bently Nevada	0-10 V
PP8	Proximity Probe Impeller 2 Y	Bently Nevada	0-10 V
PP9	Proximity Probe Shaft 3 X	Bently Nevada	0-10 V
PP10	Proximity Probe Shaft 3 Y	Bently Nevada	0-10 V
PP11	Proximity Probe Coupling X	Bently Nevada	0-10 V
PP12	Proximity Probe Coupling Y	Bently Nevada	0-10 V
PP13	Proximity Probe Coupling Z	Bently Nevada	0-10 V
OFM	Orifice Flow Meter	Lambda Square	0-10 V
CFM	Coriolis Density Meter	Emerson	4-20 mA
LS1	Tank Level Sensor L		NO/NC
LS2	Tank Level Sensor M		NO/NC
LS3	Tank Level Sensor H		NO/NC
LS4	Sand Level Sensor M	IFM	NO/NC
LS5	Sand Level Sensor L	IFM	NO/NC
PT1	Pressure Transducer Inlet ESP	Omega	4-20 mA
PT2	Pressure Transducer Outlet ESP	Omega	4-20 mA
PT3	Pressure Transducer Outlet Choke	Omega	4-20 mA
PT4	Pressure Transducer	Omega	4-20 mA
PT5	Pressure Transducer	Omega	4-20 mA
PT6	Pressure Transducer	Omega	4-20 mA
PT10	Differential Pressure OFM (FM1)	Rosemount	4-20 mA
SG1	Axial Strain Gauge	Binsfield	0-10 V
SG2	Radial Strain Gauge	Binsfield	0-10 V
TT1	ESP Inlet Temperature	Omega	
VFD1	ESP VFD	Yaskawa	4-20 mA
VFD2	Main Pump VFD	Toshiba	4-20 mA
VFD3	Slurry Pump VFD	Toshiba	4-20 mA
VFD4	Sand Handling VFD	Altivar	4-20 mA

EQUIPMENT LIST

Equipment List			
Item No.	**Item**	**Manufacturer**	**Description**
ESP1	Electrical Submersible Pump	Centrilift	3 Stage Centrifugal Pump under testing
F1	Cooling Filter		
HX1	Heat Exchanger		
P1	Feed Pump	Triflo	Auxiliary Centrifugal Pump
P2	Slurry Pump	Triflo	Auxiliary Centrifugal Pump
P3	Cooling Pump		
SC1	Sand Screw Conveyor	Flexicon	Sand auger with hopper
SS1	Sand Separator	Triflo	20 hydrocyclos with screen shaker
St1	Strainer		
T1	Tank	Triflo	5,000 gallon, weir wall-divided tank
BR1	ESP Motor Main Circuit Breaker		480 V
BR3	Auxiliary Pumps Breaker		480 V
BR4	Sand Auger Breaker		240V
SW1	Auxiliary Pumps VFDs Switch		Start/Stop Door Latch Switch
SW2	ESP E-Stop Switch		E-Stop Switch
SW3	Auxiliary Pumps E-Stop Switch		E-Stop Switch
SW4	Sand Auger E-Stop Switch		E-Stop Switch
SW5	Heat Exchanger Switch		On/Off Switch
SW6	Shaker Switch		On/Off Switch
SW7	Seal Flush Pump Switch		On/Off Switch
SW8	ESP Motor Switch Selector		480 V

VALVE LIST

Valve List			
Item No.	**Description**	**Line Size**	**Valve Class**
V1	Feed Pump Valve	5"	Butterfly Valve
V2	Slurry Pump Valve	2"	Butterfly Valve
V3	Pinch Valve	4"	Control Pinch Valve
V4	Tank Feed Pump Valve-Water Supply	6"	Butterfly Valve
V5	Tank Slurry Pump-Water Supply	4"	Butterfly Valve
V6	Tank Cooling Valve--Water Supply	4"	Butterfly Valve
V7	Tank Equalization Valve	4"	Butterfly Valve
V8	Tank Drain Valve-Clean Side	5"	Butterfly Valve
V9	Tank Drain Valve-Dirty Side	5"	Butterfly Valve
V10	Vent Valve- Outlet Feed Pump	1/2"	Ball Valve
V11-V30	20 tank separator valves		Ball Valve
V31	Vent Valve- Outlet Slurry Pump	1/2"	Ball Valve
V32	Drain Valve- Inlet Feed Pump	1/2"	Ball Valve
V33	Drain Valve- Inlet Slurry Pump	1/2"	Ball Valve
V34	Drain Valve Inlet ESP	1/2"	Ball Valve
V35	Pinch Valve Air Supply	1/2"	Ball Valve
V36	Seal Flush Pump Inlet Valve	1/2"	Ball Valve
V37	Seal Flush Control Valve	1/2"	Needle Valve
V38	Seal Flush Water Supply Valve	1/2"	Ball Valve
V39	Separator Inlet Drain Valve	1/2"	Ball Valve

Bill of Materials ESP

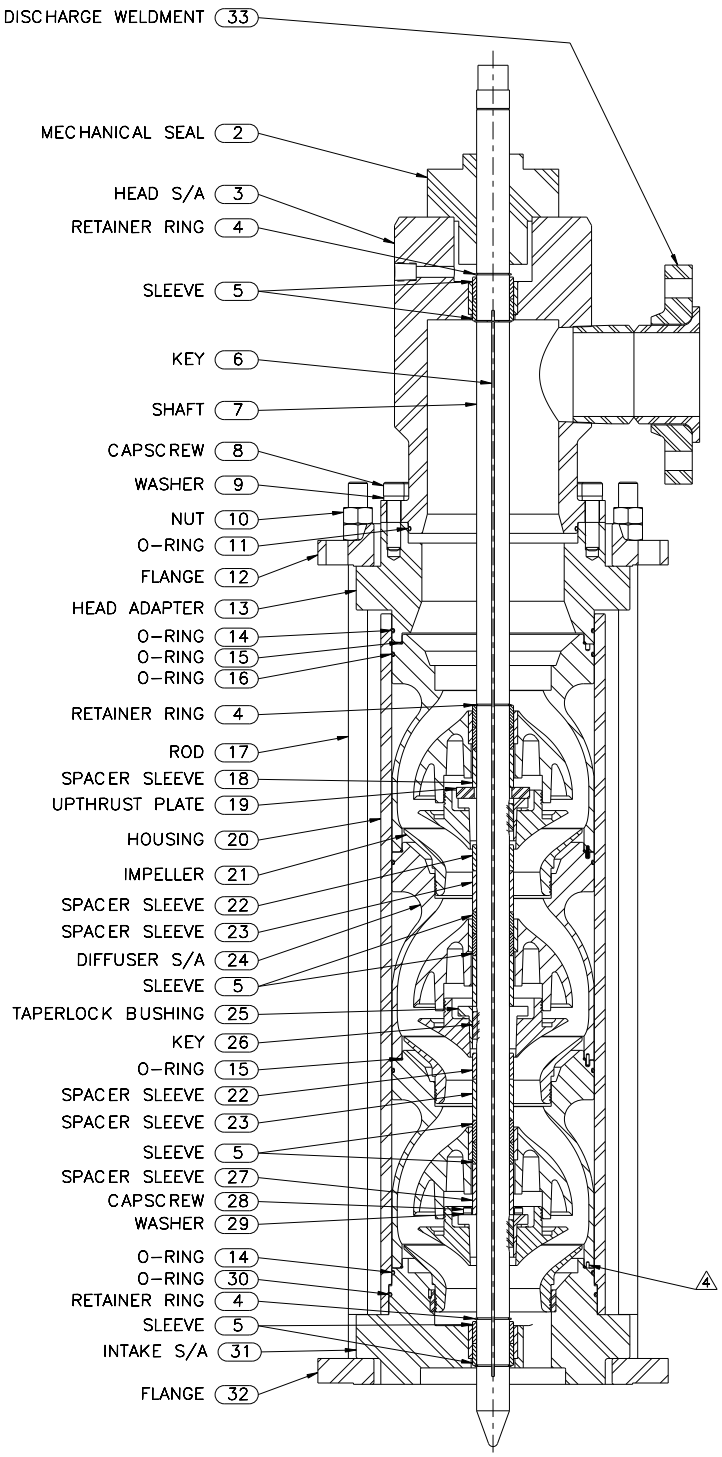

System Startup Checklist and Logbook

Date: _____ Owner: _____

Time: _____ Assistant: _____

Total Run Time: _____hrs. Total Sand Run: _____lbs.

Flow Rate: _____GPM Concentration: _____g/lit

Valve Checklist

	Item	Item No.	Required Position	✓
Tank Area				
	Tank Drain Valve-Dirty Side	V9	Closed	
	Tank Slurry Pump-Water Supply	V5	Open	
	Tank Equalization Valve	V7	Closed (OFF)	
	Tank Drain Valve-Clean Side	V8	Closed	
	Tank Cooling Valve--Water Supply	V6	Open	
	Separator Inlet Drain Valve	V39	Closed	
	Tank Feed Pump Valve-Water Supply	V4	Open	
	Slurry Pump Valve	V2	Open	
	Drain Valve- Inlet Slurry Pump	V33	Closed	
	Vent Valve- Outlet Slurry Pump	V31	Closed	
	20 tank separator valves	V11-V30	As calculated on section 4.1.1: _____.	
Test Cell Area				
	Seal Flush Water Supply Valve	V38	Open	
	Pinch Valve Air Supply	V35	Open	
	Pinch Valve	V3	Open	
	Drain Valve- Inlet Feed Pump	V32	Closed	
	Feed Pump Valve	V1	Open	
	Vent Valve- Outlet Feed Pump	V10	Closed	
	Seal Flush Pump Inlet Valve	V36	Open	
	Drain Valve Inlet ESP	V34	Closed	
	Seal Flush Control Valve[1]	V37	TBD	

Electrical Checklist

	Item	Item No.	Required Position	✓
	Sand Auger E-Stop Switch[1]	SW4	OFF (Out)	
	Shaker Switch	SW6	ON	
	Auxiliary Pumps Breaker(Slurry)	BR3	ON	
	Heat Exchanger Fan Breaker	BR5	ON	
	Heat Exchanger Fan Switch	SW9	ON(OUT)	
	Heat Exchanger Pump Breaker	BR6	ON	
	Heat Exchanger Pump Switch	SW5	ON(Top)	
	Sand Auger Breaker[1]	BR4	ON	
	Auxiliary Pumps VFD Switch	SW1	ON	
	Seal Flush Pump Switch[2,3]	SW7	ON[1,2]	
	ESP Motor Switch Selector[4]	SW8	ESP[3]	
	ESP Motor Main Circuit Breaker	BR1[3]	ON[3]	
	Auxiliary Pumps E-Stop Switch	SW3	ON (Out)	
	Auxiliary Pumps Auto/Manual Switches		Auto	

[1]Sand Auger E-Stop Switch (SW4) must be OFF before turning Sand Auger Breaker (BR4) ON.
[2]Ensure valves V36, V37 and V38 are in their correct positions before switching SW7 ON.
[3]Check for pressure immediately after switching SW7 ON.
[4]SW8 must be in ESP position before switching BR1 ON.

Miscellaneous Checklist

	Item	Item No.	Required Position	✓
	Coupling Guards		ON	
	Hopper		DRY	
	Pallet and Bag on Sand Cart			

System Shutdown Checklist and Logbook

Date: _____ Owner: _____

Time: _____ Assistant: _____

Total Run Time: _____hrs. Total Sand Run: _____lbs.

Valve Checklist

	Item	Item No.	Required Position	✓
	Seal Flush Pump Inlet Valve	V36	Closed	

Electrical Checklist

	Item	Item No.	Required Position	✓
	Seal Flush Pump Switch[1,2]	SW7	OFF[1]	
	Heat Exchanger Pump Switch	SW5	OFF(Bottom)	
	Heat Exchanger Pump Breaker	BR6	OFF	
	Heat Exchanger Fan Switch	SW9	OFF(IN)	
	Heat Exchanger Fan Breaker	BR5	OFF	
	Sand Auger Breaker	BR4	OFF	
	Auxiliary Pumps VFD Switch	SW1	OFF	
	ESP Motor Main Circuit Breaker	BR1[3]	OFF[3]	
	ESP Motor Switch Selector[3]	SW8	Center[3]	

[1]Ensure the shaft has stopped turning before turning the pump off.
[2]BR1 must be turned off before SW8.

Miscellaneous Checklist

	Item	Item No.	Required Position	✓
	Visual Inspection			
	Hopper Cover			